THE INSECT VOLTAGE-GATED SODIUM CHANNEL: STRUCTURE CONSERVATION, ROLE IN PYRETHROID RESISTANCE AND FITNESS COSTS IN THE YELLOW FEVER MOSQUITO, *AEDES AEGYPTI*

A Dissertation

Presented to the Faculty of the Graduate School

of Cornell University

In Partial Fulfillment of the Requirements for the Degree of

Doctor of Philosophy

by

Juan José Silva Fernández

December 2022

THE INSECT VOLTAGE-GATED SODIUM CHANNEL: STRUCTURE CONSERVATION, ROLE IN PYRETHROID RESISTANCE AND FITNESS COSTS IN THE YELLOW FEVER MOSQUITO, *AEDES AEGYPTI*

Juan José Silva Fernández, Ph.D.

Cornell University 2022

The focus of my research was understand the conservation of exons of the *voltage-gated sodium channel* (*Vgsc*) gene across insect Orders and the role of this gene in pyrethroid resistance and its fitness costs in the yellow fever mosquito, *Aedes aegypti*.

The VGSC is critical for the generation of action potentials in the nervous system. The proper functioning of the nervous system is necessary for the survival of organisms as it is responsible for detection, integration and response to external and internal stimuli (e.g., environmental changes, predators, etc.). The VGSC has been under strong selection pressure and resulting in a highly conserved protein. Insects have only one copy of the *Vgsc,* but they produce multiple splice variants due to differential exon usage. In fact, the VGSC is known for having mutually exclusive, optional and 5' or 3' alternative splice site exons. Alternative splicing modulates the three critical features that allow the proper function of the VGSC: voltage-sensing, ion selectivity and channel inactivation. Previous studies found that the *Vgsc* was highly conserved and some optional exons were lacking in certain insect Orders (e.g., Coleoptera lacks exons b, c and k). However, only 10 species representing five insect Orders were examined for this trend (Blattodea: *Blattella germanica,* Coleoptera: *Tribolium castaneum,* Diptera: *Aedes aegypti, Anopheles gambiae, Culex quinquefasciatus, Drosophila melanogaster, Drosophila virilis* and *Musca domestica*, Hymenoptera: *Apis mellifera,* and Lepidoptera: *Bombyx mori*), but it was impossible to claim if those trends were either species-specific or common within Orders. For this reason,

I studied the exon conservation of the VGSC between insect orders and within species. The comparison between insect orders was done across 10 different orders of insects (Blattodea, Coleoptera, Diptera, Ephemeroptera, Hemiptera, Hymenoptera, Lepidoptera, Odonata, Orthoptera, and Thysanoptera). This comparison is relevant because it showed that the amino acid sequence is highly conserved within insect orders (amino acid similarity of exons ranged from 42.5 to 100%) but evidenced the increase in the number of alternative, mutually exclusive and 5' or 3' alternative splice site exons from Diplura to Diptera. Amino acid identity was exceptionally high at the regions involved in the functionality of the VGSC (e.g. voltage sensors, selectivity filter and inactivation loop). The species comparison was done within *A. aegypti* and within *Drosophila melanogaster.* In *A. aegypti,* I compared the full-length cDNA sequences from nine strains of *A. aegypti* collected from multiple parts of the world. Then, I determined possible codon bias for the known *knockdown resistance (kdr)* mutations. In *D. melanogaster,* I examined the variation that exists in the VGSC within lines of the *Drosophila* Genome Reference Panel (DGRP). Exon amino acid conservation was highly identical across the 205 lines of the DGRP because there were only three non-synonymous mutations. The fundamental role of the VGSC in the nervous system makes it a key for toxicology and vector control programs. In fact, several insecticides (e.g. pyrethroids, DDT and oxadiazines) that target the VGSC have been used extensively in the field to control crop pests or vectors. However, there are non-synonymous mutations in the VGSC that can confer resistance to pyrethroids, DDT and oxadiazines and they are known as *knockdown resistance (kdr)* mutations.

To study the mechanisms of resistance to pyrethroids, DDT and oxadiazines, the first step was to characterize a strain of *A. aegypti* that was originally collected from a region in Colombia where insecticide resistance was previously reported but the mechanisms of resistance remained unknown. The characterization of the Colombian strain indicated that the major mechanism of resistance was the *kdr* allele (*410L+1016I+1534C*) but not enzyme-mediated detoxification. For this reason, I isolated a strain that was congenic to a pyrethroid-susceptible strain but carrying the *410L+1016I+1534C* allele. Then, I compared the levels of cross-resistance to multiple insecticides that target the VGSC and compared these

results to those previously reported for other strains that shared the same congenic background but carried different *kdr* alleles (*989P+1016G* and *1534C*). Unexpectedly, the *410L+1016I+1534C* allele did not confer higher levels of resistance relative to the 1534C allele for seven out of 12 insecticides tested between these two strains. The *410L+1016I+1534C* allele conferred higher levels of resistance to pyrethroids containing the 1*R-cis αS* conformation in the cyclopropane ring (e.g. 1*R-cis αS* cypermethrin and deltamethrin) relative to the *1534C* allele. This is the first report of increased levels of resistance to a stereoisomer conformation associated to a *kdr* allele. Furthermore, these results are relevant to understand the evolution of insecticide resistance and are useful for insecticide resistance management because I found which insecticides are most and least effective at controlling mosquitoes carrying the *410L+1016I+1534C*.

To study the fitness costs associated to the *410L+1016I+1534C kdr* allele, this allele was evaluated in the absence of insecticide exposure through 10 generations. The *410L+1016I+1534C* allele coexists with the *1534C* allele in field populations of *A. aegypti* from the Americas and the Caribbean. For this reason, I conducted a population cage experiment where the environmental conditions were controlled in the laboratory and the congenic strains carrying the *410L+1016I+1534C* and *1534C* alleles were crossed and allowed to mate through nine generations in the absence of insecticide exposure. In addition, a subset of mosquitoes of the F_9 were selected with deltamethrin and survivors were allowed to mate. The results from this experiment are relevant because they showed a dramatic decrease in the allele frequencies of the *410L+1016I+1534C* allele but it quickly recovered (frequencies increased) after deltamethrin selection. These findings suggest that the *410L+1016I+1534C* allele is highly advantageous over the *1534C* allele in field populations of *A. aegypti* where 1*R-cis αS* cypermethrin or deltamethrin are applied but use of other pyrethroids would be equally inefficient for either of these alleles. However, the frequencies of the *410L+1016I+1534C* allele would likely decrease relative to *1534C* in the absence of pyrethroid exposure under conditions similar to those tested in my project.

BIOGRAPHICAL SKETCH

Juan Jose Silva Fernandez was born and raised in the city of Bogota, Colombia. He graduated from the Universidad de Los Andes with a Bachelor's of Science in Biology and Microbiology. As an undergraduate student, he worked in the labs of Dr. Alfredo Uribe and Dr. Jenny Dussan and did two research theses to study the catalytic activity of Hexosaminidase A in leukocytes and biological control of mosquitoes using bacterial toxins. At Universidad de Los Andes, Juan focused his Master's degree to research biological control of larvae of *A. aegypti* using bacterial toxins isolated from *Lysinibacillus sphaericus* under the supervision of Dr. Jenny Dussan (2015-2016). In the Fall of 2016, Juan started his Ph.D. in Entomology at Cornell University under the supervision of Dr. Jeffrey G. Scott.

To those who inspired me.

ACKNOWLEDGEMENTS

First, I would like to thank my advisor, Jeff Scott for giving me the privilege to work in his lab and for his support, mentorship and guidance throughout my Ph.D. Dr. Jeff Scott is the best scientist I ever met and wish to retrieve his dedication and patience in my work for the rest of my career. I want to thank my special committee members, Nicolas Buchon and Ping Wang, for their fruitful advice and comments on my research, manuscripts and career. Their contributions allowed me to reinvent myself as a scientist. I want to extend my gratitude to Dr. Cole Gilbert and Dr. Katja Poveda for their continuous support during the preparation for my A exam when some hours were more stressful. A huge thank to the members of the Scott lab, especially Leticia Smith and Jamie Freeman, who gave me their friendship and support during my first years of the Ph.D. at Cornell University. Other remarkable members of the Scott lab that contributed with kindness, friendship, feedback, and support are Haina Sun, Luke Pfannenstiel, Rachel Norris, Rob Mertz and Yinjun Fan. I want to thank my hard-working undergraduate mentees who helped with my projects, Cedric Kouam and Stacie Dressel. I thank my friends from Entomology, especially, Annette Kang, Augusto Rampasso, Chhoki Sherpa, Diana Obregon, Erin Hassett, Joe Poggi, Nathalia Florez, Mark Buckner and Rey Cotto. Big thanks to Rick Fandino for teaching me how to conduct micro-injections in embryos of *Aedes aegypti* and Peter Nagy for teaching me how to do brain dissections in adult mosquitoes.

I thank the funding sources that contributed to my life and research that helped me complete my research (Sarkaria Institute of Insect Physiology and Toxicology (SIPTI), Griswold Fellowship). Thanks to the many teaching assistantships that allowed me to grow as a teaching instructor. Big thank you to every student in my classes who inspired and fed my passion to continue teaching.

I want to thank my friends in Ithaca and anywhere in the world. Alex Chauta, my best roommate who always gave great discussions about science and life, provided me with feedback and supported me those days when experiments did not work as planned. Other special thanks to my fellow latino community: Ana Porras, Andres Perez, Daniel Rojas, David Sossa, Javier Jaimes-Olaya, Jose Bastidas and Juliana Gonzalez-Tobon.

I want to thank my family. My parents, Martha Fernandez and Fernando Silva, my biggest supporters who always believed in me and gave me the tools that shaped the person I am. Special thanks my beloved sister, Maria Lucia Silva, for being a fundamental person in my life who is always there to give me her love and support. Finally, I want to thank my love, Anamaria Paez, for bringing colors to my life, filling my soul with happiness and passion.

TABLE OF CONTENTS

[1] Published in Insect Molecular Biology
[2] Published in PLOS Neglected Tropical Diseases

CHAPTER 1

INTRODUCTION

The focus of my research was to contribute the fields of entomology, toxicology and insect physiology to understand the conservation of exons of the *voltage-gated sodium channel* (*Vgsc*) gene across insect Orders and the role of this gene in pyrethroid resistance and its fitness costs in the yellow fever mosquito, *Aedes aegypti*. My research focused on two areas as described below.

The choice to study the VGSC was based on its importance for insect physiology (*e.g*., generation of action potentials) and toxicology (target site for insecticides). The *voltage-gated sodium channel* plays an essential role in the nervous system. The nervous system is necessary for the survival of organisms as it is responsible for detection, integration and response to external and internal stimuli (e.g., environmental changes, predators, etc.). Hence, the VGSC has been under strong selection pressure and resulting in a highly conserved protein. Most insects have only one copy of the *Vgsc,* but they produce multiple splice variants due to differential exon usage. In fact, the VGSC is known for having mutually exclusive, optional and 5' or 3' alternative splice site exons. Alternative splicing modulates the three critical features that allow the proper function of the VGSC: voltage-sensing, ion selectivity and channel inactivation. In fact, DDT, pyrethroid, and oxadiazine insecticides (e.g., target the VGSC have been used extensively in the field to control crop pests and vectors. However, there are non-synonymous mutations in the *Vgsc* that can confer resistance to pyrethroids, DDT and oxadiazines and they are known as *knockdown resistance (kdr)* mutations. For example, it was regarded that the *Vgsc* was highly conserved and some optional exons (exons b, c, d, i, j, k and h) were lacking in certain insect Orders (e.g., Coleoptera lacks exons b, c and k). However, only 10 species representing five insect Orders were examined for this trend (Blattodea: *Blattella germanica,* Coleoptera: *Tribolium castaneum,* Diptera: *Aedes aegypti, Anopheles gambiae, Culex quinquefasciatus, Drosophila melanogaster, Drosophila virilis*

and *Musca domestica*, Hymenoptera: *Apis mellifera,* and Lepidoptera: *Bombyx mori*), but it was impossible to claim if those trends were either species-specific or common within Orders. In terms of amino acid conservation, the regions of the VGSC involved in the functionality (voltage-sensors, selectivity filter and inactivation loop) across insect Orders remained unknown. Most studies that reported *kdr* mutations did so by sequencing specific regions of the *Vgsc,* but full-length cDNA sequences were usually rare. This was a limiting factor for studying codon bias of *kdr* mutations. Therefore, in Chapter 2 I reported on the 1) Exon comparison of the VGSC across 10 Orders of insects (68 species studied) to examine both conservation of amino acid sequences and conservation of differential exon use, 2) using all available cDNA sequences for *A. aegypti*, determine which known resistance mutations were possible more likely to occur in different populations available and 3) examine the individual VGSC variation that exists within a population of *Drosophila melanogaster*.

The research conducted in Chapters 3 and 4 used *A. aegypti* as model organism for three reasons. First, this is a primary vector of viral pathogens including chikungunya, dengue, yellow fever and Zika, and is responsible for millions of human infections that leads to death, morbidity and economic losses annually. Second, insecticide resistance in *A. aegypti* has been reported in every region where this mosquito is distributed. Third, *A. aegypti* is relatively easy to rear in laboratory under specific environmental conditions. Collectively, the previous considerations make *A. aegypti* an ideal organism to continue the scope of my research.

In the second area (Chapters 3 and 4) of my thesis, the focus was to study the mechanisms of resistance to pyrethroids, DDT and oxadiazines, and fitness costs associated with *kdr* alleles in *A. aegypti*. The mechanisms of resistance are pre-adaptive which means that they are present in field populations, but usually at low frequencies prior to insecticide exposure due to fitness costs (Freeman et al. 2021). However, exposure to insecticides in field populations imposes a selective pressure that raises the frequencies of the *kdr* alleles (*410L+1016I+1534C* and *1534C*), thus, rendering pyrethroids less effective. In the field of insect toxicology, most studies comparing insecticide resistance used strains from different

genetic backgrounds, but this made it difficult to draw conclusions regarding the mechanisms of resistance. Few studies evaluated the role of structure-activity relationship of pyrethroids, but the responses conferred by different *kdr* alleles were never investigated *in vivo*. Therefore, in Chapter 3 I report on the characterization and isolation of a congenic strain of *A. aegypti* carrying the *410L+1016I+1534C* allele, compared the levels of resistance to multiple pyrethroids, DDT and oxadiazines that target the VGSC against two other congenic strains carrying different *kdr* alleles (*989P+1016G* and *1534C*).

To study the fitness costs associated to the *410L+1016I+1534C kdr* allele, a population cage experiment was conducted. This experiment is preferred as the initial step to evaluate fitness costs because it allows to detect changes in allele frequencies due to fitness costs across generations in the absence of insecticide exposure under certain environmental parameters. The vast majority of publications that evaluated fitness costs compared resistance alleles versus susceptible alleles, but competition between resistance alleles has been largely overlooked. This is problematic because different resistance alleles already coexist in field populations, and some potentially impose more detrimental disadvantages relative to other resistance alleles in the absence of insecticide exposure. Therefore, it is valuable to understand not only the relative fitness of *kdr* alleles relative to the susceptible alleles, but also to understand the relative fitness between different resistance alleles. Such information is needed to better understand the patterns of alleles found in field populations. For this reason, I compared the changes of allele and genotype frequencies between two *kdr* alleles (*410L+1016I+1534C* and *1534C*) both in the absence of insecticide exposure and after one cycle of selection.

REFERENCES

Freeman, J. C., L. B. Smith, J. J. Silva, Y. Fan, H. Sun, and J. G. Scott. 2021. Fitness studies of insecticide resistant strains: lessons learned and future directions. Pest Man. Sci. 77: 3847–3856.

CHAPTER 2

CONSERVATION OF THE *VOLTAGE-GATED SODIUM CHANNEL* PROTEIN WITHIN THE INSECTA[3]

Authors: Juan J. Silva and Jeffrey G. Scott

Abstract

The voltage-gated sodium channel (VGSC) is essential for the generation and propagation of action potentials. VGSC kinetics can be modified by producing different splice variants. The functionality of VGSC depends on features such as the voltage-sensors, the selectivity filter and the inactivation loop. Mutations in *Vgsc* conferring resistance to pyrethroid insecticides are known as *knockdown resistance* (*kdr*). I analyzed the conservation of VGSC in both a broad scope and a narrow scope by three approaches: 1) Compare conservation of sequences and of differential exon use across orders of the Insecta, 2) determine which *kdr* mutations were possible in nine populations or *Aedes aegypti*, and 3) examine the individual VGSC variation that exists within a population of *Drosophila melanogaster*. There is an increasing amount of transcript diversity possible from Diplura towards Diptera. The residues of the voltage-sensors, selectivity filter and inactivation loop are highly conserved. The majority of exon sequences were >88.6% similar. Strain specific differences in codon constraints exist for *kdr* mutations in nine strains of *A. aegypti*. Three *Vgsc* mutations were found in one population of *D. melanogaster*. This study shows that overall *Vgsc* is highly conserved across Insecta and within a population of an insect, but that important differences do exist.

[3] Published: *Silva, J. J.*, Scott, J. G. 2020. Conservation of the voltage-sensitive sodium channel protein within the Insecta. Insect Mol Biol. 29: 9-18. (doi: 10.1111/imb.12605)

2.1 Introduction

The nervous system plays a critical role in the detection, integration and response to external and internal stimuli. Responses to stimuli are orchestrated by the propagation of action potentials across neurons mediated by the voltage-sensitive sodium channel (VGSC, also known as the voltage-gated sodium channel) and the voltage-sensitive potassium channel (Catterall 2010, Jan and Jan 2012). The VGSC is arranged in four domains (I-IV, Fig. 1A). Each domain contains six transmembrane α-helical segments (S1 to S6) (Catterall 2010). Three functional features (hereafter referred as sodium-gating regions) are critical for VGSC functioning (Catterall 2000): voltage-sensors, the selectivity filter and the inactivation loop. S4 segments from all four domains are the voltage-sensors and typically have four to eight positively charged amino acids interspaced by two hydrophobic residues (Davies et al. 2007, Payandeh et al. 2011). During the resting state, these positively charged amino acids in S4 form ionic bonds to negatively charged residues in S1, S2 and S3 which neutralizes their charge (Keynes and Elinder 1999, Catterall 2010). An increase in cations flowing through the pore leads to the rotational movement of the S4 segments outward which activates the channel. The selectivity filter is composed of inner (DEKA) and outer (EEQD) rings. The inner and outer rings are composed of four residues: I:D377, II:E985, III:K1497, IV:A1790 (Catterall 2010) and I:E380, II:E988, III:Q1501, IV:D1793, respectively (Terlau et al. 1991, Yu et al. 2005, Davies et al. 2007). The inner ring plays a critical role in Na^+ selectivity (Sun et al. 1997) while the outer ring is predicted to be critical for the permeation rate (Lipkind 2005, Vora et al. 2005). Upon depolarization, the inactivation loop located in the intracellular linker between domains III and IV folds towards the pore and blocks sodium influx. Previous studies found that the hydrophobic triad of residues methionine-phenylalanine-methionine (M1564, F1565 and M1566) is critical for fast inactivation in insects (West et al. 1992, Catterall 2000, Gosselin-Badaroudine et al. 2015).

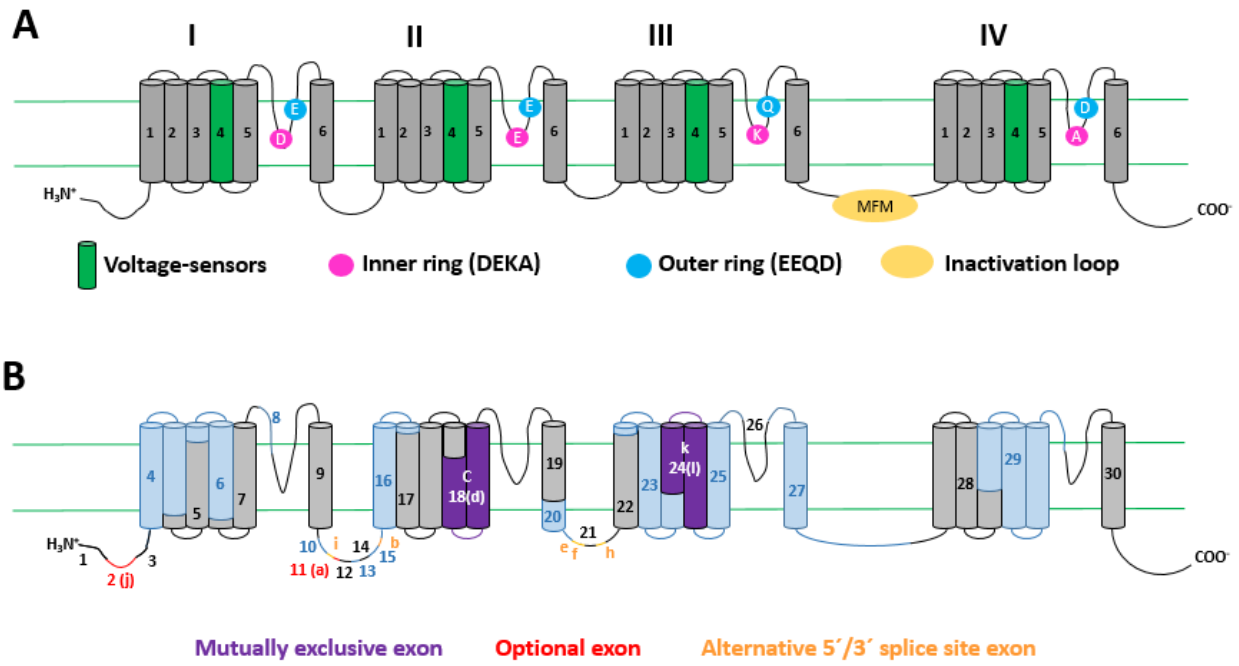

Figure 1. Structure of the voltage-sensitive sodium channel. (A) Topology of the channel indicating important regions for sodium gating. Inner and outer rings of the voltage-sensors, the selectivity filter and the inactivation loop are colored in pink, blue, green and yellow, respectively. (B) Exon organization in the topology of the channel. Numbers and letters indicate exon nomenclature based on *D. melanogaster*. Contiguous exons are differentiated by blue and gray/black colors. Mutually exclusive, optional and alternative 5´ or 3´ splice site exons are colored in purple, red and orange, respectively. Predicted transmembrane regions are based on Davies *et al*. 2007 (Davies et al. 2007).

The first several VGSC sequences revealed highly conserved sequences across metazoans, presumably because this gene is under strong selection pressure (Davies et al. 2007, Payandeh et al. 2011, Barzilai et al. 2012, Zakon 2012). Although insects are an extraordinarily diverse group of organisms, it is unknown what level of VGSC conservation exists throughout this group. Furthermore, it is unclear if amino acid conservation would be retained throughout the sequence or if there might be regions of the protein that are relatively less conserved. Given the numerous insect genomes that have been completed, the means to investigate these questions are now available.

Unlike vertebrates that have multiple *Vgsc* genes, there is only one copy of *Vgsc* in insects (however, aphids have this gene encoded by two unique heteromers (Amey et al. 2015))and VGSC diversity in insects is accomplished by differential exon usage (different splice variants) (Lin et al. 2009). Thus, there can be variable VGSC proteins in different developmental stages (Thackeray and Ganetzky 1995) and tissues (Lee et al. 2002). This has been suggested as "fine-tuning" the functionality of VGSC (Thackeray and Granetzky 1994, Lee et al. 2002, Song et al. 2004, Lin et al. 2009). Splice variants in *Vgsc* of insects can occur due to the presence of mutually exclusive, optional and alternative 5′ or 3′ splice site exons (Fig. 1B). In *Vgsc*, mutually exclusive exons c/d and k/l are present in domains II and III, respectively. Exons a and j are optional. Alternative splice site exons have more than one donor or acceptor sites in their junctions which results in longer or shorter sequences of these exons in the transcript after splicing occurs. The current nomenclature system includes five alternative 5′ or 3′ splice site exons. In fact, exons b, f and h are alternative 3′ splice sites from exons 16, 21 and 22, respectively, while exons i and e are alternative 5′ splice sites from exons 10 and 20, respectively. Previous studies have shown that the different VGSCs produced by differential exon use have different electrophsyiological and pharmacological properties (Song et al. 2004, Lin et al. 2009). However, it is unknown whether or not the mutually exclusive, optional and alternative 5′ or 3′ splice site exons are conserved throughout the insects.

The insect VGSC is the target site for pyrethroid insecticides as well as DDT and oxadiazines (O'Reilly et al. 2006, Du et al. 2013) which are used for control of crop pests and vectors of human diseases and present a tremendous selective force. Resistance to pyrethroids or DDT, due to mutations in *Vgsc* (known as *knockdown resistance*, hereafter referred as *kdr*), is a common mechanism of resistance (Scott 2019). The most recent review of the subject (Dong et al. 2014) lists 61 mutations, or combinations of mutations, that have been reported from one or more insect species through 2013; 24 of these have been tested in oocyte expression systems, and 18 have been confirmed to cause insensitivity to one or more pyrethroids and/or DDT. Since then an additional two mutations have also been confirmed to play a role in resistance. These mutations occur throughout the sequence (there is a clustering of mutations in

domain II), but it is unclear why the mutations are so varied and may or may not occur in more than one species. One possibility is that codon constraints (those requiring >1 nucleotide change to achieve the desired mutation), could be dictating which mutations are possible in different species. This was suggested as a reason why k*dr* mutations L1014F/H/S are not found in *Aedes aegypti* or *Apis mellifera* (Davies et al. 2007) and why the G119S mutation in *Ace* is found in some mosquitoes, but not *A. aegypti* (Weill et al. 2004). However, issues of codon constraint influencing the evolutionary outcome of *Vgsc* mutations are largely based on a very few sequences. There are now multiple *Vgsc* cDNA sequences available in some species (such as *A. aegypti*). I, therefore, examine the available *A. aegypti Vgsc* cDNA sequences to determine the extent with which codon bias is more of a species or population phenomenon.

Studies of *Vgsc* have commonly relied on a single sequence (protein, cDNA or gene) that was determined from multiple pooled insects, and what level of individual variation was present was largely unknown. To address this question, I used *Drosophila melanogaster* because of the availability of the *Drosophila* Genetic Reference Panel (DGRP) (Mackay et al. 2012) and because no mutations in *Vgsc* conferring pyrethroid or DDT resistance are known in this species (Schmidt et al. 2017, Duneau et al. 2018, Scott 2019) (i.e. variation seen would not be due to insecticide selection).

My goals were to examine VGSC variability, and address different questions, across three scales of analyses: 1) Compare VGSC across orders of the Insecta to examine both conservation of amino acid sequences (one exon at a time), and the conservation of differential exon use, 2) using all available cDNA sequences for *A. aegypti*, determine which known resistance mutations were possible in all, some or none of the populations represented, and 3) examine the individual VGSC variation that exists within a population of *D. melanogaster* using the DGRP lines.

2.2 Materials and Methods

Collection of Vgsc sequences

Genome assemblies were initially collected from 89 hexapods (as of January 2019) by downloading from the National Center for Biotechnology Information (NCBI) or i5k project (https://i5k.nal.usda.gov/). These genomes belong to insects, non-insect hexapods (Diplura) and crustaceans. Dipluran and crustacean genomes were used as outgroups when the presence or absence of mutually exclusive, optional and alternative 5´ or 3´ splice sites were examined (section 3.1). As a starting point, individual exon sequences were collected from house fly (Sun et al. 2016) and used to identify exons from *A. aegypti* Per-R, SMK and LVP_AGWG strains (GenBank = ACB37024.1, BAP46858.1 and XP_021708042.1, respectively) (File "*Vgsc* exons *Aedes aegypti*.fasta"). *A. aegypti* exons were used as queries to search with TBLASTN over the other insect genomes to find the *Vgsc* sequence. Exon sequences were manually inspected to match all the residues from query sequences. If the search failed to match an exon, then queries were repeated using the most closely related species. Genomes (and species) were discarded if constitutive exons were missing from the genome sequence. After applying these filters, a total of 71 *Vgsc* sequences were identified and used for this study: two crustaceans, one dipluran, one odonatan, one ephemeropteran, one orthopteran, three blattodeans, one thysanopteran, seven hemipterans, 15 hymenopterans, nine coleopterans, 14 lepidopterans and 16 dipterans (Table S1).

Selection of representative species per insect Order

To avoid bias (due to the different numbers of genomes in the different Orders) in my assessment of exon variation in *Vgsc* across hexapod Orders, only one species was selected to represent each Order. Based on sequence alignments, the species with the highest percent similarity in each Order was selected as representative. Global alignments are most accurate when sequences are similar and have approximately the same length. Thus, for each species, artificial protein sequences containing all exons were generated. All the species per Order were aligned globally with MAFFT (Katoh and Toh 2008). Multiple sequences were aligned using the iterative method G-INS-i with default parameters in MAFFT (Katoh and Standley 2013). Amino acids were clustered into eight groups (having similar chemical properties): G, AVLI, FYW, CM, ST, KRH, DENQ and P. Percent similarities were calculated by pairwise comparisons using SMS2 (Stothard 2000).

Exon similarity across insect Orders

Percent similarity was estimated for individual exons from one representative of each Order (for which a genome sequence was available) according to the same procedure described above. The difference between the highest and lowest percent similarities was divided into five quantile groups to which exons were assigned (42.5-53.9, 54.0-65.4, 65.5-77.0, 77.1-88.5 and 88.6-100 % similarity, respectively). Similarities for exons e and f were calculated only within Diptera, because these exons were only found in this Order.

Positions of kdr mutations across insect Orders

Twenty *kdr* mutations were considered for this study. Eighteen previously reported mutations in *Vgsc* that have been confirmed to confer resistance to pyrethroids (by heterologous expression/electrophysiology studies or *in vivo* using congenic strains) (Usherwood et al. 2007, Dong et al. 2014, Sun et al. 2017). Another two mutations (E435K and S989P) alone do not confer insensitivity to pyrethroids but enhance insensitivity when in combination with other mutations (E435K + L1014F and

S989P + V1016G) (Tan et al. 2002, Hirata et al. 2014). These mutations were located in the topology of the sodium channel protein (Davies et al. 2007) using numbering based on the gold standard *Musca domestica* voltage-sensitive sodium channel (Swiss-Prot = X96668.1).

Non-synonymous Vgsc mutations in exons from the DGRP lines

I analyzed the genotype data from 205 inbred lines from the *Drosophila* Genetics Reference Panel (DGRP) (Huang et al. 2014). In *D. melanogaster*, *Vgsc* is located on chromosome X. Exon coordinates and the reference sequence of chromosome X were downloaded from assembly BDGP R5/dm3 (Apr. 2006) at UCSC Table Browser (Casper et al. 2018). Non-synonymous SNPs located in exons of *Vgsc* were found with Galaxy Tool (Giardine et al. 2005, Blankenberg et al. 2010) and manually confirmed with EditSeq and MegAlign applications of Lasergene (DNAstar, Madison, WI, USA).

Identification of codon constraints for kdr mutations in A. aegypti strains

To examine if there were codon constraints for known *kdr* mutations across *A. aegypti* strains, the full-length *Vgsc* cDNA sequences from nine *A. aegypti* strains. Eight strains were downloaded from NCBI: Bora, Liverpool (LVP_AGWG), NS, Per-R, Oiapoque, Campos, SMK and Waco (GenBank = EU399179.1, XM_021852342.1, EU399180.1, EU399181.1, KY747530.1, KY747529.1, AB909019.1 and KC107440.1, respectively). The *Vgsc* cDNA sequence of the Singapore strain was provided by Dr. Shinji Kasai. Three of the nine strains are pyrethroid resistant (Oiapoque, Per-R and Singapore) and the other six are pyrethroid susceptible (Bora, Liverpool, NS, Campos, SMK and Waco) (Chang et al. 2009, Du et al. 2013, Hirata et al. 2014, Faucon et al. 2015, Haddi et al. 2017). The codons at the sites of the 20 known *kdr* mutations were collected manually using the EditSeq application of Lasergene (DNAstar, Madison, WI, USA), and were confirmed by manually comparing the amino acid sequences of the nine *A. aegypti* strains to *D. melanogaster* DmNav1 (P35500.3).

2.3 Results

The sequences of the *Vgsc* from genomes of 68 species (representing 10 Orders) of insects were collected. *Vgsc* sequences from two crustacean species (*E. affinis* and *L. salmonis*) and one dipluran (*C. aquilonaris*) were used as outgroups. There was generally an increasing number of exons associated with higher Orders, although there were noteworthy exceptions (Fig. 2). The sodium gating regions of VGSC were highly conserved with only 2, 7, 0 and 2 species having different sequences for the inner ring of the selectivity filter, outer ring of the selectivity filter, voltage sensors and inactivation loop respectively. The amino acid sequence of VGSC, evaluated between exons was highly conserved, ranging from 100% to 42.5% across all insects. Generally, the most variable regions were intracellular. Population variation in *Vgsc* was limited with only three non-synonymous mutations found in the DGRP lines. The limited number (four) of *kdr* mutations found in different populations of *A. aegypti* can be partly explained by codon bias, although this depends, at least in part, on the strains examined. Each of these findings are detailed below.

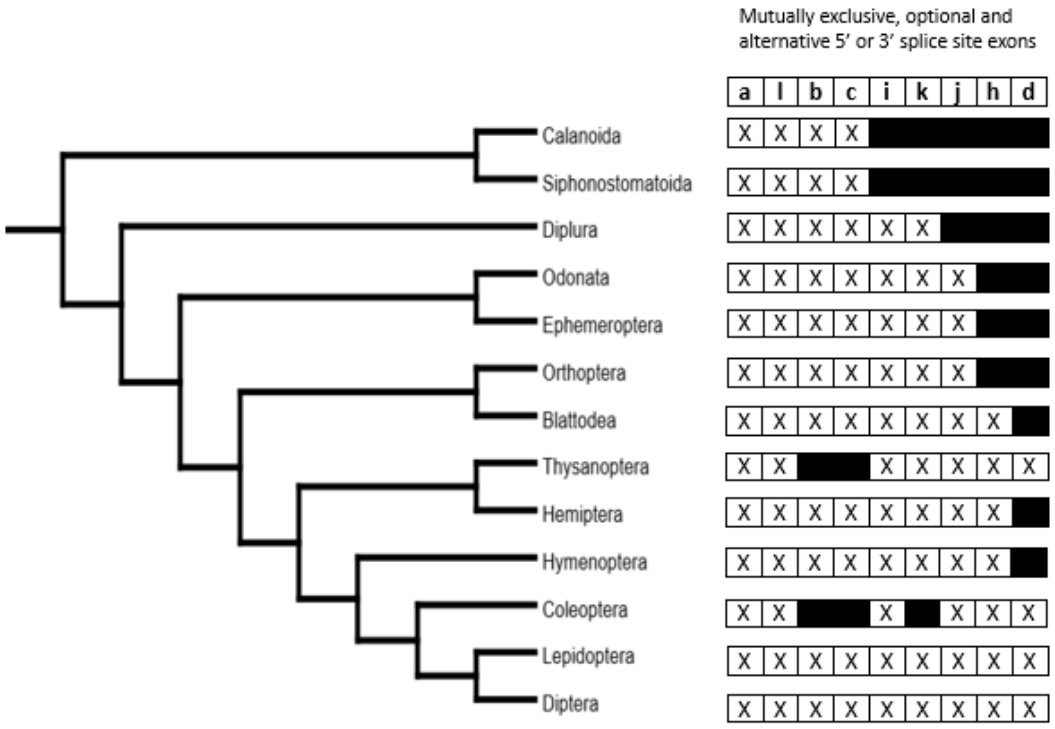

Figure 2. Phylogenetic relationships and presence/absence of *Vgsc* alternative exons in insect Orders. Phylogenetic relationships based on Misof *et al.* 2014 (Misof et al. 2014). Exons present in the Order are represented with a "X" and exons absent are represented with a black box. Exons c/d and k/l are mutually exclusive, exons a and j are optional and exons b, h and i are alternative 5´ or 3´ splice sites.

Presence or absence of mutually exclusive, optional and alternative 5´ or 3´ splice site exons

The presence or absence of mutually exclusive, optional and alternative 5´ or 3´ splice site exons for the different orders is shown in Fig. 2 and the results for all the species are shown in Table S1. Only Diptera and Lepidoptera contained both of the mutually exclusive exons c/d and k/l (*D. melanogaster* nomenclature) (Fig. 2). All of the orders contained only exon c, except for Coleoptera and Thysanoptera (and one Diptera, *C. fuscipes*) which contained only exon d (Table S1). All hexapods had both mutually exclusive exons k and l, except for Coleoptera and two Diptera (*G. austeni* and *G. fuscipes*) which lack k. Optional exon a was present in all species examined. In contrast, optional exon j was found only in insects

(not present in Crustacea and Diplura). Exons b, h and i are alternative 5′ or 3′ splice site exons. Exon h was only present in the higher orders of Insecta (Fig. 1). It is noteworthy that exon h was found in Blattodea (three species examined) and absent from Orthoptera (one species) (Table S1). As additional orthopteran genomes are sequenced this should be re-examined. Exon i is present only in hexapods (Fig. 1). Exons e and f were not included for the presence/absence analysis because these exons have short sequences (≤ 13 and ≤ 10 amino acids, respectively) which made accuracy in BLAST searches (and potentially in genome assemblies) problematic.

Overall, seven patterns were observed based on a comparison of mutually exclusive, optional and alternative 5′ or 3′ splice site exons across Orders (Table S1). First, the presence of exons i and k is a synapomorphic character in hexapods (except Coleoptera that lacks exon k). Second, the presence of exon j is a synapomorphic character in insects. Third, Ephemeroptera, Odonata and Orthoptera share exactly the same exons (a, l, b, c, k, i, and j). Fourth, Blattodea, Hemiptera and Hymenoptera had the presence of the same exons (a, l, b, c, k, i, j and h) as in the previous group with the addition of exon h. Fifth, Thysanoptera and Coleoptera are the only insect Orders containing exon d but lacking c. All the Coleoptera lacked mutually exclusive exons c and k as shown in a previous study for the flour beetle, *T. castaneum* (Davies et al. 2007). Sixth, the two crustacean Orders (Calanoida and Siphonostomatoida) contained the lowest number of mutually exclusive, optional and alternative 5′ or 3′ splice site exons whereas Diptera had the highest number of exons (11 exons including mutually exclusive, optional and alternative 5′ or 3′ splice site). Seventh, there was an increased number of mutually exclusive, optional and alternative 5′ or 3′ splice site exons from crustaceans towards holometabolous insects (as in Diptera). Conversely, no pattern was observed in the total number of exons (including constitutive, mutually exclusive, optional and alternative 5′ or 3′ splice site exons) across Orders (data not shown).

To determine the reliability of the *in silico* predictions, I compared the genome results with two datasets: 1) the full-length cDNA sequences from ten insect species (representing the only species in the analyses for which a full length *Vgsc* cDNA was available), and 2) twelve VGSC sequences predicted by automated computational analysis from NCBI (Table S2). These datasets contained predicted or cDNA

sequences from 21 species that belong to six Orders (Blattodea, Coleoptera, Diptera, Hemiptera, Hymenoptera and Lepidoptera). There was 100% agreement between my results and these datasets (Table S2). For example, Coleoptera lacked exons c and k and this was supported by the five coleopteran sequences (one cDNA and four automated annotations from NCBI): *A. plannipennis* (XP_018330935.1), *A. tumida* (XP_019866360.1), *D. ponderosae* (XP_019765194.1), *O. taurus* (XP_022915619.1) and *T. castaneum* (GQ202025.1). The available cDNA and automated sequences also agreed with my predictions for the voltage gating regions (Table S2). Thus, all available data suggests high accuracy in my sequences.

Amino acid conservation in sodium gating regions of insects

Amino acid sequences of the selectivity filter, voltage-sensors and inactivation loop were highly conserved across insects (Tables S3-S6, respectively). For the inner ring of the selectivity filter, all species had the expected DEKA residues, except for two species: *A. pisum* (Hemiptera) had DENS (i.e. K1497N and A1790S) and *D. novaeangliae* (Hymenoptera) that had a 54-nucleotide deletion that included residue K1497. The residues of the outer ring (EEQD) were more variable than the inner ring (DEKA) when compared across species (Table S3). In fact, seven insect species had residue substitutions in the outer ring: *O. fasciatus* (EIQD), *A. pisum* (EEED), *C. nemesis* (EEPN), and *B. dorsalis*, *H. halys* and *C. lectularius* had the same substitution (EEPD).*D. novaeangliae* had a 54 nucleotide deletion that included Q1501 (located in the outer ring) and K1497 in the inner ring. For the voltage-sensors, there were 32 positively charged residues (lysine or arginine) located in S4 across the four domains (exons c/d and exons k/l are included) (Tables S4-S5). From these positively charged residues, there were four, eight, six and eight located in domains I, II, III and IV, respectively. There was absolute conservation of these amino acids; all the 32 voltage sensors were positively charged amino acids across the insects. All the species had the hydrophobic triad MFM in the inactivation loop, except two beetles, *T. castaneum* (LMM) and *O. borbonicus* (LFM) (Table S6).

Amino acid similarity in VGSC across insect Orders

The VGSC sequences across the Insecta were well conserved overall, but some regions had higher or lower areas of amino acid conservation (Fig. 3A). The majority of the exons (54.0%) were highly conserved (88.6-100% similarity) and an additional 18.9% of the exons had 77.1-88.5% amino acid similarity (Fig. 3A). Four exons (j, 8, 22 and 30), had intermediate levels of amino acid similarity (65.5-77.0%). Three of these correspond to exons that code for intracellular (in whole or in part) domains of VGSC. However, exon 8 codes for an extracellular loop (in whole or in part). The least similar exons were 13, i and h (42.5-53.9% similarity), and exons 10, 14 and 21 (54.0-65.4% similarity). Again, most of these exons are located in intracellular domains of VGSC (except exon 8 that is located in an extracellular linker of domain I).

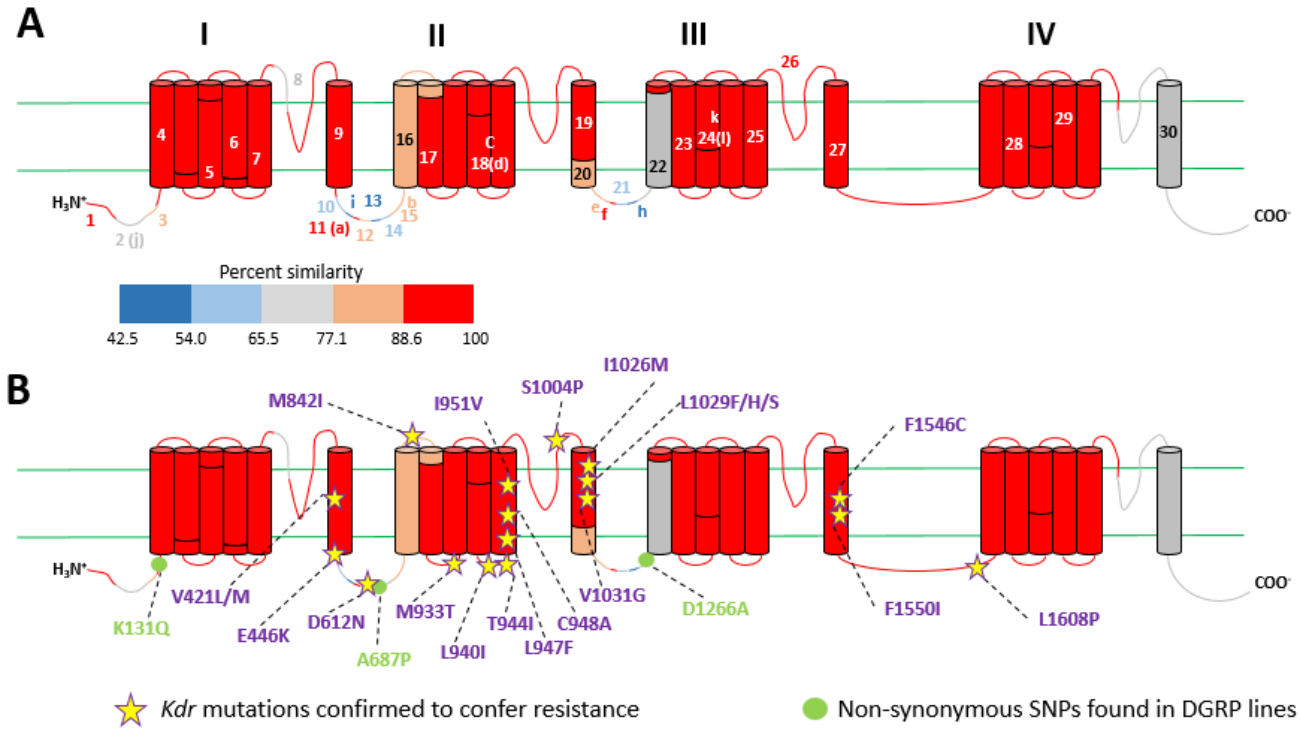

Figure 3. Relative conservation of the exons of the voltage-sensitive sodium channel across insect Orders. Numbers and letters indicate exon nomenclature based on *D. melanogaster*. (A) Individual exons are color coded according to percent similarity. Percent similarity for exons e and f was calculated only for dipteran species for reasons explained in the Experimental Procedures. (B) Mutations in the *Vgsc* that have been confirmed to confer pyrethroid-insensitivty in *Xenopus* oocytes are illustrated in yellow stars and non-synonymous mutations from DGRP lines are illustrated in green circles. Codon numbering according to *M. domestica* voltage-sensitive sodium channel (Swiss-Prot accession = X96668.1).

VGSC variation within a population of D. melanogaster

The 205 DGRP lines contain three non-synonymous mutations and none of these confer resistance to pyrethroids (Battlay et al. 2018, Duneau et al. 2018). The mutations are located in the N-terminal (K120Q) and in the linkers connecting domains I-II (A680P) and II-III (D1259A). These polymorphisms were in regions where the amino acid sequences ranged from relatively less conserved to highly conserved (Fig. 3B).

Codon comparison of kdr mutations across nine A. aegypti strains

I examined 20 *Vgsc* mutations that have been confirmed to confer resistance (alone or in combination) to pyrethroids in one or more strains of insects using full length cDNA sequences from nine populations of *A. aegypti* in order to determine if the codons would permit (need only a single nucleotide change), or not permit (>1 nt change needed) resistance mutations at that site. Nine *kdr* mutations (E435K, D610N, M827I, M918T, L925I, I936V, I1011M, F1538I and L2596P) could be achieved with a single nt change (had no codon bias) in all of the strains (unless they already had the *kdr* mutation), including the four that have previously been found in *A. aegypti* (Smith et al. 2016, Haddi et al. 2017) (Table 1). Seven *kdr* mutations (V410M, T929I, L932F, C933A and L1014F/H/S) showed codon constraint (required >1 nt change) in all nine strains. Although, the codon for C933 was different between SMK and Liverpool (TGT) relative to the other seven strains (TGC), all strains still required a two nt change to achieve the *kdr* mutation at this position. Two of the *kdr* mutations (T929I and L932F) revealed that the codon bias was strain specific when the susceptible strains were compared. The Liverpool and SMK strains (having an ACC codon) could give rise to a T929I mutation (ATC) with a single nucleotide change, while the other strains (Bora, Campos, NS, Oiapoque, Per-R, Singapore and Waco) would be highly unlikely (would require two nucleotides changes). Conversely, the L932F mutation would require two nucleotide substitutions in SMK and Liverpool, but only one in the other strains (Table 1). Additional cDNA sequences would be very informative as to how many mutations have codon bias that is strain specific compared to being a species wide phenomenon. The Oiapoque, Per-R and Singapore resistant strains contained the *kdr* mutations V410L + F1534C, V1016G + F1534C and V1016G + S989P, respectively (Table 1).

Table 1. Codon bias at the known *kdr* mutations in insects across nine strains of *A. aegypti*.

A. aegypti strain	*Drosophila* codon numbering*	V410L/M			T929I		L932F		C933A		S989P		L1014F/H/S					V1016G		F1534C	
		V	L	M	T	I	L	F	C	A	S	P	L	F	H	S	V	G	F	C
Liverpool		GTA	TTA, CTA	X	ACC	ATC	CTG	X	TGT	X	TCC	CCC	CTA	X	X	X	GTA	GGA	TTC	TGC
SMK		GTA	TTA, CTA	X	ACC	ATC	CTG	X	TGT	X	TCC	CCC	CTA	X	X	X	GTA	GGA	TTC	TGC
Bora		GTA	TTA, CTA	X	ACG	X	CTC	TTC	TGC	X	TCC	CCC	CTA	X	X	X	GTA	GGA	TTC	TGC
Campos		GTA	TTA, CTA	X	ACG	X	CTC	TTC	TGC	X	TCC	CCC	CTA	X	X	X	GTA	GGA	TTC	TGC
Waco		GTA	TTA, CTA	X	ACG	X	CTC	TTC	TGC	X	TCC	CCC	CTA	X	X	X	GTA	GGA	TTC	TGC
NS		GTA	TTA, CTA	X	ACG	X	CTC	TTC	TGC	X	TCC	CCC	CTA	X	X	X	GTA	GGA	TTC	TGC
Oiapoque			**TTA**	X	ACG	X	CTC	TTC	TGC	X	TCC	CCC	CTA	X	X	X	GTA	GGA		**TGC**
Per-R		GTA	TTA, CTA	X	ACG	X	CTC	TTC	TGC	X	TCC	CCC	CTA	X	X	X		**GGA**	TTC	TGC
Singapore		GTA	TTA, CTA	X	ACG	X	CTC	TTC	TGC	X	-	**CCC**	CTA	X	X	X		**GGA**	TTC	TGC

*Codon numbering according to *M. domestica* voltage-sensitive sodium channel (Swiss-Prot = X96668.1).

Boxes with an X represent codons in which two nucleotide substitutions are required in the wild type allele to change amino acid residue.

Codons containing *kdr* mutations found in individual *A. aegypti* strains are in bold.

The known *kdr* mutations that are not shown (E435K, D610N, M827I, M918T, L925I, I936V, I1011M, F1538I and L1596P) would all be possible with a single nucleotide change in all of the strains shown.

2.4 Discussion

In this study, I investigated the conservation of the VGSC using three parameters: 1) presence or absence of mutually exclusive, optional and alternative splice sites exons (using a dipluran and two crustaceans as outgroups), 2) conservation of the amino acids in the sodium gating regions, and 3) overall amino acid similarity. There was an increase in the presence of mutually exclusive, optional and alternative splice sites exon from Crustacea (a, l, b and c) through the lower insect Orders to the more derived holometabolous Orders, such as in Diptera (a, l, b, c, k, i, j, h and d) with only exons a, b and l found in all species. Exons i and k are found in the hexapods, but not in Crustacea. Similarly, exon j is found in insects but absent in Crustacea and Diplura.

A previous study indicated *T. castaneum* lacks mutually exclusive exons c and k (Davies et al. 2007) and my results indicate this appears to be true for all Coleoptera. A previous report (Davies et al. 2007) suggested that *T. castaneum* may lack exon b, but this species and other coleopterans contained this exon. The only Thysanoptera (*F. occidentalis*) lacked exon c. The amino acid sequences of the sodium-gating regions were highly conserved, especially the voltage-sensors in which positively charged residues (K or R) were identical for all 32 positions across 68 species. For example, the positively charged residues from the voltage-sensors of domain I are R, R, R and K across 68 species (Table S4). In the selectivity filter, the residues of the inner ring (DEKA) were more conserved than the outer ring (EEQD) when compared across species. This is concordant with the prediction that the inner ring is under higher selection pressure because it contributes to sodium selectivity as opposed to the outer ring that is involved in permeation rate. Only two species had non-DEKA residues in the inner ring of the selectivity filter *A. pisum* (DENS) and *D. novaelangliae* (18-residue deletion). The inner ring residues DENS have been described in other species of aphids (*Aphis citricidus*, *Myzus persicae* and *Rhopalosiphum padi*) and these studies found increased Ca^{2+} permeability and reduced tetrodotoxin sensitivity relative to DEKA (Amey et al. 2015, Zuo et al. 2016, Jiang et al. 2017). In the inactivation loop, the hydrophobic triad (MFM) was identical for most species except *T. castaneum* (LMM) and *O. borbonicus* (LFM). It would be valuable to evaluate the channel properties that of the VGSC with novel inner ring and hydrophobic triad sequences. Most exons

(73%) were highly conserved (77.1-100% similar) when amino acid similarities across insect Orders were considered consistent with strong selective pressure acting on VGSC. Of the 20 VGSC amino acids that can be changed to confer resistance, 18 were found in exons having the highest levels of similarity and two mutations (D610N and M827I) were in exons with the second highest levels of similarity (Fig. 3B). This may help explain the fitness costs that are commonly associated with *kdr* (Rinkevich et al. 2007, Berticat et al. 2008, Rinkevich et al. 2012, Brito et al. 2013, Rinkevich et al. 2013, Hanai et al. 2018). A previous study of house flies identified the carboxy end as the most variable region of the VGSC (Kasai et al. 2017) and this is a region of the protein that has relatively lower sequence conservation.

Knowledge of codon constraints for *kdr* mutations is important to predict what mutations are possible. The results show that such codon constraints are not necessarily species specific, but may also be population specific. For example, the T929I is more likely to occur in populations that have the same codon as SMK and Liverpool because only a single nucleotide substitution is required. In contrast, populations that have a different codon at T929I, such as found in Bora, Campos, NS, Oiapoque, Per-R, Singapore and Waco, would not be expected to have the resistance mutation due to codon bias. Conversely, the L932F mutation is less likely to occur in SMK and Liverpool relative to other strains because two nucleotide substitutions are required to change the codon from leucine (CTG) to phenylalanine (TTC or TTT). Among all the strains used in this study, *kdr* mutations V410M, C933A and L1014F/H/S are less likely to occur because all the codons in these strains require two nucleotide substitutions.

Based on the information that has been generated over the last 20 years, it is worth reconsidering the current nomenclature of *Vgsc* exons. Specifically, exons i, b, e, f and h are not actually exons. They are the alternative 5´ or 3´ splice site variant of an adjoining exon. For example, exon i is actually an optional piece of exon 10. Given the technology originally used, it is understandable that these splice site variants were originally thought to be separate exons (Thackeray and Ganetzky 1995). However, given the improved understanding of the *Vgsc* and to simplify the nomenclature, it is proposed that researchers

should stop using the “exon i, b, e, f and h” nomenclature, and instead treat these as splice variants of the exon they are part of.

In conclusion, the amino acid sequence of VGSC is highly conserved across the Orders of Insecta and interesting phylogenetic patterns associate with mutually exclusive, optional and alternative 5´ or 3´ splice site exons were observed. There is also high conservation when the residues involved in the voltage-sensors, the selectivity filter and the inactivation were considered as well as non-synonymous SNPs (based on the DGRP lines) and the codons of *kdr* mutations (based on *A. aegypti* strains). Additional cDNA sequences, from new populations and from new species, will facilitate the understanding of VGSC conservation, VGSC function and role of different mutations in insecticide resistance.

Acknowledgements

I want to thank S. Kasai, K. Dong and H. Sun for sharing unpublished data and W. Huang for his support with the analysis of the non-synonymous mutations from the DGRP lines. Thanks to Y. Fan, J. Freeman, C. Gilbert, R. Mertz, L. Smith H. Sun and P. Wang for their valuable comments and helpful suggestions.

REFERENCES

Amey, J. S., A. O. O'Reilly, M. J. Burton, A. M. Puinean, I. R. Mellor, I. R. Duce, L. M. Field, B. A. Wallace, M. S. Williamson, and T. G. E. Davies. 2015. An evolutionarily-unique heterodimeric voltage-gated cation channel found in aphids. FEBS Let. 589: 598-607.

Barzilai, M. G., Adam M. Reitzel, Johanna E. M. Kraus, D. Gordon, U. Technau, M. Gurevitz, and Y. Moran. 2012. Convergent evolution of sodium ion selectivity in metazoan neuronal signaling. Cell Reports 2: 242-248.

Battlay, P., P. B. Leblanc, L. Green, N. R. Garud, J. M. Schmidt, A. Fournier-Level, and C. Robin. 2018. Structural variants and selective sweep foci contribute to insecticide resistance in the *Drosophila* genetic reference panel. G3 8: 3489.

Berticat, C., J. Bonnet, S. Duchon, P. Agnew, M. Weill, and V. Corbel. 2008. Costs and benefits of multiple resistance to insecticides for *Culex quinquefasciatus* mosquitoes. BMC Evol. Biol. 8: 104.

Blankenberg, D., G. Von Kuster, N. Coraor, G. Ananda, R. Lazarus, M. Mangan, A. Nekrutenko, and J. Taylor. 2010. Galaxy: a web-based genome analysis tool for experimentalists. Current protocols in molecular biology 89: 19.10.11-19.10.21.

Brito, L. P., J. G. Linss, T. N. Lima-Camara, T. A. Belinato, A. A. Peixoto, J. B. Lima, D. Valle, and A. J. Martins. 2013. Assessing the effects of *Aedes aegypti kdr* mutations on pyrethroid resistance and its fitness cost. PLoS One 8: e60878.

Casper, J., A. S. Zweig, C. Villarreal, C. Tyner, M. L. Speir, K. R. Rosenbloom, B. J. Raney, C. M. Lee, B. T. Lee, D. Karolchik, A. S. Hinrichs, M. Haeussler, L. Guruvadoo, J. Navarro Gonzalez, D. Gibson, I. T. Fiddes, C. Eisenhart, M. DIekhans, H. Clawson, G. P. Barber, J. Armstrong, D. Haussler, R. M. Kuhn, and W. J. Kent. 2018. The UCSC Genome Browser database: 2018 update. Nucl. Acids Res. 46: 8.

Catterall, W. A. 2000. From ionic currents to molecular mechanisms: the structure and function of voltage-gated sodium channels. Neruon 26: 13-25.

Catterall, W. A. 2010. Ion channel voltage sensors: structure, function, and pathophysiology. Neuron 67: 915-928.

Chang, C., W. K. Shen, T. T. Wang, Y. H. Lin, E. L. Hsu, and S. M. Dai. 2009. A novel amino acid substitution in a voltage-gated sodium channel is associated with knockdown resistance to permethrin in *Aedes aegypti*. Insect Biochem. Mol. Bio. 39: 272-278.

Davies, T. G. E., L. M. Field, P. N. R. Usherwood, and M. S. Williamson. 2007. A comparative study of voltage-gated sodium channels in the Insecta: implications for pyrethroid resistance in Anopheline and other Neopteran species. Insect Mol. Biol. 16: 361-375.

Dong, K., Y. Du, F. Rinkevich, Y. Nomura, P. Xu, L. Wang, K. Silver, and B. S. Zhorov. 2014. Molecular biology of insect sodium channels and pyrethroid resistance. Insect Biochem. Mol. Biol. 50: 1-17.

Du, Y., Y. Nomura, G. Satar, Z. Hu, R. Nauen, S. Y. He, B. S. Zhorov, and K. Dong. 2013. Molecular evidence for dual pyrethroid-receptor sites on a mosquito sodium channel. Proc. Natl. Acad. Sci. USA 110: 11785-11790.

Duneau, D., H. Sun, J. Revah, K. San Miguel, H. D. Kunerth, I. V. Caldas, P. W. Messer, J. G. Scott, and N. Buchon. 2018. Signatures of insecticide selection in the genome of *Drosophila melanogaster*. G3 8: 3469-3480.

Faucon, F., I. Dusfour, T. Gaude, V. Navratil, F. Boyer, F. Chandre, P. Sirisopa, K. Thanispong, W. Juntarajumnong, R. Poupardin, T. Chareonviriyaphap, R. Girod, V. Corbel, R. Reynaud, and J.-P. David. 2015. Identifying genomic changes associated with insecticide resistance in the dengue mosquito *Aedes aegypti* by deep targeted sequencing. Genome Res. 25: 1347-1359.

Giardine, B., C. Riemer, R. C. Hardison, R. Burhans, L. Elnitski, P. Shah, Y. Zhang, D. Blankenberg, I. Albert, J. Taylor, W. Miller, W. J. Kent, and A. Nekrutenko. 2005. Galaxy: A platform for interactive large-scale genome analysis. Genome Res. 15: 1451-1455.

Gosselin-Badaroudine, P., A. Moreau, L. Delemotte, T. Cens, C. Collet, M. Rousset, P. Charnet, M. L. Klein, and M. Chahine. 2015. Characterization of the honeybee AmNaV1 channel and tools to assess the toxicity of insecticides. Sci. Rep. 5: 12475.

Haddi, K., H. V. V. Tomé, Y. Du, W. R. Valbon, Y. Nomura, G. F. Martins, K. Dong, and E. E. Oliveira. 2017. Detection of a new pyrethroid resistance mutation (V410L) in the sodium channel of *Aedes aegypti*: a potential challenge for mosquito control. Sci. Rep. 7: 46549.

Hanai, D., M. H. Yoshimizu, and J. G. Scott. 2018. The insecticide resistance allele *kdr-his* has a fitness cost in the absence of insecticide use. J. Econ. Entomol. 111: 2992-2995.

Hirata, K., O. Komagata, K. Itokawa, A. Yamamoto, T. Tomita, and S. Kasai. 2014. A single crossing-over event in voltage-sensitive Na^+ channel genes may cause critical failure of dengue mosquito control by insecticides. PLoS Negl. Trop. Dis. 8: e3085.

Huang, W., A. Massouras, Y. Inoue, J. Peiffer, M. Ramia, A. M. Tarone, L. Turlapati, T. Zichner, D. Zhu, R. F. Lyman, M. M. Magwire, K. Blankenburg, M. A. Carbone, K. Chang, L. L. Ellis, S. Fernandez, Y. Han, G. Highnam, C. E. Hjelmen, J. R. Jack, M. Javaid, J. Jayaseelan, D. Kalra, S. Lee, L. Lewis, M. Munidasa, F. Ongeri, S. Patel, L. Perales, A. Perez, L. Pu, S. M. Rollmann, R. Ruth, N. Saada, C. Warner, A. Williams, Y.-Q. Wu, A. Yamamoto, Y. Zhang, Y. Zhu, R. R. H. Anholt, J. O. Korbel, D. Mittelman, D. M. Muzny, R. A. Gibbs, A. Barbadilla, J. S. Johnston, E. A. Stone, S. Richards, B. Deplancke, and T. F. C. Mackay. 2014. Natural variation in genome architecture among 205 *Drosophila melanogaster* Genetic Reference Panel lines. Genome Res. 24: 1193-1208.

Jan, L. Y., and Y. N. Jan. 2012. Voltage-gated potassium channels and the diversity of electrical signalling. J. Physiol. 590: 2591-2599.

Jiang, X.-Z., Y.-X. Pei, W. Lei, K.-Y. Wang, F. Shang, H.-B. Jiang, and J.-J. Wang. 2017. Characterization of an insect heterodimeric voltage-gated sodium channel with unique alternative splicing mode. Comparative Biochemistry and Physiology Part B: Biochemistry and Molecular Biology 203: 149-158.

Kasai, S., H. Sun, and J. G. Scott. 2017. Diversity of knockdown resistance alleles in a single house fly population facilitates adaptation to pyrethroid insecticides. Insect Mol. Biol. 26: 13-24.

Katoh, K., and H. Toh. 2008. Recent developments in the MAFFT multiple sequence alignment program. Brief Bioinform 9: 286-298.

Katoh, K., and D. M. Standley. 2013. MAFFT multiple sequence alignment software version 7: improvements in performance and usability. Mol. Biol. Evol. 30: 772-780.

Keynes, R. D., and F. Elinder. 1999. The screw-helical voltage gating of ion channels. Proc. Biol. Sci. 266: 843-852.

Lee, S. H., P. J. Ingles, D. C. Knipple, and D. M. Soderlund. 2002. Developmental regulation of alternative exon usage in the house fly *Vssc1* sodium channel gene. Invertebr. Neurosci. 4: 125-133.

Lin, W.-H., D. E. Wright, N. I. Muraro, and R. A. Baines. 2009. Alternative splicing in the voltage-gated sodium channel $DmNa_v$ regulates activation, inactivation, and persistent current. J. Neurophys. 102: 1994-2006.

Lipkind, G. M. 2005. Molecular modeling of local anesthetic drug binding by voltage-gated sodium channels. Molec. Pharmacol. 68: 1611-1622.

Mackay, T. F. C., S. Richards, E. A. Stone, A. Barbadilla, J. F. Ayroles, D. Zhu, S. Casillas, Y. Han, M. M. Magwire, J. M. Cridland, M. F. Richardson, R. R. H. Anholt, M. Barron, C. Bess, K. P. Blankenburg, M. A. Carbone, D. Castellano, L. Chaboub, L. Duncan, Z. Harris, M. Javaid, J. C. Jayaseelan, S. N. Jhangiani, K. W. Jordan, F. Lara, F. Lawrence, S. L. Lee, P. Librado, R. S. Linheiro, R. F. Lyman, A. J. Mackey, M. Munidasa, D. M. Muzny, L. Nazareth, I. Newsham, L. Perales, L.-L. Pu, C. Qu, M. Ramia, J. G. Reid, S. M. Rollmann, J. Rozas, N. Saada, L. Turlapati, K. C. Worley, Y.-Q. Wu, A. Yamamoto, Y. Zhu, C. M. Bergman, K. R. Thornton, D. Mittelman, and R. A. Gibbs. 2012. The *Drosophila melanogaster* genetic reference panel. Nature 482: 173-178.

Misof, B., S. Liu, K. Meusemann, R. S. Peters, A. Donath, C. Mayer, P. B. Frandsen, J. Ware, T. Flouri, R. G. Beutel, O. Niehuis, M. Petersen, F. Izquierdo-Carrasco, T. Wappler, J. Rust, A. J. Aberer, U. Aspock, H. Aspock, D. Bartel, A. Blanke, S. Berger, A. Bohm, T. R. Buckley, B. Calcott, J. Chen, F. Friedrich, M. Fukui, M. Fujita, C. Greve, P. Grobe, S. Gu, Y. Huang, L. S. Jermiin, A. Y. Kawahara, L. Krogmann, M. Kubiak, R. Lanfear, H. Letsch, Y. Li, Z. Li, J. Li, H. Lu, R. Machida, Y. Mashimo, P. Kapli, D. D. McKenna, G. Meng, Y. Nakagaki, J. L. Navarrete-Heredia, M. Ott, Y. Ou, G. Pass, L. Podsiadlowski, H. Pohl, B. M. von Reumont, K. Schutte, K. Sekiya, S. Shimizu, A. Slipinski, A. Stamatakis, W. Song, X. Su, N. U. Szucsich, M. Tan, X. Tan, M. Tang, J. Tang, G. Timelthaler, S. Tomizuka, M. Trautwein, X. Tong, T. Uchifune, M. G. Walzl, B. M. Wiegmann, J. Wilbrandt, B. Wipfler, T. K. Wong, Q. Wu, G. Wu, Y. Xie, S. Yang, Q. Yang, D. K. Yeates, K. Yoshizawa, Q. Zhang, R. Zhang, W. Zhang, Y. Zhang, J. Zhao, C. Zhou, L. Zhou, T. Ziesmann, S. Zou, Y. Li, X. Xu, Y. Zhang, H. Yang, J. Wang, J. Wang, K. M. Kjer, et al. 2014. Phylogenomics resolves the timing and pattern of insect evolution. Science 346: 763-767.

O'Reilly, A. O., B. P. S. Khambay, M. S. Williamson, L. A. Field, B. A. Wallace, and T. G. E. Davies. 2006. Modelling insecticide-binding sites in the voltage-gated sodium channel. Biochem. J. 396: 255-263.

Payandeh, J., T. Scheuer, N. Zheng, and W. A. Catterall. 2011. The crystal structure of a voltage-gated sodium channel. Nature 475: 353-359.

Rinkevich, F. D., R. L. Hamm, C. J. Geden, and J. G. Scott. 2007. Dynamics of insecticide resistance alleles in two different climates over an entire field season. Insect Biochem. Mol. Biol. 37: 550-558.

Rinkevich, F. D., C. A. Leichter, T. A. Lazo, M. C. Hardstone, and J. G. Scott. 2013. Variable fitness costs for pyrethroid resistance alleles in the house fly, *Musca domestica*, in the absence of insecticide pressure. Pestic. Biochem. Physiol. 105: 161-168.

Rinkevich, F. D., C. Su, T. A. Lazo, D. J. Hawthorne, W. M. Tingey, S. Naimov, and J. G. Scott. 2012. Multiple evolutionary origins of knockdown resistance (*kdr*) in pyrethroid-resistant Colorado potato beetle, *Leptinotarsa decemlineata*. Pestic. Biochem. Physiol. 104: 192-200.

Schmidt, J. M., P. Battlay, R. S. Gledhill-Smith, R. T. Good, C. Lumb, A. Fournier-Level, and C. Robin. 2017. Insights into DDT resistance from the *Drosophila melanogaster* genetic reference panel. Genetics 207: 1181-1193.

Scott, J. G. 2019. Life and death at the voltage-sensitive sodium channel: Evolution in response to insecticide use. Ann. Rev. Entomol. 64: 243-257.

Smith, L. B., S. Kasai, and J. G. Scott. 2016. Pyrethroid resistance in *Aedes aegypti* and *Aedes albopictus*: important mosquito vectors of human diseases. Pestic. Biochem. Physiol. 133: 1-12.

Song, W., Z. Liu, J. Tan, Y. Nomura, and K. Dong. 2004. RNA editing generates tissue-specific sodium channels with distinct gating properties. J. Biol. Chem. 279: 32554-32561.

Stothard, P. 2000. The Sequence Manipulation Suite: JavaScript programs for analyzing and formatting protein and DNA sequences. Biotechniques 28: 1102-1104.

Sun, H., S. Kasai, and J. G. Scott. 2017. Two novel house fly *Vssc* mutations, D600N and T929I, give rise to new insecticide resistance alleles. Pestic. Biochem. Physiol. 143: 116-121.

Sun, H., K. P. Tong, S. Kasai, and J. G. Scott. 2016. Overcoming *super-kdr* mediated resistance: Multi-halogenated benzyl pyrethroids are more toxic to *super-kdr* than *kdr* house flies. Insect Mol. Biol. 25: 126-137.

Sun, Y.-M., I. Favre, L. Schild, and E. Moczydlowski. 1997. On the structural basis for size-selective permeation of organic cations through the voltage-gated sodium channel effect of alanine mutations at the DEKA locus on selectivity, inhibition by Ca^{+2} and H^{+}, and molecular sieving. J. Gen. Physiol. 110: 693-715.

Tan, J., Z. Liu, T.-D. Tsai, S. M. Valles, A. L. Goldin, and K. Dong. 2002. Novel sodium channel gene mutations in *Blattella germanica* reduce the sensitivity of expressed channels to deltamethrin. Insect Biochem. Molec. Biol. 32: 445-454.

Terlau, H., S. H. Heinemann, W. Stühmer, M. Pusch, F. Conti, K. Imoto, and S. Numa. 1991. Mapping the site of block by tetrodotoxin and saxitoxin of sodium channel II. FEBS Letters 293: 93-96.

Thackeray, J. R., and B. Granetzky. 1994. Developmentally regulated alternative splicing generates a complex array of *Drosophila para* sodium channel isoforms. J. Neurosci. 14: 2569–2578.

Thackeray, J. R., and B. Ganetzky. 1995. Conserved alternative splicing patterns and splicing signals in the gene *para*. Genetics 141: 203-214.

Usherwood, P. N. R., T. G. E. Davies, I. R. Mellor, A. O. O'Reilly, F. Peng, H. Vais, B. P. S. Khambay, L. M. Field, and M. S. Williamson. 2007. Mutations in DIIS5 and the DIIS4-S5 linker of *Drosophila melanoaster* sodium channel define binding domains for pyrethroids and DDT. FEBS Lett. 581: 5485-5492.

Vora, T., B. Corry, and S.-H. Chung. 2005. A model of sodium channels. Biochim Biophys Acta 1668: 106-116.

Weill, M., A. Berthomieu, C. Berticat, G. Lutfalla, V. Negre, N. Pasteur, A. Philips, J.-P. Leonetti, P. Fort, and M. Raymond. 2004. Insecticide resistance: a silent base prediction. Current-Biology 14: R552-R553.

West, J. W., D. E. Patton, T. Scheuer, Y. Wang, A. L. Goldin, and W. A. Catterall. 1992. A cluster of hydrophobic amino acid residues required for fast Na^+-channel inactivation. P. Natl. Acad. Sci. USA 89: 10910-10914.

Yu, F. H., V. Yarov-Yarovoy, G. A. Gutman, and W. A. Catterall. 2005. Overview of molecular relationships in the voltage-gated ion channel superfamily. Pharmacol. Rev. 57: 387-395.

Zakon, H. H. 2012. Adaptive evolution of voltage-gated sodium channels: The first 800 million years. P. Natl. Acad. Sci. USA 109: 10619-10625.

Zuo, Y., X. Peng, K. Wang, F. Lin, Y. Li, and M. Chen. 2016. Expression patterns, mutation detection and RNA interference of *Rhopalosiphum padi* voltage-gated sodium channel genes. Sci. Rep. 6: 30166 |.

2.5 Supplementary materials

Table S1. List of 71 species of arthropods used in this study.

Order	Organism	Mutually exclusive, optional and alternative 5' or 3' splice site exons^								
		a	**l**	**b**	**c**	**k**	**i**	**j**	**h**	**d**
Calanoida	***Eurytemora affinis***	X	X	X	X					
Siphonostomatoida	***Lepeophtheirus salmonis***	X	X	X	X					
Diplura	***Catajapyx aquilonaris***	X	X	X	X	X	X			
Odonata	***Calopteryx splendens***	X	X	X	X	X	X	X		
Ephemeroptera	***Ephemera danica***	X	X	X	X	X	X	X		
Orthoptera	***Laupala kohalensis***	X	X	X	X	X	X	X		
Blattodea	***Periplaneta americana***	X	X	X	X	X	X	X	X	
	Blattella germanica	X	X	X	X	X	X	X	X	
	Zootermopsis nevadensis	X	X	X	X	X	X	X	X	
Thysanoptera	***Frankliniella occidentalis***	X	X	X		X	X	X	X	X
Hemiptera	***Halyomorpha halys***	X	X	X	X	X	X	X	X	
	Bemisia tabaci	X	X	X	X	X	X	X	X	
	Acyrthosiphon pisum	X	X	X	X	X	X	X	X	
	Cimex lectularius	X	X	X	X	X	X	X	X	
	Nilaparvata lugens	X	X	X	X	X	X	X	X	
	Oncopeltus fasciatus	X	X	X	X	X	X	X	X	
	Rhodnius prolixus	X	X	X	X	X	X	X	X	
Hymenoptera	***Apis mellifera***	X	X	X	X	X	X	X	X	
	Ceratosolen solmsi	X	X	X	X	X	*X*	X	X	
	Diachasma alloeum	X	X	X	X	X	X	X	X	
	Cephus cinctus	X	X	X	X	X	X	X	X	
	Neodiprion lecontei	X	X	X	X	X	X	X	X	
	Copidosoma floridanum	X	X	X	X	X	X	X	X	
	Camponotus floridanus	X	X	X	X	X	X	X	X	
	Linepithema humile	X	X	X	X	X	X	X	X	
	Dufourea novaeangliae	X	X	X	X	X	X	X	X	
	Megachile rotundata	X	X	X	X	X	X	X	X	
	Orussus abietinus	X	X	X	X	X	X	X	X	
	Nasonia longicornis	X	X	X	X	X	X	X	X	
	Athalia rosae	X	X	X	X	X	X	X	X	
	Trichogramma pretiosum	X	X	X	X	X	X	X	X	
	Polistes dominula	X	X	X	X	X	X	X	X	
Coleoptera	***Anoplophora glabripennis***	X	X	X			X	X	X	X
	Pogonus chalceus	X	X	X			X	X	X	X
	Agrilus planipennis	X	X	X			X	X	X	X
	Dendroctonus ponderosae	X	X	X			X	X	X	X
	Aethina tumida	X	X	X			X	X	X	X
	Onthophagus taurus	X	X	X			*X*	X	X	X
	Oryctes borbonicus	X	X	X			X	X	X	X
	Nicrophorus vespilloides	X	X	X			*X*	X	X	X
	Tribolium castaneum	X	X	X			X	X	X	X

Table S1. Continuation.

Order	**Organism**	Mutually exclusive, optional and alternative 5’ or 3’ splice site exons^								
		a	**l**	**b**	**c**	**k**	**i**	**j**	**h**	**d**
	Helicoverpa zea	X	X	X	X	X	X	X	X	X
	Bombyx mori	X	X	X	X	X	X	X	X	X
	Operophtera brumata	X	X	X	X	X	X	X	X	X
	Calycopis cecrops	X	X	X	X	X	X	X	X	X
	Spodoptera frugiperda	X	X	X	X	X	X	X	X	X
	Heliothis virescens	X	X	X	X	X	X	X	X	X
	Danaus plexippus	X	X	X	X	X	X	X	X	X
	Papilio machaon	X	X	X	X	X	X	X	X	X
	Leptidea sinapis	X	X	X	X	X	X	X	X	X
	Phoebis sennae	X	X	X	X	X	X	X	X	X
	Plodia interpunctella	X	X	X	X	X	X	X	X	X
	Amyelois transitella	X	X	X	X	X	X	X	X	X
	Calephelis nemesis	X	X	X	X	X	X	X	X	X
	Manduca sexta	X	X	X	X	X	X	X	X	X
Diptera	***Teleopsis dalmanni***	X	X	X	X	X	X	X	X	X
	Lucilia cuprina	X	X	X	X	X	X	X	X	X
	Belgica antarctica	X	X	X	X	X	X	X	X	X
	Anopheles gambiae	X	X	X	X	X	X	X	X	X
	Aedes aegypti	X	X	X	X	X	X	X	X	X
	Culex quinquefasciatus	X	X	X	X	X	X	X	X	X
	Drosophila melanogaster	X	X	X	X	X	X	X	X	X
	Glossina pallidipes	X	X	X	X	X	X	X	X	X
	Glossina austeni	X	X	X	X		X	X	X	X
	Glossina fuscipes	X	X	X	X		X	X	X	
	Glossina brevipalpis	X	X	X	X	X	X	X	X	X
	Musca domestica	X	X	X	X	X	X	X	X	X
	Stomoxys calcitrans	X	X	X	X	X	*X*	X	X	X
	Lutzomyia longipalpis	X	X	X	X	X	X	X	X	X
	Coboldia fuscipes	X	X	X		X	*X*	X	X	X
	Bactrocera dorsalis	X	X	X	X	X	X	X	X	X

^ Exons c/d and k/l are mutually exclusive, exons a and j are optional and exons b, h and i are alternative 5’ or 3’ splice site.

*Species selected to represent an Order are in bold.

Gray boxes indicate exon absent and boxes with an X inside indicate exon presence.

Table S2. Full-length cDNA and automated sequences from NCBI used for validation of the *in silico* sequences collected in this study.

Order	Species	Sequence predicted from NCBI or cDNA	Accession number (GenBank)	Accession number from NCBI	Agree/Disagree with predicted exon structure	Agree/Disagree with predicted AA of voltage gating regions
Blattodea	*Blattella germanica*	cDNA	AAC47484.1	2366*	Agree	Agree
		cDNA	U73583.1			Agree
Hemiptera	*Halyomorpha halys*	automated	XP_024214521.1	NW_014467146.1	Agree	Agree
	Cimex lectularius	cDNA	FJ031997.1	NW_014465016.1	Agree	Agree
	Nilaparvata lugens	automated	XP_022195780.1	NW_019106694.1	Agree	Agree
Hymenoptera	*Apis mellifera*	automated	XM_006561527.2	NW_003377999.1	Agree	Agree
	Diachasma alloeum	automated	XP_015109206.1	NW_015145028.1	Agree	Agree
	Dufourea novaeangliae	automated	XM_015580858.1	NW_015374150.1	Agree	Agree
Coleoptera	*Agrilus planipennis*	automated	XP_018330935.1	NW_017259880.1	Agree	Agree
	Dendroctonus ponderosae	automated	XP_019765194.1	NW_017852166.1	Agree	Agree
	Aethina tumida	automated	XP_019866360.1	NW_017853006.1	Agree	Agree
	Onthophagus taurus	automated	XP_022915619.1	NW_019286126.1	Agree	Agree
	Tribolium castaneum	cDNA	GQ202025.1	GCF_000002335.3	Agree	Agree
Lepidoptera	*Bombyx mori*	cDNA	EU822499.1	NP_001136084.1	Agree	Agree
	Spodoptera frugiperda	cDNA	*S. exigua* (MF461351.1)	NJHR01000040.1	Agree	Agree
	Papilio Machaon	automated	XM_014501979.1	NW_014506857.1	Agree	Agree
Diptera	*Anopheles gambiae*	cDNA	CAM12801.1	NT_078265.2	Agree	Agree
	Aedes aegypti	cDNA	ACB37024.1	CM008045.1	Agree	Agree
		cDNA	BAP46858.1			Agree
		automated	XP_021708042.1			Agree
	Culex quinquefasciatus	cDNA	AB453977.1	NW_001886882.1	Agree	Agree
		cDNA	BAI77917.1			Agree
		cDNA	JX424548.1			Agree
	Drosophila melanogaster	cDNA	NP_001188635.1	FBgn0264255	Agree	Agree
		cDNA	NP_001188647.1			Agree
		cDNA	NP_001285332.1			Agree
		cDNA	P35500.3			Agree
	Musca domestica	cDNA	X96668.1	MDOA002080	Agree	Agree
		cDNA	KT897924.1			Agree
		cDNA	KT289928.1			Agree
		cDNA	KT289929.1			Agree
	Bactrocera dorsalis	automated	*B. oleae* (XP_014089682.1)	NW_011876389.1	Agree	Agree

*The genome sequence from *B. germanica* was collected from i5k database.

Table S3. Sequence alignment of the selectivity filter across 68 insect species. Residues of the inner (DEKA) and outer (EEQD) rings are colored in red and blue, respectively. Highlighted strains and sequences have exceptions to the conserved sequences.

Species	Domain I	Domain II	Domain III	Domain IV
Calopteryx splendens	AFRLMTQDYWENLYQ	FRVLCGEWIESMWDC	FQVATFKGWIQIMND	LFQMSTSAGWDGVLD
Ephemera danica	AFRLMTQDYWENLYQ	FRVLCGEWIESMWDC	FQVATFKGWIQIMND	LFQMSTSAGWDGVLD
Laupala kohalensis	AFRLMTQDYWENLYQ	FRVLCGEWIESMWDC	FQVATFKGWIQIMND	LFQMSTSAGWDGVLD
Blattella germanica	AFRLMTQDYWENLYQ	FRVLCGEWIESMWDC	FQVATFKGWIQIMND	LFQMSTSAGWDGVLD
Periplaneta americana	AFRLMTQDYWENLYQ	FRVLCGEWIESMWDC	FQVATFKGWIQIMND	LFQMSTSAGWDGVLD
Zootermopsis nevadensis	AFRLMTQDYWENLYQ	FRVLCGEWIESMWDC	FQVATFKGWIQIMND	LFQMSTSAGWDGVLD
Bemisia tabaci	AFRLMTQDYWESLYQ	FRVLCGEWIESMWDC	FQVATFKGWIQIMND	LFQISTSAGWDGVLD
Acyrthosiphon pisum	AFRLMTQDNWEALYQ	FRVLCGEWIESMWDC	FQVATFNGWMEIMRD	LFMLSTSSGWDAVLD
Cimex lectularius	AFRLMTQDYWENLYQ	FRVLCGEWIESMWDC	FQVATFKGWIPIMND	LFQMSTSAGWDGVLD
Nilaparvata lugens	AFRLMTQDYWENLYQ	FRVLCGEWIESMWDC	FQVATFKGWIQIMND	LFQMSTSAGWDGVLD
Oncopeltus fasciatus	KLGQNTQDTYIHLYQ	FRVLCGEWIESMWDC	FQVATFKGWIQIMND	LFQMSTSAGWDGVLD
Halyomorpha halys	AFRLMTQDYWENLYQ	FRVLCGEWIESMWDC	FQVATFKGWIPIMND	LFQMSTSAGWDGVLD
Rhodnius prolixus	AFRLMTQDYWENLYQ	FRVLCGEWIESMWDC	FQVATFKGWIQIMND	LFQMSTSAGWDSVLD
Frankliniella occidentalis	AFRLMTQDYWENLYQ	FRVLCGEWIESMWDC	FQVATFKGWIQIMND	LFQMSTSAGWDGVLD
Agrilus planipennis	AFRLMTQDYWENLYQ	FRVLCGEWIESMWDC	FQVATFKGWIQIMND	LFQMSTSAGWDGVLD
Pogonus chalceus	AFRLMTQDYWENLYQ	FRVLCGEWIESMWDC	FQVATFKGWIQIMND	LFQMSTSAGWDGVLD
Anoplophora glabripennis	AFRLMTQDYWENLYQ	FRVLCGEWIESMWDC	FQVATFKGWIQIMND	LFQMSTSAGWDGVLD
Dendroctonus ponderosae	AFRLMTQDYWENLYQ	FRVLCGEWIESMWDC	FQVATFKGWIQIMND	LFQMSTSAGWDGVLD
Aethina tumida	AFRLMTQDYWENLYQ	FRVLCGEWIESMWDC	FQVATFKGWIQIMND	LFQMSTSAGWDGVLD
Onthophagus taurus	AFRLMTQDYWENLYQ	FRVLCGEWIESMWDC	FQVATFKGWIQIMND	LFQMSTSAGWDGVLD
Oryctes borbonicus	AFRLMTQDYWENLYQ	FRVLCGEWIESMWDC	FQVATFKGWIQIMND	LFQMSTSAGWDGVLD
Nicrophorus vespilloides	AFRLMTQDYWENLYQ	FRVLCGEWIESMWDC	FQVATFKGWIQIMND	LFQMSTSAGWDGVLD
Tribolium castaneum	AFRLMTQDYWENLYQ	FRVLCGEWIESMWDC	FQVATFKGWIQIMND	LFQMSTSAGWDGVLD
Ceratosolen solmsi	AFRLMTQDYWENLYQ	FRVLCGEWIESMWDC	FQVATFKGWIQIMND	LFQMSTSAGWDGVLD
Apis mellifera	AFRLMTQDYWENLYQ	FRVLCGEWIESMWDC	FQVATFKGWIQIMND	LFQMSTSAGWDGVLD
Diachasma alloeum	AFRLMTQDYWENLYQ	FRVLCGEWIESMWDC	FQVATFKGWIQIMND	LFQMSTSAGWDGVLD
Cephus cinctus	AFRLMTQDYWENLYQ	FRVLCGEWIESMWDC	FQVATFKGWIQIMND	LFQMSTSAGWDGVLD
Neodiprion lecontei	AFRLMTQDYWENLYQ	FRVLCGEWIESMWDC	FQVATFKGWIQIMND	LFQMSTSAGWDGVLD
Copidosoma floridanum	AFRLMTQDYWENLYQ	FRVLCGEWIESMWDC	FQVATFKGWIQIMND	LFQMSTSAGWDGVLD
Camponotus floridanus	AFRLMTQDYWENLYQ	FRVLCGEWIESMWDC	FQVATFKGWIQIMND	LFQMSTSAGWDGVLD
Linepithema humile	AFRLMTQDYWENLYQ	FRVLCGEWIESMWDC	FQVATFKGWIQIMND	LFQMSTSAGWDSVLD
Dufourea novaeangliae	AFRLMTQDYWENLYQ	FRVLCGEWIESMWDC	----------ND	LFQMSTSAGWDGVLD
Megachile rotundata	AFRLMTQDYWENLYQ	FRVLCGEWIESMWDC	FQVATFKGWIQIMND	LFQMSTSAGWDGVLD
Orussus abietinus	AFRLMTQDYWENLYQ	FRVLCGEWIESMWDC	FQVATFKGWIQIMND	LFQMSTSAGWDGVLD
Nasonia longicornis	AFRLMTQDYWENLYQ	FRVLCGEWIESMWDC	FQVATFKGWIQIMND	LFQMSTSAGWDGVLD
Athalia rosae	AFRLMTQDYWENLYQ	FRVLCGEWIESMWDC	FQVATFKGWIQIMND	LFQMSTSAGWDGVLD
Trichogramma pretiosum	AFRLMTQDYWENLYQ	FRVLCGEWIESMWDC	FQVATFKGWIQIMND	LFQMSTSAGWDGVLD
Polistes dominula	AFRLMTQDYWENLYQ	FRVLCGEWIESMWDC	FQVATFKGWIQIMND	LFQMSTSAGWDGVLD
Bombyx mori	AFRLMTQDYWENLYQ	FRVLCGEWIESMWDC	FQVATFKGWIQIMND	LFQMSTSAGWDGVLD
Operophtera brumata	AFRLMTQDYWENLYQ	FRVLCGEWIESMWDC	FQVATFKGWIQIMND	LFQMSTSAGWDGVLD
Calycopis cecrops	AFRLMTQDYWENLYQ	FRVLCGEWIESMWDC	FQVATFKGWIQIMND	LFQMSTSAGWDGVLD
Spodoptera frugiperda	AFRLMTQDYWENLYQ	FRVLCGEWIESMWDC	FQVATFKGWIQIMND	LFQMSTSAGWDGVLD
Heliothis virescens	AFRLMTQDYWENLYQ	FRVLCGEWIESMWDC	FQVATFKGWIQIMND	LFQMSTSAGWDGVLD

Table S3. Continuation.

	Domain I	**Domain II**	**Domain III**	**Domain IV**
Helicoverpa zea	AFRLMTQDYWENLYQ	FRVLCGEWIESMWDC	FQVATFKGWIQIMND	LFQMSTSAGWDGVLD
Danaus plexippus	AFRLMTQDYWENLYQ	FRVLCGEWIESMWDC	FQVATFKGWIQIMND	------MSTSAGWDGVLD
Papilio machaon	AFRLMTQDYWENLYQ	FRVLCGEWIESMWDC	FQVATFKGWIQIMND	LFQMSTSAGWDGVLD
Leptidea sinapis	AFRLMTQDYWENLYQ	FRVLCGEWIESMWDC	FQVATFKGWIQIMND	LFQMSTSAGWDGVLD
Phoebis sennae	AFRLMTQDYWENLYQ	FRVLCGEWIESMWDC	FQVATFKGWIQIMND	LFQMSTSAGWDGVLD
Plodia interpunctella	AFRLMTQDYWENLYQ	FRVLCGEWIESMWDC	FQVATFKGWIQIMND	LFQMSTSAGWDGVLD
Amyelois transitella	AFRLMTQDYWENLYQ	FRVLCGEWIESMWDC	FQVATFKGWIQIMND	LFQMSTSAGWDGVLD
Calephelis nemesis	AFRLMTQDYWENLYQ	FRVLCGEWIESMWDC	FQVATFKGWIQIMND	LFQM--TSAGWNDVLE
Manduca sexta	AFRLMTQDYWENLYQ	FRVLCGEWIESMWDC	FQVATFKGWIQIMND	LFQMSTSAGWDGVLD
Lucilia cuprina	AFRLMTQDFWEDLYQ	FRVLCGEWIESMWDC	FQVATFKGWIQIMND	LFQMSTSAGWDGVLD
Belgica antarctica	AFRLMTQDYWENLYQ	FRVLCGEWIESMWDC	FQVATFKGWIQIMND	LFQMSTSAGWDGVLD
Anopheles gambiae	AFRLMTQDYWENLYQ	FRVLCGEWIESMWDC	FQVATFKGWIQIMND	LFQMSTSAGWDGVLD
Aedes aegypti	AFRLMTQDYWENLYQ	FRVLCGEWIESMWDC	FQVATFKGWIQIMND	LFQMSTSAGWDGVLD
Culex quinquefasciatus	AFRLMTQDYWENLYQ	FRVLCGEWIESMWDC	FQVATFKGWIQIMND	LFQMSTSAGWDGVLD
Teleopsis dalmanni	AFRLMTQDFWEDLYQ	FRVLCGEWIESMWDC	FQVATFKGWIQIMND	LFQMSTSAGWDGVLD
Drosophila melanogaster	AFRLMTQDFWEDLYQ	FRVLCGEWIESMWDC	FQVATFKGWIQIMND	LFQMSTSAGWDGVLD
Glossina pallidipes	AFRLMTQDFWEDLYQ	FRVLCGEWIESMWDC	FQVATFKGWIQIMND	LFQMSTSAGWDGVLD
Glossina austeni	AFRLMTQDFWEDLYQ	FRVLCGEWIESMWDC	FQVATFKGWIQIMND	LFQMSTSAGWDGVLD
Glossina fuscipes	AFRLMTQDFWEDLYQ	FRVLCGEWIESMWDC	FQVATFKGWIQIMND	LFQMSTSAGWDGVLD
Glossina brevipalpis	AFRLMTQDFWEDLYQ	FRVLCGEWIESMWDC	FQVATFKGWIQIMND	LFQMSTSAGWDGVLD
Musca domestica	AFRLMTQDFWEDLYQ	FRVLCGEWIESMWDC	FQVATFKGWIQIMND	LFQMSTSAGWDGVLD
Stomoxys calcitrans	AFRLMTQDFWEDLYQ	FRVLCGEWIESMWDC	FQVATFKGWIQIMND	LFQMSTSAGWDGVLD
Lutzomyia longipalpis	AFRLMTQDFWENLYQ	FRVLCGEWIESMWDC	FQVATFKGWIQIMND	LFQMSTSAGWDSVLD
Coboldia fuscipes	AFRLMTQDYWENLYQ	FRVLCGEWIESMWDC	FQVATFKGWIQIMND	LFQMSTSAGWDGVLD
Bactrocera dorsalis	AFRLMTQDFWEDLYQ	FRVLCGEWIESMWDC	FQVATFKGWIPIMND	LFQMSTSAGWDGVLD

Table S4. Sequence alignment of the voltage-sensors across 68 insect species (includes domains I and II). Positively charged residues are colored in red.

Species	Exons Voltage sensor (DI)	Exons Voltage sensor (DII)	
		Exon c	Exon d
Calopteryx splendens	LRTFRVLRALK	VLRSFRLLRVFKLAK	----------
Ephemera danica danica	LRTFRVLRALK	VLRSFRLLRVFKLAK	----------
Laupala kohalensis	LRTFRVLRALK	VLRSFRLLRVFKLAK	----------
Blattella germanica	LRTFRVLRALK	VLRSFRLLRVFKLAK	----------
Periplaneta americana	LRTFRVLRALK	VLRSFRLLRVFKLAK	----------
Zootermopsis nevadensis	LRTFRVLRALK	VLRSFRLLRVFKLAK	----------
Bemisia tabaci	LRTFRVLRALK	VLRSFRLLRVFKLAK	----------
Acyrthosiphon pisum	LRTFRVLRALK	VLRSFRLLRVFKLAK	----------
Cimex lectularius	LRTFRVLRALK	VLRSFRLLRVFKLAK	----------
Nilaparvata lugens	LRTFRVLRALK	VLRSFRLLRVFKLAK	----------
Oncopeltus fasciatus	LRTFRVLRALK	VLRSFRLLRVFKLAK	----------
Halyomorpha halys	LRTFRVLRALK	VLRSFRLLRVFKLAK	----------
Rhodnius prolixus	LRTFRVLRALK	VLRSFRLLRVFKLAK	----------
Frankliniella occidentalis	LRTFRVLRALK	----------	VLRSFRLLRVFKLAK
Agrilus planipennis	LRTFRVLRALK	----------	VLRSLRLLRVFKLAK
Pogonus chalceus	LRTFRVLRALK	----------	VLRSFRLLRVFKLAK
Anoplophora glabripennis	LRTFRVLRALK	----------	VLRSLRLLRVFKLAK
Dendroctonus ponderosae	LRTFRVLRALK	----------	VLRSFRLLRVFKLAK
Aethina tumida	LRTFRVLRALK	----------	VLRSFRLLRVFKLAK
Onthophagus taurus	LRTFRVLRALK	----------	VLRSFRLLRVFKLAK
Oryctes borbonicus	LRTFRVLRALK	----------	VLRSFRLLRVFKLAK
Nicrophorus vespilloides	LRTFRVLRALK	----------	VLRSFRLLRVFKLAK
Tribolium castaneum	LRTFRVLRALK	----------	VLRSFRLLRVFKLAK
Ceratosolen solmsi	LRTFRVLRALK	VLRSFRLLRVFKLAK	----------
Apis mellifera	LRTFRVLRALK	VLRSFRLLRVFKLAK	----------
Diachasma alloeum	LRTFRVLRALK	VLRSFRLLRVFKLAK	----------
Cephus cinctus	LRTFRVLRALK	VLRSFRLLRVFKLAK	----------
Neodiprion lecontei	LRTFRVLRALK	VLRSFRLLRVFKLAK	----------
Copidosoma floridanum	LRTFRVLRALK	VLRSFRLLRVFKLAK	----------
Camponotus floridanus	LRTFRVLRALK	VLRSFRLLRVFKLAK	----------
Linepithema humile	LRTFRVLRALK	VLRSFRLLRVFKLAK	----------
Dufourea novaeangliae	LRTFRVLRALK	VLRSFRLLRVFKLAK	----------
Megachile rotundata	LRTFRVLRALK	VLRSFRLLRVFKLAK	----------
Orussus abietinus	LRTFRVLRALK	VLRSFRLLRVFKLAK	----------
Nasonia longicornis	LRTFRVLRALK	VLRSFRLLRVFKLAK	----------
Athalia rosae	LRTFRVLRALK	VLRSFRLLRVFKLAK	----------
Trichogramma pretiosum	LRTFRVLRALK	VLRSFRLLRVFKLAK	----------
Polistes dominula	LRTFRVLRALK	VLRSFRLLRVFKLAK	----------
Bombyx mori	LRTFRVLRALK	VLRSFRLLRVFKLAK	VLRSFRLLRVFKLAK
Operophtera brumata	LRTFRVLRALK	VLRSFRLLRVFKLAK	VLRSFRLLRVFKLAK
Calycopis cecrops	LRTFRVLRALK	VLRSFRLLRVFKLAK	VLRSFRLLRVFKLAK
Spodoptera frugiperda	LRTFRVLRALK	VLRSFRLLRVFKLAK	VLRSLRLLRVFKLAK
Heliothis virescens	LRTFRVLRALK	VLRSFRLLRVFKLAK	VLRSFRLLRVFKLAK
Helicoverpa zea	LRTFRVLRALK	VLRSFRLLRVFKLAK	VLRSFRLLRVFKLAK
Danaus plexippus	LRTFRVLRALK	VLRSFRLLRVFKLAK	VLRSFRLLRVFKLAK
Papilio machaon	LRTFRVLRALK	VLRSFRLLRVFKLAK	VLRSFRLLRVFKLAK
Leptidea sinapis	LRTFRVLRALK	VLRSFRLLRVFKLAK	VLRSFRLLRVFKLAK
Phoebis sennae	LRTFRVLRALK	VLRSFRLLRVFKLAK	VLRSFRLLRVFKLAK
Plodia interpunctella	LRTFRVLRALK	VLRSFRLLRVFKLAK	VLRSFRLLRVFKLAK
Amyelois transitella	LRTFRVLRALK	VLRSFRLLRVFKLAK	VLRSFRLLRVFKLAK
Calephelis nemesis	LRTFRVLRALK	VLRSFRLLRVFKLAK	VLRSFRLLRVFKLAK
Manduca sexta	LRTFRVLRALK	VLRSFRLLRVFKLAK	VLRSFRLLRVFKLAK
Lucilia cuprina	LRTFRVLRALK	VLRSFRLLRVFKLAK	VLRSFRLLRVFKLAK

Table S4. Continued.

Species	Exons Voltage sensor (DI)	Exons Voltage sensor (DII)	
		Exon c	Exon d
Belgica antarctica	LRTFRVLRALK	VLRSFRLLRVFKLAKS	VLRSFRLLRVFKLAKS
Anopheles gambiae	LRTFRVLRALK	VLRSFRLLRVFKLAKS	VLRSFRLLRVFKLAKS
Aedes aegypti	LRTFRVLRALK	VLRSFRLLRVFKLAKS	VLRSFRLLRVFKLAKS
Culex quinquefasciatus	LRTFRVLRALK	VLRSFRLLRVFKLAKS	VLRSFRLLRVFKLAKS
Teleopsis dalmanni	LRTFRVLRALK	VLRSFRLLRVFKLAKS	VLRSFRLLRVFKLAKS
Drosophila melanogaster	LRTFRVLRALK	VLRSFRLLRVFKLAKS	VLRSFRLLRVFKLAKS
Glossina pallidipes	LRTFRVLRALK	VLRSFRLLRVFKLAKS	VLRSFRLLRVFKLAKS
Glossina austeni	LRTFRVLRALK	VLRSFRLLRVFKLAKS	VLRSFRLLRVFKLAKS
Glossina fuscipes	LRTFRVLRALK	VLRSFRLLRVFKLAKS	----------
Glossina brevipalpis	LRTFRVLRALK	VLRSFRLLRVFKLAKS	VLRSFRLLRVFKLAKS
Musca domestica	LRTFRVLRALK	VLRSFRLLRVFKLAKS	VLRSFRLLRVFKLAKS
Stomoxys calcitrans	LRTFRVLRALK	VLRSFRLLRVFKLAKS	VLRSFRLLRVFKLAKS
Lutzomyia longipalpis	LRTFRVLRALK	VLRSFRLLRVFKLAKS	VLRSFRLLRVFKLAKS
Coboldia fuscipes	LRTFRVLRALK	----------	VLRSFRLLRVFKLAKS
Bactrocera dorsalis	LRTFRVLRALK	VLRSFRLLRVFKLAKS	VLRSFRLLRVFKLAKS

Table S5. Sequence alignment of the voltage-sensors across 68 insect species (includes domains III and IV). Positively charged residues are colored in red.

Species	Exons Voltage sensor (DIII)		Exons Voltage sensor (DIV)
	Exon k	Exon l	
Ephemera danica	AFRSMRTLRALRPLRAVSR WE	AFKTMRTLRALRPLRAMSR MQ	LLRVVRVAKVGRVLRLVKGAKGIR TLL
Calopteryx splendens	AFRSMRTLRALRPLRAVSR WE	AFKTMRTLRALRPLRAMSR MQ	LLRVVRVAKVGRVLRLVKGAKGIR TLL
Laupala kohalensis	AFRSMRTLRALRPLRAVSR WE	AFKTMRTLRALRPLRALSR MQ	LLRVVRVAKVGRVLRLVKGAKGIR TLL
Blattella germanica	AFRSMRTLRALRPLRAVSR WE	AFKTMRTLRALRPLRAMSR MQ	LLRVVRVAKVGRVLRLVKGAKGIR TLL
Periplaneta americana	AFRSMRTLRALRPLRAVSR WE	AFKTMRTLRALRPLRAMSR MQ	LLRVVRVAKVGRVLRLVKGAKGIR TLL
Zootermopsis nevadensis	AFRSMRTLRALRPLRAVSR WE	AFKTMRTLRALRPLRAMSR MQ	LLRVVRVAKVGRVLRLVKGAKGIR TLL
Bemisia tabaci	AFRSMRTLRALRPLRAVSR WE	----------	LLRVVRVAKVGRVLRLVKGAKGIR TLL
Acyrthosiphon pisum	AFRSMRTLRALRPLRAVSR WE	AFKTMRTLRALRPLRAMSR MQ	LLRVVRVAKVGRVLRLVKGAKGIR TLL
Cimex lectularius	AFRSMRTLRALRPLRAVSR WE	AFKTMRTLRALRPLRAMSR MQ	LLRVVRVAKVGRVLRLVKGAKGIR TLL
Nilaparvata lugens	AFRAMRTLRALRPLRAVSR WE	AFKTMRTLRALRPLRAMSR MQ	LLRVVRVAKVGRVLRLVKGAKGIR TLL
Oncopeltus fasciatus	AFRSMRTLRALRPLRAVSR WE	AFKTMRTLRALRPLRAMSR MQ	LLRVVRVAKVGRVLRLVKGAKGIR TLL
Halyomorpha halys	AFRSMRTLRALRPLRAVSR WE	AFKTMRTLRALRPLRAMSR MQ	LLRVVRVAKVGRVLRLVKGAKGIR TLL
Rhodnius prolixus	AFRSMRTLRALRPLRAVSR WE	AFKTMRTLRALRPLRAMSR MQ	LLRVVRVAKVGRVLRLVKGAKGIR TLL
Frankliniella	AFRSMRTLRALRPLRAVSR WE	AFKTMRTLRALRPLRAMSR MQ	LLRVVRVAKVGRVLRLVKGAKGIR TLL
Agrilus planipennis	----------	AFKTMRTLRALRPLRAMSR MQ	LLRVVRVAKVGRVLRLVKGAKGIR TLL
Pogonus chalceus	----------	AFKTMRTLRALRPLRAMSR MQ	LLRVVRVAKVGRVLRLVKGAKGIR TLL
Anoplophora	----------	AFKTMRTLRALRPLRAMSR MQ	LLRVVRVAKVGRVLRLVKGAKGIR TLL
Dendroctonus	----------	AFKTMRTLRALRPLRAMSR MQ	LLRVVRVAKVGRVLRLVKGAKGIR TLL
Aethina tumida	----------	AFKTMRTLRALRPLRAMSR MQ	LLRVVRVAKVGRVLRLVKGAKGIR TLL
Onthophagus taurus	----------	AFKTMRTLRALRPLRAMSR MQ	LLRVVRVAKVGRVLRLVKGAKGIR TLL
Oryctes borbonicus	----------	AFKTMRTLRALRPLRALSR MQ	LLRVVRVAKVGRVLRLVKGAKGIR TLL
Nicrophorus vespilloides	----------	AFKTMRTLRALRPLRAMSR MQ	LLRVVRVAKVGRVLRLVKGAKGIR TLL
Tribolium castaneum	----------	AFKTMRTLRALRPLRAMSR MQ	LLRVVRVAKVGRVLRLVKGAKGIR TLL
Ceratosolen solmsi	AFRSMRTLRALRPLRGVSR WE	AFKTMRTLRALRPLRAMSR MQ	LLRVVRVAKVGRVLRLVKGAKGIR TLL
Apis mellifera	AFRSMRTLRALRPLRAVSR WE	AFKTMRTLRALRPLRAMSR MQ	LLRVVRVAKVGRVLRLVKGAKGIR TLL
Diachasma alloeum	AFRSMRTLRALRPLRAVSR WE	AFKTMRTLRALRPLRAMSR MQ	LLRVVRVAKVGRVLRLVKGAKGIR TLL
Cephus cinctus	AFRSMRTLRALRPLRAVSR WE	AFKTMRTLRALRPLRAMSR MQ	LLRVVRVAKVGRVLRLVKGAKGIR TLL
Neodiprion lecontei	AFRSMRTLRALRPLRAVSR WE	AFKTMRTLRALRPLRAMSR MQ	LLRVVRVAKVGRVLRLVKGAKGIR TLL
Copidosoma floridanum	AFRSMRTLRALRPLRGVSR WE	AFKTMRTLRALRPLRAMSR MQ	LLRVVRVAKVGRVLRLVKGAKGIR TLL
Camponotus floridanus	AFRSMRTLRALRPLRAVSR WE	AFKTMRTLRALRPLRAMSR MQ	LLRVVRVAKVGRVLRLVKGAKGIR TLL
Linepithema humile	AFRSMRTLRALRPLRAVSR WE	AFKTMRTLRALRPLRAMSR MQ	LLRVVRVAKVGRVLRLVKGAKGIR TLL
Dufourea novaeanglia	AFRSMRTLRALRPLRAVSR WE	AFKTMRTLRALRPLRAMSR MQ	LLRVVRVAKVGRVLRLVKGAKGIR TLL
Megachile rotundata	AFRSMRTLRALRPLRAVSR WE	AFKTMRTLRALRPLRAMSR MQ	LLRVVRVAKVGRVLRLVKGAKGIR TLL
Orussus abietinus	AFRSMRTLRALRPLRAVSR WE	AFKTMRTLRALRPLRAMSR MQ	LLRVVRVAKVGRVLRLVKGAKGIR TLL
Nasonia longicornis	AFRSMRTLRALRPLRGVSR WE	AFKTMRTLRALRPLRAMSR MQ	LLRVVRVAKVGRVLRLVKGAKGIR TLL

Table S5. Continued.

Species	**Exons Voltage sensor (DIII)**		
	Exon k	**Exon l**	**Exons Voltage sensor (DIV)**
Athalia rosae	AFRSMRTLRALRPLRAVS RWE	AFKTMRTLRALRPLRAMS RMQ	LLRVVRVAKVGRVLRLVKGAKGI RTLL
Trichogramma pretiosum	AFRSMRTLRALRPLRGVS RWE	AFKTMRTLRALRPLRAMS RMQ	LLRVVRVAKVGRVLRLVKGAKGI RTLL
Polistes dominula	AFRSMRTLRALRPLRAVS RWE	AFKTMRTLRALRPLRAMS RMQ	LLRVVRVAKVGRVLRLVKGAKGI RTLL
Bombyx mori	AFRSMRTLRALRPLRAVS RWE	AFKTMRTLRALRPLRAMS RMQ	LLRVVRVAKVGRVLRLVKGAKGI RTLL
Operophtera brumata	AFRSMRTLRALRPLRAVS RWE	AFKTMRTLRALRPLRAMS RMQ	LLRVVRVAKVGRVLRLVKGAKGI RTLL
Calycopis cecrops	AFRSMRTLRALRPLRAVS RWE	AFKTMRTLRALRPLRAMS RMQ	LLRVVRVAKVGRVLRLVKGAKGI RTLL
Spodoptera frugiperda	AFRSMRTLRALRPLRAVS RWE	AFKTMRTLRALRPLRAMS RMQ	LLRVVRVAKVGRVLRLVKGAKGI RTLL
Heliothis virescens	AFRSMRTLRALRPLRAVS RWE	AFKTMRTLRALRPLRAMS RMQ	LLRVVRVAKVGRVLRLVKGAKGI RTLL
Helicoverpa zea	AFRSMRTLRALRPLRAVS RWE	AFKTMRTLRALRPLRAMS RMQ	LLRVVRVAKVGRVLRLVKGAKGI RTLL
Danaus plexippus	AFRSMRTLRALRPLRAVS RWE	AFKTMRTLRALRPLRAMS RMQ	LLRVVRVAKVGRVLRLVKGAKGI RTLL
Papilio machaon	AFRSMRTLRALRPLRAVS RWE	AFKTMRTLRALRPLRAMS RMQ	LLRVVRVAKVGRVLRLVKGAKGI RTLL
Leptidea sinapis	AFRSMRTLRALRPLRAVS RWE	AFKTMRTLRALRPLRAMS RMQ	LLRVVRVAKVGRVLRLVKGAKGI RTLL
Phoebis sennae	AFRSMRTLRALRPLRAVS RWE	AFKTMRTLRALRPLRAMS RMQ	LLRVVRVAKVGRVLRLVKGAKGI RTLL
Plodia interpunctella	AFRSMRTLRALRPLRAVS RWE	AFKTMRTLRALRPLRAMS RMQ	LLRVVRVAKVGRVLRLVKGAKGI RTLL
Amyelois transitella	AFRSMRTLRALRPLRAVS RWE	AFKTMRTLRALRPLRAMS RMQ	LLRVVRVAKVGRVLRLVKGAKGI RTLL
Calephelis nemesis	AFRSMRTLRALRPLRAVS RWE	AFKTMRTLRALRPLRAMS RMQ	LLRVVRVAKVGRVLRLVKGAKGI RTLL
Manduca sexta	AFRSMRTLRALRPLRAVS RWE	AFKTMRTLRALRPLRAMS RMQ	LLRVVRVAKVGRVLRLVKGAKGI RTLL
Lucilia cuprina	AFRSMRTLRALRPLRAVS RWE	AFKTMRTLRALRPLRAMS RMQ	LLRVVRVAKVGRVLRLVKGAKGI RTLL
Belgica antarctica	AFRSMRTLRALRPLRAVS RWE	AFKTMRTLRALRPLRAMS RMQ	LLRVVRVAKVGRVLRLVKGAKGI RTLL
Anopheles gambiae	AFRSMRTLRALRPLRAVS RWE	AFKTMRTLRALRPLRAMS RMQ	LLRVVRVAKVGRVLRLVKGAKGI RTLL
Aedes aegypti	AFRSMRTLRALRPLRAVS RWE	AFKTMRTLRALRPLRAMS RMQ	LLRVVRVAKVGRVLRLVKGAKGI RTLL
Culex quinquefasciat	AFRSMRTLRALRPLRAVS RWE	AFKTMRTLRALRPLRAMS RMQ	LLRVVRVAKVGRVLRLVKGAKGI RTLL
Teleopsis dalmanni	AFRSMRTLRALRPLRAVS RWE	AFKTMRTLRALRPLRAMS RMQ	LLRVVRVAKVGRVLRLVKGAKGI RTLL
Drosophila melanogaster	AFRSMRTLRALRPLRAVS RWE	AFKTMRTLRALRPLRAMS RMQ	LLRVVRVAKVGRVLRLVKGAKGI RTLL
Glossina pallidipes	AFRSMRTLRALRPLRAVS RWE	AFKTMRTLRALRPLRAMS RMQ	LLRVVRVAKVGRVLRLVKGAKGI RTLL
Glossina austeni	----------	AFKTMRTLRALRPLRAMS RMQ	LLRVVRVAKVGRVLRLVKGAKGI RTLL
Glossina fuscipes	----------	AFKTMRTLRALRPLRAMS RMQ	LLRVVRVAKVGRVLRLVKGAKGI RTLL
Glossina brevipalpis	AFRSMRTLRALRPLRAVS RWE	AFKTMRTLRALRPLRAMS RMQ	LLRVVRVAKVGRVLRLVKGAKGI RTLL
Musca domestica	AFRSMRTLRALRPLRAVS RWE	AFKTMRTLRALRPLRAMS RMQ	LLRVVRVAKVGRVLRLVKGAKGI RTLL
Stomoxys calcitrans	AFRSMRTLRALRPLRAVS RWE	AFKTMRTLRALRPLRAMS RMQ	LLRVVRVAKVGRVLRLVKGAKGI RTLL
Lutzomyia longipalpis	AFRSMRTLRALRPLRAVS RWE	AFKTMRTLRALRPLRAMS RMQ	LLRVVRVAKVGRVLRLVKGAKGI RTLL
Coboldia fuscipes	AFRSMRTLRALRPLRAVS RWE	AFKTMRTLRALRPLRAMS RMQ	LLRVVRVAKVGRVLRLVKGAKGI RTLL
Bactrocera dorsalis	AFRSMRTLRALRPLRAVS RWE	AFKTMRTLRALRPLRAMS RMQ	LLRVVRVAKVGRVLRLVKGAKGI RTLL

Table S6. Sequence alignment of the inactivation loop across 68 species. Positively charged residues are colored in brown. Highlighted species are exceptions to the conserved MFM sequence.

	Inactivation loop
Species	**Sequence**
Calopteryx splendens	KKAGGSLE**MFM**TEDQ
Ephemera danica	KKAGGSLE**MFM**TDDQ
Laupala kohalensis	KKAGGSLE**MFM**TEDQ
Blattella germanica	KKAGGSLE**MFMT**EDQ
Periplaneta americana	KKAGGSLE**MFM**TEDQ
Zootermopsis nevadensis	KKAGGSLE**MFM**TEDQ
Bemisia tabaci	KKAGGSLE**MFM**TEDQ
Acyrthosiphon pisum	KKSGASLE**MFM**TEDQ
Cimex lectularius	KKAGGSLE**MFM**TEDQ
Nilaparvata lugens	KKAGGSLE**MFM**TEDQ
Oncopeltus fasciatus	KKAGGSLE**MFM**TEDQ
Halyomorpha halys	KKAGGSLE**MFM**TEDQ
Rhodnius prolixus	KKAGGSLE**MFM**TEDQ
Frankliniella occidentalis	KKAGGSLE**MFM**TEDQ
Agrilus planipennis	KKAGGSLE**MFM**TEDQ
Pogonus chalceus	KKAGGSLE**MFM**TEDQ
Anoplophora glabripennis	KKAGGSLE**MFM**TEDQ
Dendroctonus ponderosae	KKAGGSLE**MFM**TEDQ
Aethina tumida	KKAGGSLE**MFM**TEDQ
Onthophagus taurus	KKAGGSLE**MFM**TEDQ
Oryctes borbonicus	KKAGGSLE**LFM**TEDQ
Nicrophorus vespilloides	KKAGGSLE**MFM**TEDQ
Tribolium castaneum	KKGGDSLA**LMM**TDAQ
Ceratosolen solmsi	KKAGGSLE**MFM**TEDQ
Apis mellifera	KKAGGSLE**MFM**TEDQ
Diachasma alloeum	KKAGGSLE**MFM**TEDQ
Cephus cinctus	KKAGGSLE**MFM**TEDQ
Neodiprion lecontei	KKAGGSLE**MFM**TEDQ
Copidosoma floridanum	KKAGGSLE**MFM**TEDQ
Camponotus floridanus	KKAGGSLE**MFM**TEDQ
Linepithema humile	KKAGGSLE**MFM**TEDQ
Dufourea novaeangliae	KKAGGSLE**MFM**TEDQ
Megachile rotundata	KKAGGSLE**MFM**TEDQ
Orussus abietinus	KKAGGSLE**MFM**TEDQ
Nasonia longicornis	KKAGGSLE**MFM**TEDQ
Athalia rosae	KKAGGSLE**MFM**TEDQ
Trichogramma pretiosum	KKAGGSLE**MFM**TEDQ
Polistes dominula	KKAGGSLE**MFM**TEDQ
Bombyx mori	KKAGGSLE**MFM**TEDQ
Operophtera brumata	KKAGGSLE**MFM**TEDQ
Calycopis cecrops	KKAGGSLE**MFM**TEDQ
Spodoptera frugiperda	KKAGGSLE**MFM**TEDQ
Heliothis virescens	KKAGGSLE**MFM**TEDQ
Helicoverpa zea	KKAGGSLE**MFM**TEDQ

Table S6. Continued.

Species	Inactivation loop Sequence
Danaus plexippus	KKAGGSLE**MFM**TEDQ
Papilio machaon	KKAGGSLE**MFM**TEDQ
Leptidea sinapis	KKAGGSLE**MFM**TEDQ
Phoebis sennae	KKAGGSLE**MFM**TEDQ
Plodia interpunctella	KKAGGSLE**MFM**TEDQ
Amyelois transitella	KKAGGSLE**MFM**TEDQ
Calephelis nemesis	KKAGGSLE**MFM**TEDQ
Manduca sexta	KKAGGSLE**MFM**TEDQ
Lucilia cuprina	KKAGGSLE**MFM**TEDQ
Belgica antarctica	KKAGGSLE**MFM**TDDQ
Anopheles gambiae	KKAGGSLE**MFM**TEDQ
Aedes aegypti	KKAGGSLE**MFM**TEDQ
Culex quinquefasciatus	KKAGGSLE**MFM**TEDQ
Teleopsis dalmanni	KKAGGSLE**MFM**TEDQ
Drosophila melanogaster	KKAGGSLE**MFM**TEDQ
Glossina pallidipes	KKAGGSLE**MFM**TEDQ
Glossina austeni	KKAGGSLE**MFM**TEDQ
Glossina fuscipes	KKAGGSLE**MFM**TEDQ
Glossina brevipalpis	KKAGGSLE**MFM**TEDQ
Musca domestica	KKAGGSLE**MFM**TEDQ
Stomoxys calcitrans	KKAGGSLE**MFM**TEDQ
Lutzomyia longipalpis	KKAGGSLE**MFM**TEDQ
Coboldia fuscipes	KKAGGSLE**MFM**TEDQ
Bactrocera dorsalis	KKAGGSLE**MFM**TEDQ

CHAPTER 3

LEVELS OF CROSS-RESISTANCE TO PYRETHROIDS CONFERRED BY THE *KNOCKDOWN RESISTANCE* ALLELE *410L+1016I+1534C* IN *AEDES AEGYPTI*[4]

Authors: Juan J. Silva, Cedric N. Kouam and Jeffrey G. Scott

Abstract

Aedes aegypti is a primary vector of viral pathogens and is responsible for millions of human infections annually that represent critical public health and economic costs. Pyrethroids are one of the most commonly used classes of insecticides to control adult *A. aegypti*. The insecticidal activity of pyrethroids depends on their ability to bind and disrupt the voltage-gated sodium channel (VGSC). In mosquitoes, a common mechanism of resistance to pyrethroids is due to mutations in *Vgsc (*hereafter referred as *knockdown resistance, kdr).* In this study, I found that a *kdr* (*410L+1016I+154C*) allele was the main mechanism of resistance in a pyrethroid-resistant strain of *A. aegypti* collected in Colombia. To characterize the level of resistance conferred by these mutations, a pyrethroid resistant strain (LMRKDR:RK, LKR) that was congenic to the susceptible Rockefeller (ROCK) strain was isolated. The full-length cDNA of *Vgsc* was cloned from LKR and no additional resistance mutations were present. The levels of resistance to different pyrethroids varied from 3.9- to 56-fold. The levels of resistance to pyrethroids, DCJW and DDT between LKR and two other congenic strains that share the same pyrethroid-susceptible background from ROCK strain, but carry different *kdr* alleles (*1534C* and *989P + 1016G*) were compared. The resistance conferred by *kdr* alleles can be dependent on the stereochemistry of the pyrethroids used. The validation of *kdr* mutations through heterologous expression does not reflect the role of *kdr* mutations *in vivo.* The *410L+1016I+1534C kdr* allele does not confer higher levels of resistance to many pyrethroids relative to the *1534C* allele. The importance of these results to understand the evolution of insecticide resistance and mosquito control are discussed.

[4] Published: *Silva, J. J.*, Kouam, C. N., Scott, J. G. July 2021. Levels of cross-resistance to pyrethroids conferred by the *Vssc knockdown resistance* allele *410L+1016I+1534C* in *Aedes aegypti.* PLoS Negl Trop Dis. 15(7): e0009549.

3.1 Introduction

Aedes aegypti is the primary vector of viral pathogens including chikungunya, dengue, yellow fever, and Zika and is responsible for millions of human infections annually that results in a critical threat for public health. Chikungunya has caused more than 440,000 cases of disease in more than 20 countries throughout the Americas (excluding North America) and the Caribbean by 2014 (Morrison 2014). According to the Global Burden of Disease Study 2013, dengue is estimated to cause approximately 58.4 million annual symptomatic cases resulting in 10,000 deaths per year (Shepard et al. 2016). Yellow fever is endemic to 47 countries and is responsible for 60,000 deaths annually (WHO 2014). Zika has been a public health problem due to its fast dispersion primarily in the Americas and the Caribbean (Gatherer and Kohl 2016, Baud et al. 2017). It is estimated that Zika virus infected 440,000 to 1,300,000 people in South America by 2016 (Plourde and Bloch 2016).

Pyrethroid insecticides are widely used to control adult *A. aegypti*, and the insecticidal activity of pyrethroids depends on their ability to disrupt the voltage-gated sodium channel (VGSC). Previous studies have characterized the importance of pyrethroid stereochemistry to insecticidal activity. These studies found differential toxicity between enantiomers (*R* or *S* conformations of the chiral carbons of the cyclopropane ring and α-cyano group) and diastereomers (*cis/trans* of the cyclopropane ring). Regarding the absolute configuration, the 1*R* conformation of the cyclopropane ring is generally more toxic than the 1*S* conformation (Nishimura and Narahashi 1978, Soderlund et al. 1983, Ford et al. 1989, Coats 1990). The *S* conformation of the *α*-cyano group (*αS*) usually has higher insecticidal activity than the *αR* conformation (Ford et al. 1989, Khambay and Jewess 2005). Regarding the geometric isomerism, contrasting results were obtained between chrysanthemate and tetrafluorobenzyl pyrethroids relative to phenoxybenzyl pyrethroids. In chrysanthemate (e.g. bioallethrin and bioresmethrin) and tetrafluorobenzyl pyrethroids (e.g. 1*R-trans* fenfluthrin, tefluthrin and transfluthrin), *trans* isomers are more toxic to insects than *cis*-isomers (Naumann 1998, Khambay and Jewess 2005). Regarding the *cis/trans* configuration of the cyclopropane ring, it was found that the *cis* isomers of phenoxybenzyl pyrethroids are usually more toxic to insects than *trans* isomers (Verschoyle and Aldridge 1980). Other patterns were found when both the absolute configuration and geometric isomerism were considered. It was found that 1*R-cis αS* phenoxybenzyl pyrethroids (e.g. deltamethrin) display higher insecticidal activity relative to the other conformations (e.g. 1*S-cis αS,* 1*R-trans αS,* etc.) (Nishimura and Narahashi 1978, Casida and Lawrence 1985).

In mosquitoes, a common mechanism of resistance to pyrethroids is target-site mutations in *Vgsc (*hereafter referred as *knockdown resistance* mutations or *kdr)*. The *kdr* mutations that have been found in *A. aegypti* are V410L, G923V, L982W, S989P, I1011V/M, V1016G/I, T1520I, F1534C and D1763Y (codon numbering based on *Musca domestica* VGSC, GenBank: CAA65448.1) (Williamson et al. 1996).

In addition, the following alleles have been found in *A. aegypti*: *410L+1534C* (Haddi et al. 2017), *410L+1016I+1534C* (Saavedra-Rodriguez et al. 2018), *989P+1016G* (Srisawat et al. 2010), *989P+1016G+1534C* (Kawada et al. 2014), *1520I+1534C* (Kushwah et al. 2015), *1011M+923V* (Brengues et al. 2003), *1016I+1534C* (Harris et al. 2010), and *1016G+1763Y)* (Chang et al. 2009). The two most common *kdr* alleles in Asia are *1534C* and *989P+1016G*, while the most common alleles in the Americas are *410L+1016I+1534C*, *410L+1534C* and *1534C* (Fan and Scott 2020). Previous studies using congenic strains found that the *989P+1016G* allele conferred 21- to 107-fold resistance to multiple pyrethroids (Smith et al. 2017). Another study found that *1534C* allele conferred only 7- to 16-fold resistance to pyrethroids (Fan and Scott 2020). Among *kdr* mutations and alleles, only a few have been confirmed to alter pyrethroid sensitivity based on heterologous expression in *Xenopus* oocytes (V410L, *1534C*, *V410+1534C*, *1016G*, *989P+1016G*, *989P+1016G+1534C*, I1011M and *1016G+1763Y* (Hirata et al. 2014, Du et al. 2016a, Haddi et al. 2017). A previous study using heterologous expression in *Xenopus* oocytes confirmed that *1016G+1763Y* alters the sensitivity of the VGSC in the presence of permethrin or deltamethrin, but D1763Y alone does not alter the sensitivity of VGSC. Another study confirmed that V1016I mutation does not alter permethrin or deltamethrin sensitivity in VGSC (Du et al. 2016a). Similarly, V1016I mutation has been associated with F1534C and it was hypothesized that this double mutation enhances pyrethroid resistance (Vera-Maloof et al. 2016).

In this study, I found that the major mechanism of resistance to pyrethroids in the LM-R strain of *A. aegypti* collected in Colombia was a *kdr* allele (*410L+1016I+1534C*). A strain that was congenic to the susceptible strain, but carried these *kdr* mutations (LMRKDR:RK, LKR) was isolated. The resistance levels in LKR to 19 insecticides that target the VGSC were measured and compared to those previously found for two other *kdr* alleles (*989P+1016G* and *1534C*), as well as what has been reported using heterologous expression in oocytes. The importance of these results to understanding the evolution of insecticide resistance and improving mosquito control is discussed.

3.2 Materials and methods

A. aegypti strains and rearing conditions

Four strains of *A. aegypti* were used in this study: Rockefeller (ROCK) is an insecticide susceptible strain, KDR:ROCK is a pyrethroid-resistant strain which is congenic to ROCK, but contains the *kdr* allele *989P+1016G* (Smith et al. 2017), 1534C:ROCK is a pyrethroid-resistant strain which is congenic to ROCK, but contains the *kdr* allele *1534C* (Fan and Scott 2020), and La Mesa (LM). The LM strain was from eggs that were collected in ovitraps according to the protocol of the World Health Organization (Reiter and Nathan 2001) in April 2016 in the town of La Mesa, Colombia (04° 38' 09" N, 74° 27' 59" W) and sent to Cornell University. The La Mesa (LM) strain was then selected with cyhalothrin for three consecutive generations (as described in the next section).

Mosquitoes were reared in cages (35 X 25 X 25 cm) with one Erlenmeyer flask containing 10% sugar water. Adult females were blood-fed using a membrane-covered water-jacketed glass feeder with cow blood (Owasco Meat Co Inc, Owasco NY) containing 0.3% sodium citrate to prevent clotting. Larvae were reared in containers (27.5 X 21.5 X 27.5 cm) with approximately 2 L of distilled water and fed with Cichlid Goldfish food pellets (Hikari Sales USA Inc., Hayward CA). Mosquitoes were reared at 27 ± 1°C and 50 – 60% relative humidity.

Selection of the LM-R strain

Adult mosquitoes that were 3-7-day old from the LM strain were selected over three consecutive generations. For each generation, an average of 2,790 unmated females and 1,164 males were treated with cyhalothrin. Mosquitoes were knocked down with CO_2 and placed in a paper cup on a bucket filled with ice to keep them anesthetized for approximately 10 minutes. Insecticide doses were applied topically to individual mosquitoes with a PB600-1 repeating dispenser and a 10 µL Hamilton syringe (Hamilton Company, Reno NV). The selection doses were designed to kill ~80% of the individuals. Following cyhalothrin applications, 40 mosquitoes were placed in a paper cup covered with nylon tulle and a cotton ball saturated with distilled water and held at 25˚C for 24 hours. Both male and unmated female survivors were released in cages and allowed to mate *en masse.* The resulting strain is referred as LM-R. This strain was tested for resistance due to enzyme-mediated detoxification (section Adult female bioassays) and used to obtain a congenic strain with the LM-R resistance alleles in a pyrethroid-susceptible background (section Isolation of the LMRKDR:RK strain).

Isolation of the LKR strain

To obtain the congenic LKR strain, unmated females of the susceptible ROCK strain were crossed with LM-R males and reared *en masse*. The F_1 males were backcrossed with ROCK unmated females. The male progeny were genotyped for the V1016I *kdr* mutation (see next section) and heterozygotes were backcrossed with ROCK unmated females. This process was repeated another four times (Fig. 1). Males and unmated females from the fifth backcross were genotyped. Heterozygotes were crossed *en masse*. The offspring from this cross were genotyped, and *kdr* homozygotes (30 males and 66 unmated females) were used to establish the new strain named LKR, which shares approximately 98.4% of its genomic background with ROCK. The genotype of individuals from the LKR strain were validated by Sanger sequencing of the three *kdr* mutations.

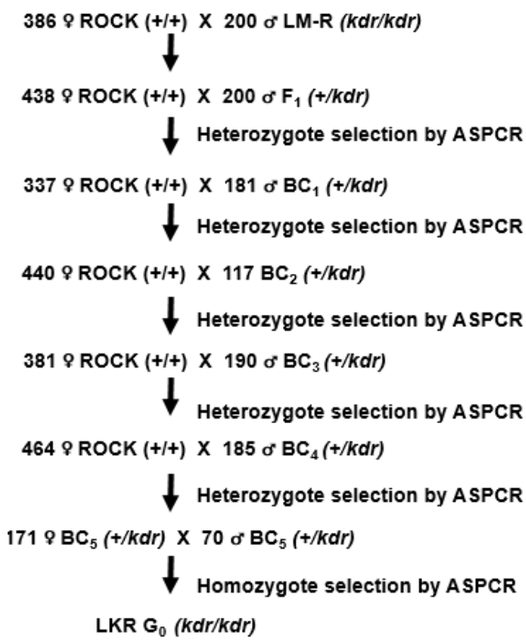

Figure 1. Protocol for the isolation of the congenic strain containing the *410L+1016I+1534C kdr* allele. Number of heterozygous (+/*kdr*) males included in each backcross varied depending on the number of females added to the cage (approximately half the number of females).

Genotyping using allele specific polymerase chain reaction (ASPCR)

The genomic DNA from the hind tarsi of mosquito males was extracted using an alkali extraction method (Smith et al. 2017). Legs were removed and placed into individual wells of a 96-well PCR plate (Bio-Rad, Hercules CA) with approximately three 2-3-mm diameter Zirconia/Silica beads (BioSpec Products, Bartlesville OK) and 10 µL of 0.2 M NaOH per well. Samples were vortexed for 1 minute to pulverize tissue and incubated at 70°C for 10 minutes. After incubation, 10 µL of neutralization buffer (360 mM Tris-HCl pH 8.0 and 10 mM EDTA) and 80 µL of nuclease-free water (VWR International,

Radnor PA) were added to each well. Each mosquito was stored individually (no longer than 24 hours) in a P5000 tip (Gilson Inc., Middleton WI) stoppered with Kimwipe paper balls saturated with 10% sugar water until genotype was determined and heterozygotes were released in a cage.

To determine the genotype for V1016I, two allele specific PCR (ASPCR) reactions with gDNA extracted from each adult mosquito were done. One PCR reaction contained a primer specific for the susceptible allele (F1-V) and a reverse primer (M2-Rev) that is not allele specific. The second PCR reaction contained a primer specific for the resistance allele (F1-I) and the M2-Rev reverse primer. The PCR conditions used were: 94 °C for 3 min, then 35 cycles of 94 °C for 30s, 60°C for 30 s and 72 °C for 1 min, followed by one cycle of 72 °C for 7 min (36 cycles of amplification were used for PCR with the F1-V primer). PCR products were evaluated on 1% agarose gels. Adult males were considered heterozygous if ASPCR products were amplified with both sets of allele specific primers or homozygous if PCR products were amplified in only one of the two ASPCR reactions mentioned above. The ASPCR primers for each PCR reaction was validated by using control DNA from ROCK, LKR and heterozygotes (genotype determined by sequencing).

RNA isolation, cDNA synthesis and sequencing of the full-length Vgsc cDNA sequences from LKR and ROCK

Total RNA was extracted from 10 unmated 3-to-7-day old female mosquitoes of the LKR and ROCK strains using TRIzol Reagent (Invitrogen, Carlsbad CA) according to manufacturer's instructions. Samples were treated with DNase I TURBO DNase (Life Technologies Co., Carlsbad CA). Total RNA concentration was determined using a NanoDrop 2000 (Thermo Fisher Scientific) and cDNA was synthesized using 5 µg of total RNA using the GoScript Reverse Transcription System (Promega, Madison WI) according to manufacturer's instructions.

To obtain the full-length cDNA of *Vgsc*, four overlapping pieces (also referred as op1-4) were amplified using PrimeStar GXL DNA high fidelity polymerase (Takara Bio Inc., Shiga, Japan) (Fig 2). For op1, L1F3 and R7 primers were used. For op2, 410-for and R5 primers were used. For op3, a PCR reaction was done using F2 and S3R primers and the products were used as templates for a nested PCR using F3 and S3R primers. For op4, a PCR reaction was done using F10 and S4R primers and the products were used as templates for a nested PCR using F11 and S4R primers. The overlap between op1-op2, op2-op3 and op3-op4 was approximately 393, 279 and 312 nucleotides, respectively. PCR reactions were done using Bio-Rad T100 Thermal Cycler (Bio-Rad, Hercules CA) under the following conditions: 95°C for 3 min, followed by 35 cycles of PCR (98°C for 10 s, 60°C for 15 s and 68°C for 4 min) and an extension at 68°C for 10 min. The PCR products from op2, op3 and op4 were gel excised from 1% agar

gel stained with ethidium bromide under UV light. PCR products were purified using the Promega Wizard SV Gel and PCR Clean-up System (Promega, Madison WI). Purified cDNA fragments were inserted in pGEM-T Easy Vector (Promega, Madison WI) according to manufacturer's instructions. Ligated plasmids were cloned into JM109 *Escherichia coli* competent cells (Promega, Madison WI). Transformed cells were grown on Luria Bertani plus ampicillin in agar plates and incubated at 37°C overnight. Confirmation of transformed colonies was assessed by PCR with primers T7 and SP6. PCR products were sequenced using primers R12, F9, S3R (Fig 2). Four clones of op2 and op3 from ROCK and LKR were sequenced. I had technical difficulties trying to clone op1, so instead the PCR products of op1 (from three independent reactions) were sequenced directly without cloning. Sequences were confirmed by multiple alignments using Clustal W in MegAlign Pro software (DNAStar).

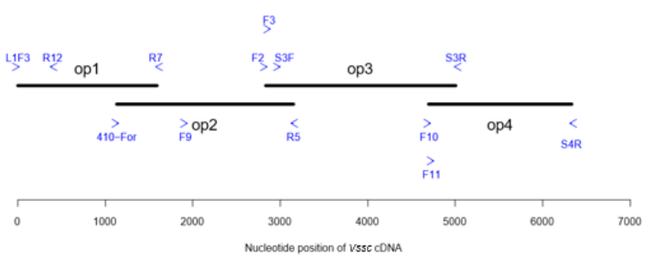

Primer name	Sequence (5' to 3')	Purpose
L1F3	AGACAATGACCGAAGACTCCGATTCG	PCR and sequencing
R12	GGAGATAATCCAAATTACGGG	Sequencing
R7	ACATCTTCTCCTTGTTGTTGTCG	PCR and sequencing
410-For	TATCTGCCTTTCGTCTAATGACCC	PCR
R5	CCAGTTGGAGAAGCGCGATATCCGATT	PCR
F9	CGGCATGACGAAGGAGAGC	Sequencing
F2	GACAATGTGGATCGCTTCCC	PCR
F3	GTGGAACTTCACCGACTTCA	PCR
S3F	TCCGTTCTTTTTGGCCACC	Sequencing
S3R	ACCTGTTCGATTTCGTCGTC	Sequencing
S4R	TCAGACATCCGCCGATCGTGAA	PCR
F10	TACAACGCCATGAAAAAGATGGGC	PCR
F11	TGAAAGCTATTCCACGGCCTAGG	PCR
T7	TAATACGACTCACTATAGGG	PCR and sequencing
SP6	ATTTAGGTGACACTATAG	PCR and sequencing

Figure 2. The *Vgsc* cDNA from the ROCK and LKR strains was obtained by PCR and cloning of four overlapping fragments. The overlapping pieces and relative position of primers (blue arrows) are shown in the diagram. List of primers, sequences and purposes are also included.

Insecticides

A total of 19 insecticides and three synergists were used (Fig 3): 1*R-cis αS* cypermethrin (100%, Roussel Uclaf), 1*R-trans* fenfluthrin (100%, Bayer CropScience, Leverkusen, Germany), *alpha*-cypermethrin (99.5%, Chem Service, West Chester, PA, USA), bioallethrin (3.8% *cis* and 95.7% *trans*, Chem Service), bioresmethrin (99.5%, Chem Service), *cis*-permethrin (99.4%, Zeneca Ag products), cyfluthrin (99.2%, Chem Service), cyhalothrin (90.2%, ICI Americas), cypermethrin (44.8% *cis* and 53.9% *trans*, Chem Service), DCJW (98%, DuPont), DDT (98%, Sigma-Aldrich, St. Louis, MO, USA), deltamethrin (99.5%, Chem Service), diethyl maleate (DEM) (97%, Sigma-Aldrich), etofenprox (96.3%, Mitsui Toatsu Chemicals, Tokyo Japan), flumethrin (100%, Bayer CropScience), permethrin (24% *cis* and 76% *trans*, Chem Service), piperonyl butoxide (PBO) (90%, Sigma-Aldrich), S,S,S-tributyl phosphorotrithioate (DEF) (97.3%, Chem Service), *tau*-fluvalinate (96%, Chem Service), tefluthrin (96%,

Sigma-Aldrich), transfluthrin (99.5%, Chem Service), *trans*-permethrin (99%, FMC, Philadelphia, PA, USA).

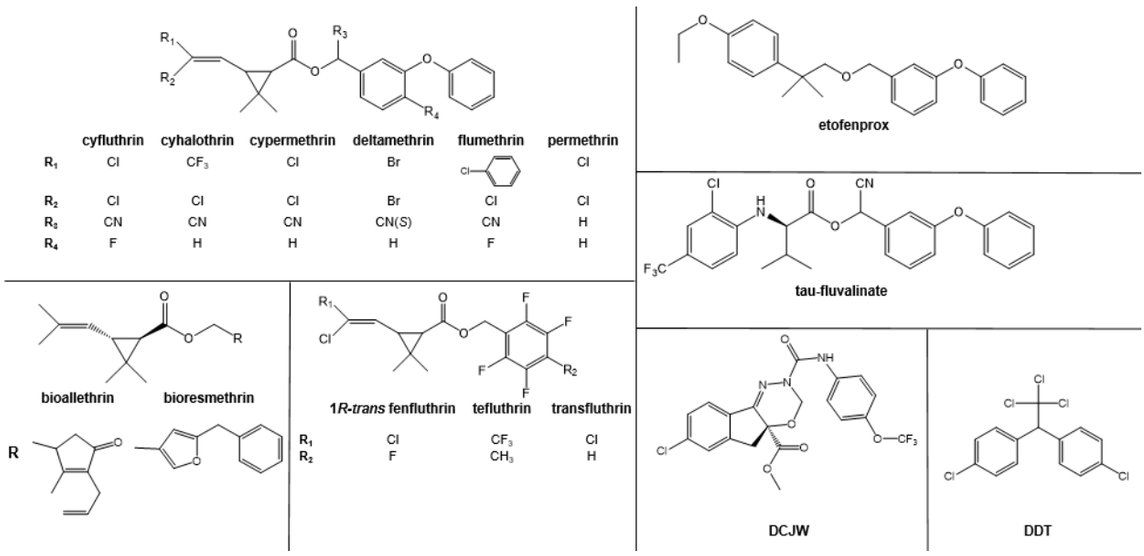

Figure 3. Structures of the insecticides tested. Stereochemistry is not indicated for all structures.

Adult female bioassays

Insecticide bioassays were conducted for three purposes: to determine the levels of resistance to insecticides, to determine if enzyme-mediated detoxification is a major mechanism of resistance by using synergists, and to calculate the degree of dominance of pyrethroid resistance. To determine the levels of resistance to insecticides, solutions were dissolved in acetone and serial dilutions were prepared to find the range of doses that provided mortality values between 0% and 100%. Acetone was applied as control. Dosing of mosquitoes was conducted as outlined for cyhalothrin selections except, 20 adult females were treated per dose. Bioassays for each insecticide were repeated 5 times per strain. To determine if enzyme-mediated detoxification is a major mechanism of resistance in the LM-R strain, I conducted bioassays with cyhalothrin and the synergists PBO, DEM and DEF which inhibit CYPs, GSTs and hydrolases, respectively (Scott 1990). Bioassays were done as described above, except that 2.5 µg PBO, 5 µg DEM or 0.31 µg DEF (the maximal sublethal dose of each) were applied in the thorax of each adult female 1 hour prior to cyhalothrin application. For each replicate, controls included double acetone and an acetone plus synergist application.

Determination of the degree of dominance of pyrethroid resistance in LKR relative to ROCK and KDR:ROCK was meant to understand how pyrethroid resistance is inherited when the *410L+1016I+1534C* allele is paired with a susceptible allele or the *989P+1016G* allele. To compare the dominance of resistance between LKR and ROCK, 400 unmated females of LKR were crossed with 200 ROCK males. Bioassays were done with adult females from the F_1 using cyhalothrin (cyhalothrin was

chosen to calculate the degree of dominance because this is the pyrethroid used to select LM-R strains based on a previous study (Santacoloma Varón et al. 2010). Reciprocal crosses were not conducted because *Vgsc* is not sex linked (Saavedra-Rodriguez et al. 2008). The degree of dominance (D) was calculated according to Stone (Stone 1968). To compare the mode of inheritance between LKR and KDR:ROCK, 549 unmated females of KDR:ROCK strain were crossed with 220 males of LKR strain. Bioassays using permethrin and transfluthrin were done with F_1 adult females and D was calculated as described above. Permethrin and transfluthrin were tested because these two pyrethroids had some of the highest fold difference in the resistance ratios between KDR:ROCK and LKR (9.2- and 9.5-fold difference between KDR:ROCK and LKR, respectively).

For each insecticide, data from all replicates were pooled and assessed by probit analysis using R software version 3.6.3 (R Development Core Team 2022) and a script that is publicly available (https://github.com/JuanSilva89/Probit-analysis/commit/2eaaff05da0f89294788bd0bed564e1bf257acf2) to determine the LD_{50} and 95% confidence intervals (CI 95%). Control mortality was corrected according to Abbott's formula (Abbott 1925). For each insecticide, the resistance ratios were calculated by dividing the LD_{50} of LKR by the LD_{50} of ROCK strain.

3.3. Results

Selection of LM strain using cyhalothrin

To reduce the presence of pyrethroid-susceptible alleles from LM-R strain, I conducted insecticide selections with cyhalothrin. An average of 2,790 virgin females and 1,164 males of LM strain were selected using cyhalothrin doses to kill approximately 80% of males and females (Table 1). I did not conduct more than three generations of selection because the LD_{50} of females between the second and third selections did not differ significantly which suggests that mosquitoes carrying cyhalothrin-susceptible alleles had been removed from the strain (CI 95% of LD_{50} for second and third selection were 6.8 - 8.5 and 6.4 - 8.8 ng cyhalothrin/female, respectively). Twelve individuals of LKR G_0 were sequenced and all of them were homozygous for the three *kdr* mutations (V410L + V1016I + F1534C).

Table 1. Cyhalothrin selection of the LM strain.

Generation of selection	Sex	Dose (ng/mosquito)	Total individuals	Mortality (%)
1	Female	7.1	2941	85.2
	Male	1.8	1523	95.5
2	Female	10	2983	86.7
	Male	2.5	1048	78.7
3	Female	14	2445	85.2
	Male	5.0	920	85.4

Synergist bioassays

The use of synergists DEF, DEM, or PBO in conjunction with cyhalothrin did not significantly decrease the levels of resistance in LM-R strain (Table 2). These results suggest that enzyme-mediated detoxification by CYPs, GSTs or hydrolases are not the main mechanisms of resistance in LM-R strain.

Table 2. Bioassays using synergists and cyhalothrin to adult females of ROCK and LM-R strains.

Synergist	Strain	LD_{50} ng/female (95% CI*)	RR_{50} (95% CI)
---	ROCK	0.049 (0.043 - 0.057)	
	LM-R	4.53 (4.27 - 4.81)	92.4 (74.9 - 112)
DEF	ROCK	0.014 (0.010 - 0.019)	
	LM-R	1.38 (1.19 - 1.61)	98.5 (62.6 - 161)
DEM	ROCK	0.024 (0.020 - 0.028)	
	LM-R	2.62 (2.44 - 2.81)	109 (87.1 - 141)
PBO	ROCK	0.005 (0.004 - 0.005)	
	LM-R	0.62 (0.52 - 0.74)	124 (103 - 186)

*95% CI: Confidence Intervals 95%.

Vgsc cDNA sequences

There were three non-synonymous mutations in the LKR strain that were different from the ROCK strain (V410L + V1016I + F1534C) based on the deduced amino acid sequence alignment using Clustal W. In addition, LKR has a fourth non-synonymous mutation (S723T), but this mutation is not associated with insecticide resistance as it is also found in the pyrethroid-susceptible NS strain (Chang et al. 2009). I obtained two splice variants of the LKR strain (GenBank accession numbers MW202399 and MW202400 for LKR splice variants 1 and 2, respectively) and one splice variant of the ROCK strain (GenBank accession number MW202398). In LKR, splice variant 1 included exons b, e, f, h and i (but lacked exon a) whereas splice variant 2 included exons a, e and h (but lacked exon b, f and i). In ROCK, the splice variant included exons a, b and f (but lacked exons e, i and h).

Levels of resistance in LKR

The levels of cross-resistance to pyrethroids, DCJW and DDT between LKR strain were compared in two general categories (Table 3). The first comparison included insecticides with different structures, whereas the second comparison included insecticides with similar structures, but different isomers. For the first comparison, nine insecticides (bioallethrin, bioresmethrin, cyfluthrin, cyhalothrin, DCJW, DDT, etofenprox, flumethrin and tau-fluvalinate) (Fig 4) were used. For these insecticides, resistance levels ranged from 6-fold (bioallethrin) to 57-fold (flumethrin) across the pyrethroids. LKR was also resistant to DCJW (6-fold) and DDT (8-fold). For the next comparisons, three sets of insecticides were included. The first set of insecticides included 1*R*-*cis* α*S* cypermethrin, alpha-cypermethrin (mix of the (1*R*)-*cis* α*S* and

(1*S*)-*cis* α*R* isomers), cypermethrin (mix of eight isomers) and deltamethrin (Fig 5). There was no difference in resistance levels between cypermethrin and alpha-cypermethrin in LKR. However, there was significantly higher resistance to 1*R*-*cis* α*S* cypermethrin and deltamethrin (also a 1*R*-*cis* α*S* enantiomer). The second set of insecticides included permethrin (mix of four isomers), *cis*-permethrin (mix of two isomers) and *trans*-permethrin (mix of two isomers) (Fig 6). LKR had significantly higher levels of resistance to *trans*-permethrin (RR_{50} = 16) than *cis*-permethrin (RR_{50} = 7) and permethrin (RR_{50} = 6) in LKR. The third set of insecticides included pyrethroids with tetrafluorobenzyl alcohol (tefluthrin, transfluthrin, 1*R*-*trans* fenfluthrin and 1*R*-*trans* tefluthrin) (Fig 7). In LKR, 1*R*-*trans* fenfluthrin (RR_{50} = 18) had the highest levels of resistance followed by tefluthrin (RR_{50} = 5) and transfluthrin (RR_{50} = 6), whereas 1*R*-*trans* tefluthrin (RR_{50} = 2.8) had the lowest levels of resistance.

Table 3. Toxicity of insecticides that target the VGSC against susceptible (ROCK) and resistant (1534C:ROCK, KDR:ROCK and LKR) strains of *A. aegypti*.

Insecticide[¥]	Strain	LD_{50}* (95% CI)	Slope (±SEM)	Sample size (*n*)
1*R-cis-αS* cypermethrin	ROCK	0.008 (0.007-0.008)	3.0 (0.2)	680
	1534C:ROCK	0.088 (0.072-0.107)	2.3 (0.2)	506
	KDR:ROCK	0.12 (0.10-0.15)	2.1 (0.3)	520
	LKR	0.19 (0.15-0.23)	1.2 (0.1)	884
1*R-trans* fenfluthrin	ROCK	0.63 (0.53-0.75)	2.8 (0.3)	880
	LKR	11.1 (8.38-14.9)	1.8 (0.3)	600
1*R-trans* tefluthrin	ROCK	0.67 (0.65-0.70)	4.5 (0.1)	540
	KDR:ROCK	26.9 (25.8-28.2)	1.3 (0.1)	720
	LKR	1.87 (1.55-2.27)	1.3 (0.1)	680
alpha-cypermethrin	ROCK	0.032 (0.027-0.039)	3.5 (0.6)	817
	1534C:ROCK	0.43 (0.376-0.49)	2.5 (0.2)	578
	KDR:ROCK	0.53 (0.44-0.63)	1.8 (0.1)	712
alpha-cypermethrin	ROCK	0.048 (0.043-0.053)	2.7 (0.2)	520
	LKR	0.19 (0.13-0.29)	1.1 (0.1)	740
bioallethrin	ROCK	3.85 (3.61-4.11)	4.2 (0.2)	620
	LKR	21.9 (19.0-25.2)	2.7 (0.2)	420
bioresmethrin	ROCK	0.43 (0.392-0.472)	4.8 (0.4)	520
	LKR	4.54 (3.48-5.94)	1.0 (0.1)	820
cis-permethrin	ROCK	0.55 (0.54-0.57)	3.8 (0.1)	620
	1534C:ROCK	4.96 (4.07-6.05)	2.2 (0.3)	689
cis-permethrin	ROCK	0.70 (0.64-0.76)	1.5 (0.1)	480
	LKR	4.78 (4.06-5.64)	1.4 (0.1)	800
cyfluthrin	ROCK	0.023 (0.019-0.029)	2.1 (0.2)	640
	LKR	0.51 (0.38-0.69)	1.01 (0.1)	1100
cyhalothrin	ROCK	0.025 (0.023-0.026)	3.7 (0.2)	840
	LKR	0.25 (0.21-0.32)	1.4 (0.1)	760
	LKR x ROCK F_1	0.050 (0.042-0.060)	2.2 (0.2)	620
cypermethrin	ROCK	0.075 (0.066-0.084)	3.2 (0.3)	837
	LKR	0.61 (0.50-0.74)	1.4 (0.1)	940
deltamethrin	ROCK	0.005 (0.004-0.006)	2.4 (0.4)	615
	LKR	0.21 (0.18-0.25)	1.1 (0.1)	820
etofenprox	ROCK	2.94 (2.85-3.04)	4.6 (0.1)	712
	LKR	42.2 (24.9-71.3)	1.2 (0.3)	700
flumethrin	ROCK	0.70 (0.59-0.83)	2.7 (0.3)	620
	LKR	39.7 (28.3-55.8)	0.7 (0.1)	1040
permethrin	ROCK	0.23 (0.23-0.24)	3.6 (0.04)	800
	LKR	1.30 (0.94-1.81)	1.15 (0.09)	814
	KDR:ROCK	12.1 (10.2-14.3)	4.4 (0.3)	660
	KDR:ROCK x LKR F_1	10.5 (9.01 - 12.3)	2.2 (0.2)	520
tau-fluvalinate	ROCK	0.69 (0.59-0.82)	3.2 (0.5)	440
	LKR	4.99 (3.94-6.34)	1.1 (0.1)	800
tefluthrin	ROCK	4.97 (4.62-5.33)	4.2 (0.3)	540
	LKR	25.2 (19.5-32.5)	2.1 (0.4)	720
transfluthrin	ROCK	0.63 (0.60-0.66)	4.8 (0.2)	520
	LKR	3.83 (3.17-4.63)	1.6 (0.1)	540
	KDR:ROCK	14.8 (13.8-15.8)	3.1 (0.2)	520
	KDR:ROCK x LKR F_1	11.3 (9.37 - 13.6)	2.0 (0.2)	571
trans-permethrin	ROCK	0.45 (0.41-0.49)	3.8 (0.3)	513
	1534C:ROCK	4.45 (3.79-5.21)	3.2 (0.2)	520
trans-permethrin	ROCK	0.63 (0.53-0.76)	3.6 (0.5)	900
	LKR	10.4 (7.56-14.3)	1.3 (0.1)	520
DCJW	ROCK	1.84 (1.72-1.96)	4.0 (0.2)	720
	LKR	11.3 (9.63-13.3)	1.9 (0.2)	727
DDT	ROCK	15.7 (15.2-16.3)	3.8 (0.1)	640
	LKR	118 (96.7-144)	1.4 (0.1)	994

[¥]Bioassays done with the same insecticide solutions for different strains share the same insecticide name.

*LD_{50}, ng/mosquito.

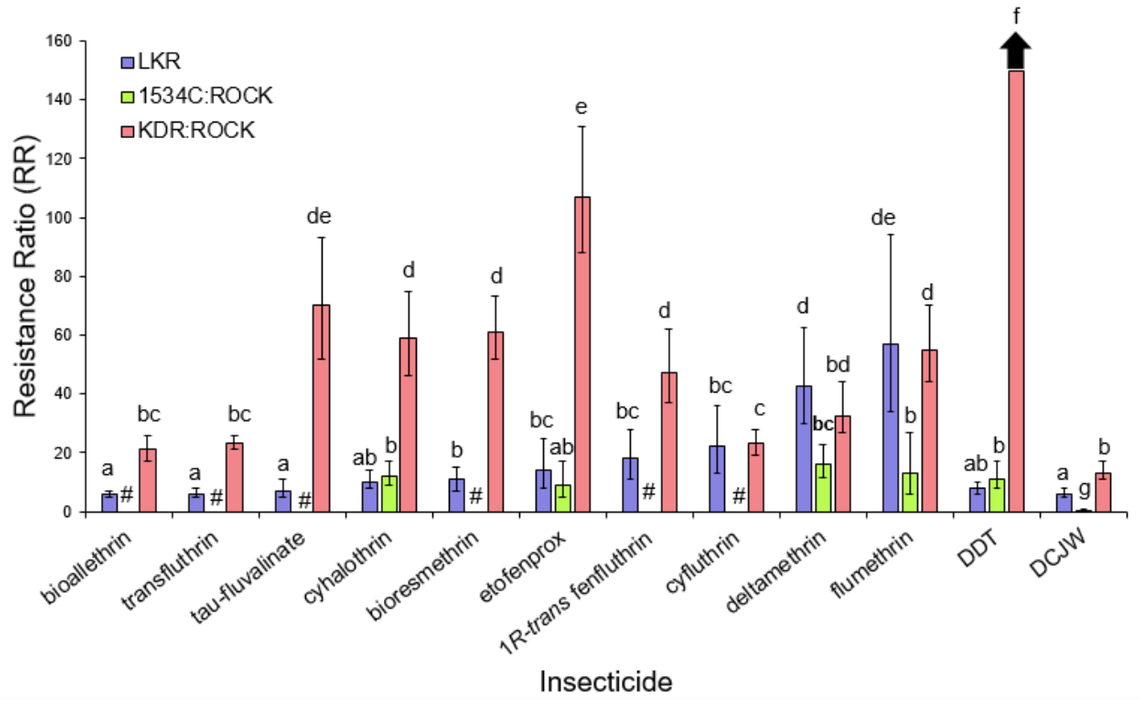

Figure 4. Comparison of resistance levels amongst LKR, 1534C:ROCK and KDR:ROCK for insecticides targeting the VGSC. RRs for KDR:ROCK were previously published (Smith et al. 2017)and given here for comparison purposes. RRs for 1534C:ROCK for bioallethrin, cyhalothrin, etofenprox, flumethrin, DDT and DCJW were previously reported (Fan and Scott 2020) and are given here for comparison purposes. Insecticides that were not tested for 1534C:ROCK in a previous study (Fan and Scott 2020) are denoted with a pound sign (#).

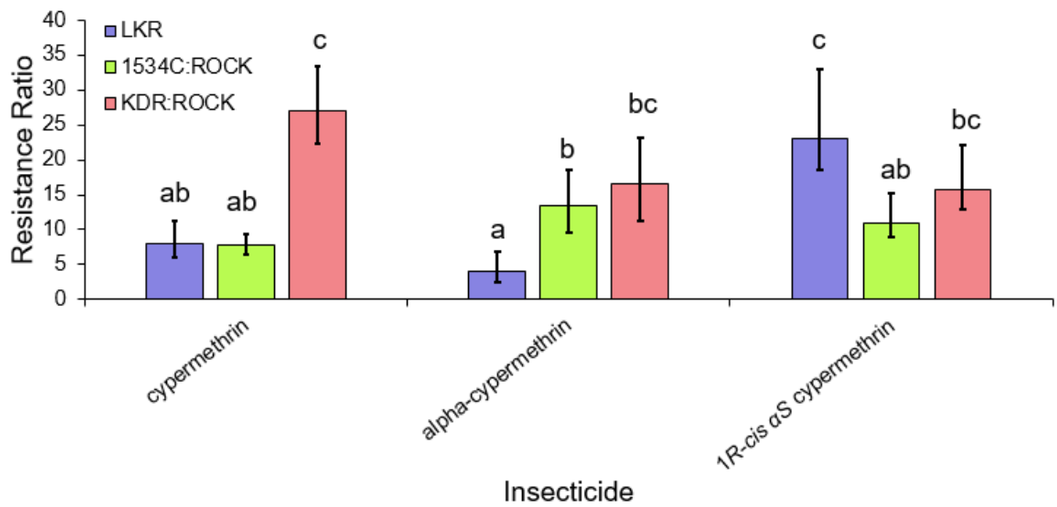

Figure 5. Comparison between 1*R-cis αS* cypermethrin, alpha-cypermethrin (mix of the 1*R-cis αS* and 1*S-cis αR* isomers), cypermethrin (mix of eight isomers) and deltamethrin. RRs for KDR:ROCK to cypermethrin and deltamethrin were previously published (Smith et al. 2017) and given here for comparison purposes. Bars with different letters are significantly different based on the 95% confidence intervals.

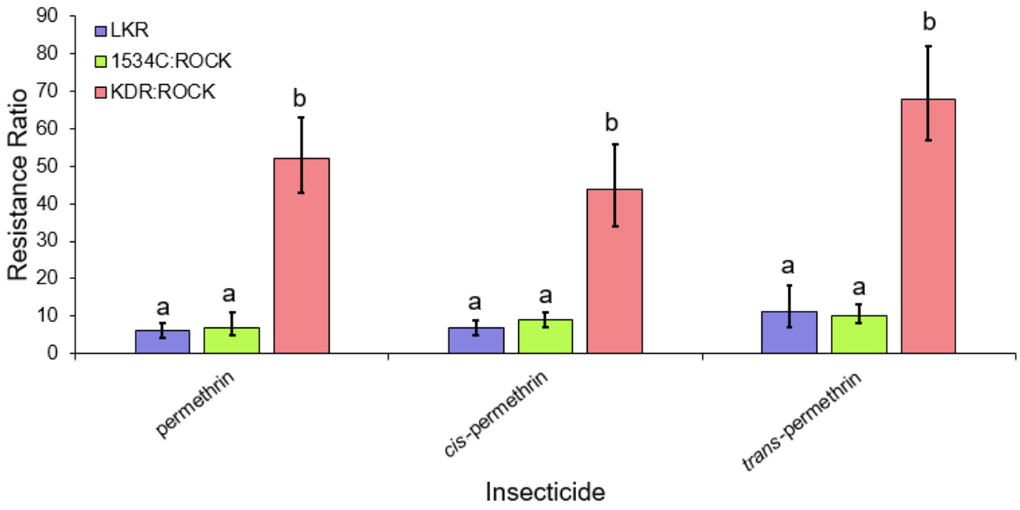

Figure 6. Comparison between *cis*-permethrin, permethrin and *trans*-permethrin. RRs for KDR:ROCK to *cis*-permethrin, permethrin and *trans*-permethrin were previously published (Smith et al. 2017) and given here for comparison purposes. Bars with different letters are significantly different based on the 95% confidence intervals.

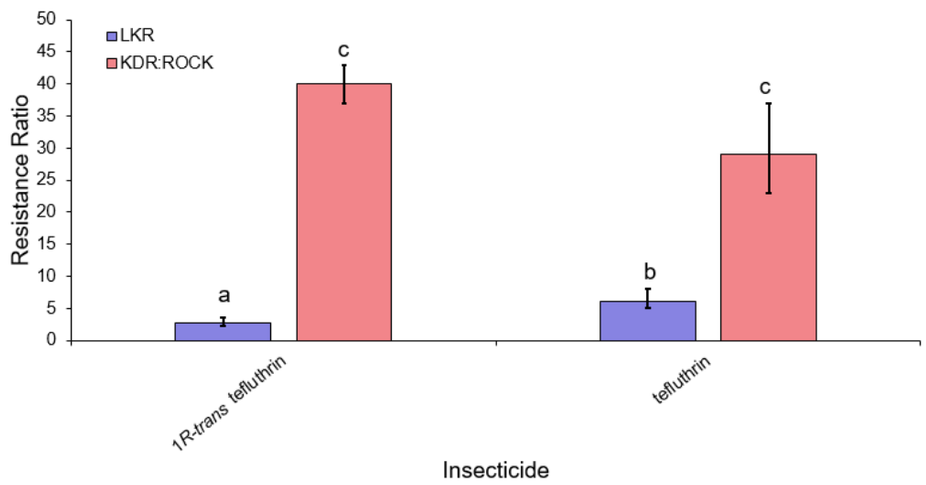

Figure 7. Comparison between pyrethroids containing tetrafluorobenzyl alcohol (tefluthrin, transfluthrin, 1*R-trans* tefluthrin and 1*R-trans* fenfluthrin). RRs for KDR:ROCK were previously published (Smith et al. 2017) (except for 1*R-trans* tefluthrin) and given here for comparison purposes. Bars with different letters are significantly different based on the 95% confidence intervals.

I also determined the inheritance of pyrethroid resistance in LKR relative to a susceptible strain and a resistant strain (ROCK and KDR:ROCK, respectively). Relative to ROCK strain, the inheritance of cyhalothrin resistance in LKR is incompletely recessive (D = -0.42). In crosses with the KDR:ROCK strain, resistance was inherited as incompletely recessive traits, with D values of -0.87 (permethrin) and -0.60 (transfluthrin).

3.4 Discussion

The isolation of a congenic resistant strain having the *410L+1016I+1534C kdr* allele allowed the opportunity to compare resistance levels of two other *kdr* alleles (*1534C* and *989P+1016G*) that had been isolated in the same genetic background (Smith et al. 2017, Fan and Scott 2020). Relative to the *1534C* allele, the *410L+1016I+1534C* allele conferred similar levels of resistance relative to seven insecticides (cyhalothrin, cypermethrin, etofenprox, DDT, cypermethrin, permethrin, *cis*-permethrin and *trans*-permethrin), conferred higher levels of resistance to flumethrin, DCJW, 1*R-cis* α*S* cypermethrin and deltamethrin), and conferred lower levels of resistance only to alpha-cypermethrin (Figs 4-5). The similar resistance levels conferred to cyhalothrin, cypermethrin, etofenprox, DDT, cypermethrin, permethrin, *cis*-permethrin and *trans*-permethrin by the *410L+1016I+1534C* and *1534C* alleles suggests that resistance to these insecticides is conferred by the F1534C mutation. In contrast, the *410L+1016I+1534C* allele did confer higher levels of resistance to flumethrin, DCJW, 1*R-cis* α*S* cypermethrin and deltamethrin, relative to the *1534C* allele, suggesting addition of the V410L and/or V1016I mutations to F1534C enhances resistance to these insecticides. Comparision of the *989P+1016G* (KDR:ROCK) and *410L+1016I+1534C* (LKR) alleles revealed that there was higher levels of resistance conferred by the *989P+1016G* allele for eleven of the insecticides tested. For cyfluthrin, flumethrin, alpha-cypermethrin, 1*R-cis* α*S* cypermethrin and deltamethrin the resistance levels were not significantly different between the alleles. The importance of pyrethroid stereochemistry to the resistance levels is exemplified by the finding of similar resistance levels for 1*R-cis* α*S* cypermethrin between the *989P+1016G* and *410L+1016I+1534C* alleles that was not observed for cypermethrin or alpha-cypermethrin (Fig 5A). In addition, the *410L+1016I+1534C* allele had higher resistance to *trans*-permethrin, compared to permethrin or *cis*-permethrin (Fig. 5).

There are non-synonymous mutations in *Vgsc* that do not cause resistance (Silva and Scott 2020) making it necessary to evaluate the resistance of each allele found. In some cases, sequential accumulation of mutations can give rise to alleles that give greater levels of resistance. The best example of this is house flies, where the first *Vgsc* mutation was L1014F (*kdr*). Subsequently a second mutation (M918T) evolved, giving rise to a new allele (*918T+1014F* or *super-kdr*) which gave higher levels of resistance to most pyrethroids (Sun et al. 2016). A subsequent mutation gave rise to a new allele *600N+918T+1014F* giving even higher levels of resistance (Kasai et al. 2017, Sun et al. 2017). This does not appear to be the case for *A. aegypti*, at least not for the *410L+1016I+1534C* and *1534C* alleles, making it unclear why these two alleles are among the most common (Fan et al. 2020). One possibility is that the triple mutation could be at a selective advantage if it conferred higher levels of resistance. The only insecticide that fits this idea is deltamethrin (Fig. 5), but there is a lack of records to connect deltamethrin use with an increased frequency of the triple mutation. A second possibility is that the

410L+1016I allele was present in a population, the *1534C* allele occurred in the *410L+1016I* background to generate the triple mutation allele, and the selective advantage of the allele to most pyrethroids is simply due to the F1534C mutation. A third possibility is that the V410L and/or V1016I mutations do not contribute to insecticide resistance, but ameliorates the fitness cost of the F1534C mutation. Previous studies in Latin America found that the *410L+1016I+1534C* allele has higher frequencies relative to *410L+1534C* allele presumably because the V1016I mutation compensates for negative fitness effects (Saavedra-Rodriguez et al. 2018, Scott 2019). The idea that V1016I may act as a fitness modifier is supported by the fact that the *1016I+1534C* allele is the most frequent allele (relative to the susceptible allele *V1016+F1534* and the resistance allele *1534C*) from over 20 field-collected populations from Brazil (Brito et al. 2018).

How *kdr* mutations alter VGSC sensitivity to pyrethroids has been tested by heterologous expression in *Xenopus* oocytes (Du et al. 2016b, Yan et al. 2020), but discrepancies between oocytes and *in vivo* results have been previously observed and my results add additional discrepancies. In heterologous expression studies, the *1534C* allele conferred insensitivity to permethrin, but not deltamethrin (Du et al. 2013, Hirata et al. 2014). However, the *1534C* allele confers resistance to both permethrin and deltamethrin *in vivo* (Fan and Scott 2020) and the *410L+1016I+1534C* allele (this study) confers higher resistance to deltamethrin than permethrin. Heterologous expression studies also found that the *410L+1534C* allele conferred higher insensitivity to permethrin than *1534C* allele (Haddi et al. 2017). Although the resistance levels in the *410L+1016I+1534C* allele were measured, my results show that the addition of V410L to F1534C did not increase the levels of resistance to permethrin (or *cis*-permethrin or *trans*-permethrin). Overall, these discrepancies support the need to quantify resistance conferred by different *kdr* mutations *in vivo*. Furthermore, use of genome editing tools such as CRISPR/Cas9 to *knock in* the *kdr* mutations allows opportunities to explore mutations and combinations of mutations that are not necessarily found in nature. Isolation of congenic strains with different *kdr* mutations also allows for studies on the impacts of these mutations on multiple aspects of mosquito biology (e.g. fitness costs).

Different *kdr* alleles are more likely to increase in frequency within populations under pyrethroid selection depending on the resistance levels they confer. For example, the *989P+1016G* allele is likely to increase in populations that carry also the *410L+1016I+1534C* or *1534C* alleles in environments exposed to permethrin and transfluthrin and this has been observed (Kasai et al. 2014). Knowing the levels of resistance conferred by different *kdr* alleles allows vector control personnel to choose the pyrethroid having the lowest levels of resistance for the alleles found in their region.

The main mechanism of resistance in a pyrethroid-resistant strain of *A. aegypti* collected in Colombia was *kdr* (*410L+1016I+1534C*) allele, and I quantified the levels of resistance to different insecticides conferred by this allele. Resistance conferred by *kdr* alleles can be dependent on the stereochemistry of the pyrethroids used. Further experimentation should be done with individual pyrethroid diastereomers to investigate the role of other *kdr* mutations in insecticide resistance. The validation of *kdr* mutations through heterologous expression does not reflect the role of *kdr* mutations *in vivo.* In this regard, it is proposed that further studies are done using either congenic strains or genome editing techniques such as CRISPR-Cas9 to validate the role of *kdr* mutations instead of using heterologous expression in *Xenopus* oocytes. The *410L+1016I+1534C* allele does not confer higher levels of resistance to many pyrethroids relative to the *1534C* allele. These results improve the understanding of the evolution of insecticide resistance. My findings help understand how different *kdr* mutations confer variable levels of resistance to pyrethroids with different chemical structures. These results are useful for insecticide resistance management because it is shown which insecticides are not effective at controlling mosquitoes carrying the *410L+1016I+1534C* and *1534C* alleles.

Acknowledgements

I thank P. Fuya, N. Pinto and M. Salgado for collecting mosquito eggs from La Mesa, Colombia. I thank Z. Wen (Syngenta) for donating 1*R-trans* tefluthrin. I thank Y. Fan and L. Smith for providing the 1534C:ROCK and KDR:ROCK strains, respectively. I thank N. Buchon and P. Wang for their comments on the experimental design and manuscript. I thank L. Smith, Y. Fan, H. Sun, R. Mertz, J. Freeman, L. Pfannenstiel, and R. Norris for their valuable comments and helpful suggestions. This project was funded by a Griswold Fellowship (to JJS) and the National Institutes of Health (to JGS).

REFERENCES

Abbott, W. S. 1925. A method of computing the effectiveness of an insecticide. J. Econ. Entomol. 18: 265-267.

Baud, D., D. J. Gubler, B. Schaub, M. C. Lanteri, and D. Musso. 2017. An update on Zika virus infection. Lancet 390: 2099-2109.

Brengues, C., N. J. Hawkes, F. Chandre, L. McCarroll, S. Duchon, P. Guillet, S. Manguin, J. C. Morgan, and J. Hemingway. 2003. Pyrethroid and DDT cross-resistance in *Aedes aegypti* is correlated with novel mutations in the voltage-gated sodium channel gene. Med. Vet. Entomol. 17: 87-94.

Brito, L. P., L. Carrara, R. M. de Freitas, J. B. P. Lima, and A. J. Martins. 2018. Levels of resistance to pyrethroid among distinct *kdr* alleles in *Aedes aegypti* laboratory lines and frequency of *kdr* alleles in 27 natural populations from Rio de Janeiro, Brazil. Biomed Res Int 2018: 2410819.

Casida, J. E., and L. J. Lawrence. 1985. Structure-activity correlations for interactions of bicyclophosphorus esters and some polychlorocycloalkane and pyrethroid insecticides withthe brain-specific t-butylbicyclophosphorothionate receptor. Environ. Health Perspect 61: 123-132.

Chang, C., W. K. Shen, T. T. Wang, Y. H. Lin, E. L. Hsu, and S. M. Dai. 2009. A novel amino acid substitution in a voltage-gated sodium channel is associated with knockdown resistance to permethrin in *Aedes aegypti*. Insect Biochem. Mol. Bio. 39: 272-278.

Coats, J. R. 1990. Mechanisms of toxic action and structure- activity relationships for organochlorine and synthetic pyrethroid insecticides. Environ. Health Perspect 87: 255-262.

Du, Y., Y. Nomura, B. Zhorov, and K. Dong. 2016a. Sodium channel mutations and pyrethroid resistance in *Aedes aegypti*. Insects 7: 60.

Du, Y., Y. Nomura, B. S. Zhorov, and K. Dong. 2016b. Evidence for dual binding sites for 1,1,1-trichloro-2,2-bis(*p*-chlorophenyl)ethane (DDT) in insect sodium channels. J. Biol. Chem. 291: 4638-4648.

Du, Y., Y. Nomura, G. Satar, Z. Hu, R. Nauen, S. Y. He, B. S. Zhorov, and K. Dong. 2013. Molecular evidence for dual pyrethroid-receptor sites on a mosquito sodium channel. Proc. Natl. Acad. Sci. USA 110: 11785-11790.

Fan, Y., and J. G. Scott. 2020. The F1534C *voltage sensitive sodium channel* mutation confers 7- to 16-fold resistance to pyrethroid insecticides in *Aedes aegypti*. Pest Man. Sci. 76: 2251-2259.

Fan, Y., P. O'Grady, M. Yoshimizu, A. Ponlawat, P. E. Kaufman, and J. G. Scott. 2020. Evidence for both recombination and mutations in the evolution of *kdr* alleles in *Aedes aegypti*. PLoS Negl Trop Dis 14: e0008154.

Ford, M. G., R. Greenwood, and C. H. Turner. 1989. The structure activity relationships of pyrethroid insecticides 1. A novel approach based on the use of multivariate QSAR and computational chemistry. Pestic. Sci. 27: 305-326.

Gatherer, D., and A. Kohl. 2016. Zika virus: a previously slow pandemic spreads rapidly through the Americas. J. Gen. Virol. 97: 269-273.

Haddi, K., H. V. V. Tomé, Y. Du, W. R. Valbon, Y. Nomura, G. F. Martins, K. Dong, and E. E. Oliveira. 2017. Detection of a new pyrethroid resistance mutation (V410L) in the sodium channel of *Aedes aegypti*: a potential challenge for mosquito control. Sci. Rep. 7: 46549.

Harris, A. F., S. Rajatileka, and H. Ranson. 2010. Pyrethroid resistance in *Aedes aegypti* from Grand Cayman. Am. J. Trop. Med. Hyg. 83: 277-284.

Hirata, K., O. Komagata, K. Itokawa, A. Yamamoto, T. Tomita, and S. Kasai. 2014. A single crossing-over event in voltage-sensitive Na^+ channel genes may cause critical failure of dengue mosquito control by insecticides. PLoS Negl. Trop. Dis. 8: e3085.

Kasai, S., H. Sun, and J. G. Scott. 2017. Diversity of knockdown resistance alleles in a single house fly population facilitates adaptation to pyrethroid insecticides. Insect Mol. Biol. 26: 13-24.

Kasai, S., O. Komagata, K. Itokawa, T. Shono, L. C. Ng, M. Kobayashi, and T. Tomita. 2014. Mechanisms of pyrethroid resistance in the dengue mosquito vector, *Aedes aegypti*: target site insensitivity, penetration, and metabolism. PLoS Negl. Trop. Dis. 8: e2948.

Kawada, H., S. Z. M. Oo, S. Thaung, K. E., Y. N. M. Maung, H. M. Thu, K. Z. Thant, and N. Minakawa. 2014. Co-occurrence of point mutations in the voltage-gated sodium channel of pyrethroid-resistant *Aedes aegypti* populations in Myanmar. PLoS Negl. Trop. Dis. 8: e3032.

Khambay, B. P. S., and P. J. Jewess. 2005. Pyrethroids, pp. 1-29. In L. I. Gilbert, K. Iatrou and S. S. Gill (eds.), Comprehensive Molecular Insect Science, vol. 6. Elsevier, Boston.

Kushwah, R. B. S., C. L. Dykes, N. Kapoor, T. Adak, and O. P. Singh. 2015. Pyrethroid-resistance and presence of two knockdown resistance (*kdr*) mutations, F1534C and a novel mutation T1520I, in Indian *Aedes aegypti*. PLoS Negl. Trop. Dis. 9: e3332.

Morrison, T. E. 2014. Reemergence of chikungunya virus. J. Virol. 88: 11644-11647.

Naumann, K. 1998. Research into fluorinated pyrethroid alcohols - an episode in the history of pyrethroid discovery. Pestic. Sci. 52: 3-20.

Nishimura, K., and T. Narahashi. 1978. Structure-activity relationships of pyrethroids based on direct action on nerve. Pestic. Biochem. Physiol. 8: 53-64.

Plourde, A. R., and E. M. Bloch. 2016. A Literature Review of Zika Virus. Emerg Infect Dis 22: 1185-1192.

R Development Core Team 2020. R: A language and environment for statistical computing computer program, version By R Development Core Team, Vienna, Austria.

Reiter, P., and M. B. Nathan. 2001. Guidelines for Assessing the Efficacy of Insecticidal Space Sprays for Control of the Dengue Vector *Aedes aegypti*. Geneva: World Health Organization. Available from http://www.who.int/iris/handle/10665/67047.

Saavedra-Rodriguez, K., C. Strode, A. Suarez, I. Salas, H. Ranson, J. Hemingway, and W. Black. 2008. Quantitative trait loci mapping of genome regions controlling permethrin resistance in the mosquito *Aedes aegypti*. Genetics 180: 1137-1152.

Saavedra-Rodriguez, K., F. V. Maloof, C. L. Campbell, J. Garcia-Rejon, A. Lenhart, P. Penilla, A. Rodriguez, A. A. Sandoval, A. E. Flores, G. Ponce, S. Saul Lozano, and W. C. Black. 2018. Parallel evolution of *vgsc* mutations at domains IS6, IIS6 and IIIS6 in pyrethroid resistant *Aedes aegypti* from Mexico. Sci. Rep. 8: 6747.

Santacoloma Varón, L., B. Chaves Córdoba, and H. L. Brochero. 2010. Susceptibility of *Aedes aegypti* to DDT, deltamethrin, and lambda-cyhalothrin in Colombia. Revista Panamericana de Salud Pública 27: 66–73.

Scott, J. G. 1990. Investigating mechanisms of insecticide resistance: methods, strategies and pitfalls, pp. 39-57. In R. T. Roush and B. Tabashnik (eds.), Pesticide Resistance in Arthropods. Chapman and Hall, New York.

Scott, J. G. 2019. Life and death at the voltage-sensitive sodium channel: Evolution in response to insecticide use. Ann. Rev. Entomol. 64: 243-257.

Shepard, D. S., E. A. Undurraga, Y. A. Halasa, and J. D. Stanaway. 2016. The global economic burden of dengue: a systematic analysis. Lancet Infect. Dis. 16: 935-941.

Silva, J. J., and J. G. Scott. 2020. Conservation of the voltage-sensitive sodium channel protein within the Insecta Insect Mol. Bio. 29: 9-18.

Smith, L. B., S. Kasai, and J. G. Scott. 2017. Voltage-sensitive sodium channel mutations S989P+V1016G in *Aedes aegypti* confer variable resistance to pyrethroids, DDT and oxadiazines. Pest Manag. Sci. 74: 737-745.

Soderlund, D. M., C. W. Hessney, and D. W. Helmuth. 1983. Pharmacokinetics of *cis*- and *trans*-substituted pyrethroids in the American cockroach. Pestic. Biochem. Physiol. 20: 161-168.

Srisawat, R., N. Komalamisra, Y. Eshita, M. Zheng, K. Ono, T. Q. Itoh, A. Matsumoto, S. Petmitr, and Y. Rongsriyam. 2010. Point mutations in domain II of the voltage-gated sodium channel gene in deltamethrin-resistant *Aedes aegypti* (Diptera: Culicidae). Appl. Entomol. Zool. 45: 275–282.

Stone, B. F. 1968. A formula for determining degree of dominance in cases of monofactorial inheritance of resistance to chemicals. Bull. World Health Org. 38: 325-326.

Sun, H., S. Kasai, and J. G. Scott. 2017. Two novel house fly *Vssc* mutations, D600N and T929I, give rise to new insecticide resistance alleles. Pestic. Biochem. Physiol. 143: 116-121.

Sun, H., K. P. Tong, S. Kasai, and J. G. Scott. 2016. Overcoming *super-kdr* mediated resistance: Multi-halogenated benzyl pyrethroids are more toxic to *super-kdr* than *kdr* house flies. Insect Mol. Biol. 25: 126-137.

Vera-Maloof, F. Z., K. Saavedra-Rodriguez, A. E. Elizondo-Quiroga, S. Lozano-Fuentes, and W. C. I. Black. 2016. Coevolution of the Ile1,016 and Cys1,534 mutations in the voltage gated sodium channel gene of *Aedes aegypti* in Mexico. PLoS Negl. Trop. Dis. 9: e0004263.

Verschoyle, R. D., and W. N. Aldridge. 1980. Structure-activity relationships of some pyrethroids in rats. Arch. Toxicol. 45: 325-329.

WHO. 2014. Yellow Fever. World Health Organization, Geneva.

Williamson, M., D. Martinez-Torres, C. Hick, and A. Devonshire. 1996. Identification of mutations in the housefly *para*-type sodium channel gene associated with knockdown resistance (*kdr*) to pyrethroid insecticides. Mol. Gen. Genet. 252: 51-60.

Yan, R., Q. Zhou, Z. Xu, G. Zhu, K. Dong, B. S. Zhorov, and M. Chen. 2020. Three sodium channel mutations from Aedes albopictus confer resistance to Type I, but not Type II pyrethroids. Insect Biochemistry and Molecular Biology 123: 103411.

CHAPTER 4

FITNESS COSTS IN THE PRESENCE AND ABSENCE OF INSECTICIDE USE EXPLAINS ABUNDANCE OF TWO COMMON *AEDES AEGYPTI KNOCKDOWN RESISTANCE* ALLELES FOUND IN THE AMERICAS[5]

Authors: Juan J. Silva, Cera R. Fisher, Anastacia E. Dressel and Jeffrey G. Scott

Abstract

Aedes aegypti is the vector of viruses such as chikungunya, dengue, yellow fever and Zika that have a critical impact in human health. Control of adult mosquitoes is widely done using pyrethroids, but resistance has reduced the effectiveness of this class of insecticides. Resistance to pyrethroids in mosquitoes is commonly due to mutations in the *voltage-gated sodium channel* (*Vgsc)* gene (these mutations are known as *knockdown resistance, kdr*). In the Americas and the Caribbean, the most common *kdr* alleles are *410L+1016I+1534C* and *1534C*. In this study, I conducted a population cage experiment to evaluate the changes in the allele and genotype frequencies of the *410L+1016I+1534C* allele by crossing two pyrethroid-susceptible congenic strain, but carrying the *410L+1016I+1534C* and 1534C alleles. Changes in allele frequencies were measured over 10 generations in the absence of deltamethrin exposure. I also applied a cycle of selection with deltamethrin at F_9 to evaluate the changes in allele and genotype frequencies. The changes in genotype frequencies due to fitness costs (out of Hardy-Weinberg Equilibrium) or genetic drift were also evaluated. My findings suggest that fitness costs were higher with the *410L+1016I+1534C* allele, relative to the *1534C* allele, in the absence of deltamethrin exposure, but this allele provides a stronger advantage when exposed to

[5] In preparation for submission in Proceedings of the National Academy of Sciences of the United States of America (PNAS)

deltamethrin relative to the *1534C* allele. Changes in genotype frequencies were not in Hardy-Weinberg equilibrium nor genetic drift which indicates the mosquito populations tested did not follow the assumptions of the Hardy-Weinberg Equilibrium. These results suggest a likely reason for the variations in frequencies between the *410L+1016I+1534C* and *1534C* alleles in field populations.

4.1 Introduction

Aedes aegypti is the vector of viruses that have devastating impacts on public health and insecticide control of adult mosquitoes is most commonly carried out using pyrethroids. *A. aegypti* is the vector of viruses such as chikungunya, dengue, yellow fever and Zika (Bhatt et al. 2013, WHO 2013, ECDC 2015, CDC 2016, Yactayo et al. 2016). To reduce the burden caused by these diseases, control of adult mosquitoes is mainly done using a class of insecticides known as pyrethroids (e.g. deltamethrin, permethrin and cyhalothrin). Being deltamethrin one of the most common pyrethroids applied for control of *A. aegypti* in the field. For example, a rigorous State such as California in terms of reporting insecticide use per county, where the top five counties that applied the highest amounts of deltamethrin (pounds per year) in 2018 were; Los Angeles (1720), Sacramento (926), Kern (880), Orange (712) and Riverside (662) (CDPR 2018). In Colombia, deltamethrin applications in Ultra Low Volume (ULV) are commonly used for control of mosquitoes (INS 2018). Pyrethroid toxicity occurs due to the binding and disruption of the voltage-gated sodium channel (VGSC) which is a critical protein involved in the depolarization of neuronal membranes and firing of action potentials in the nervous system.

Resistance to pyrethroids in mosquitoes is commonly due to mutations in the *Vgsc* gene (mutations that cause pyrethroid resistance are known as *knockdown resistance* or *kdr*). There are 10 *kdr* alleles in *A. aegypti* based on the sequencing of either full-length cDNA or PCR products of domains I, II or III of the *Vgsc* gene were previously reported *kdr* mutations were found *(Table S1)* (Chang et al. 2009, Harris et al. 2010, Srisawat et al. 2012, Kawada et al. 2014, Kushwah et al. 2015, Haddi et al. 2017, Granada et al. 2018, Saavedra-Rodriguez et al. 2018, Murcia et al. 2019, Fan et al. 2020).. *1534C* is a common allele with a wide distribution in America and Asia (amino acid numbering based on *Musca domestica* VGSC, GenBank: CAA65448.1)(Granada et al. 2018, Saavedra-Rodriguez et al. 2018, Costa et al. 2020, Fan et al. 2020) (Moyes et al. 2017). The most common alleles found in the Americas are *410L+1016I+1534C*, and *1534C* (Granada et al. 2018, Saavedra-Rodriguez et al. 2018, Costa et al. 2020, Fan et al. 2020). The levels of resistance conferred by these alleles revealed the *1534C* allele conferred 7- to 16-fold resistance to pyrethroids. The *410L+1016I+1534C* allele did not confer higher levels of resistance (compared to

1534C) except for deltamethrin (Fan and Scott 2020, Silva et al. 2021). The levels of resistance for deltamethrin conferred by the *410L+1016I+1534C* and *1534C* alleles were 42 (30-63) and 16 (11-23), respectively.

Relative to insecticide susceptible alleles, resistance alleles commonly have a fitness cost in the absence of insecticide exposure (Freeman et al. 2021). However, field populations often include multiple resistance alleles. Thus, the fitness of the different resistance alleles to each other (in both the presence and absence of insecticide) is as important to understanding the evolution of resistance, as comparisons resistant and susceptible alleles. For example, in *Musca domestica* the relative fitness in the presence of pyrethroids of the different *kdr* alleles is *super-kdr* (*918T+1014F*) >*kdr* (*1014F*) > *kdr-his* (*1014H*), but in the absence of insecticide the relative fitness is *susceptible* > *kdr-his* > *kdr* > *super-kdr (Rinkevich et al. 2013)*, suggesting that alleles with multiple mutations might have a greater fitness cost than those with a single mutation. In *A. aegypti*, although the fitness advantage of some resistance alleles in the presence of insecticide has been investigated (see paragraph above), the fitness costs of different *kdr* alleles in the absence of insecticide in *A. aegypti* is much less studied, although fitness costs for the *989P+1016G* (Smith et al. 2021) and *1534C* (Fisher et al. 2022) alleles were shown to have a fitness cost relative to the susceptible allele (Smith et al. 2021). Fitness costs can be evaluated by numerous experimental means, with one common method being population cage experiments (Freeman et al. 2021). In *A. aegypti*, three previous publications identified fitness costs of different *kdr* alleles by conducting population cage experiments: *1534C* allele (allele frequencies decreased from 0.50 to 0.31 after seven generations) (Fisher et al. 2022), *989P+1534C* allele (0.46 to 0.32 after nine generations)(Smith 2019), and *1016I+1534C* allele (0.50 to 0.22 after 15 generations) (Brito et al. 2013). In population cage experiments, resistant and susceptible strains are placed in a population cage study where the frequencies of resistance alleles are monitored over generations. This method allows to measure the overall presence and magnitude of a cost in a given environment, but the components responsible for this cost remain unknown.. Thus, population cage experiments are preferred as the initial experiment to evaluate overall fitness costs under defined environmental conditions, because more variables are evaluated. To date, most publications that evaluated

fitness costs compared resistance alleles versus susceptible alleles, but competition between resistance alleles have been vastly neglected for many decades. This is problematic because many resistance alleles already coexist in field populations, and some potentially impose more detrimental disadvantages relative to other resistance alleles in the absence of insecticide exposure. Therefore, it is valuable to understand not only the relative fitness of *kdr* alleles relative to the susceptible alleles, but also to understand the relative fitness of the different and resistance alleles. Such information is needed to better understand the patterns of alleles found in field populations.

In this study, I investigated the relative fitness of two *A. aegypti kdr* alleles (*410L+1016I+1534C* and *1534C*) relative to each other, in the absence and presence of insecticide exposure. I wanted to assess whether a resistance allele with multiple mutations imposed greater fitness costs relative to the allele with only one mutation (in accordance to what was previously found in *M. domestica*). Overall, the *410L+1016I+1534C* allele imposes both an astonishing fitness cost in the absence of insecticide and a strong advantage relative to *1534C* in the presence of deltamethrin exposure. Such fitness cost and strong advantage are evidenced in the extremely low frequencies of homozygous *410L+1016I+1534C/410L+1016I+1534C* mosquitoes that are later increased following deltamethrin exposure. Genotype frequencies across generations do not follow the assumptions of Hardy-Weinberg Equilibrium and are not due to genetic drift suggesting that these mosquito populations have fitness costs.

4.2 Materials and methods

Mosquito strains

Two congenic strains of *A. aegypti* were used in this study. Both strains share the same pyrethroid-susceptible background from the Rockefeller strain (ROCK), but carry different *kdr* alleles. The LMRKDR:ROCK (LKR) is a pyrethroid-resistant strain which is congenic to ROCK, but contains the *kdr* allele *410L+1016I+1534C* (Silva et al. 2021). The 1534C:ROCK is a pyrethroid-resistant strain which is congenic to ROCK, but contains the *1534C* allele (Fan and Scott 2020). In both congenic strains, the *kdr* alleles are the only mechanism of resistance to pyrethroids (Fan and Scott 2020, Silva et al. 2021).

Allele competition experiments

To conduct the allele competition experiments (population cage experiment), the two congenic strains described in the previous section were crossed: Cross A (LKR females x 1534C:ROCK males) and reciprocal cross B (1534C:ROCK females x LKR males). For each reciprocal cross, 400 unmated females and 200 males were released into a cage and were allowed to mate *en masse* for seven days. The offspring resulting from crosses A and B were split into three cages (A1, A2, A3, B1, B2 and B3) as shown in Fig. S1. Mosquitoes were reared in a room with temperatures ranging from 25.0 – 28.5°C (average = 25.6), 26.8 – 54.5% (average = 47.9%) relative humidity, and a 14:10-h (light/dark) photoperiod. Females were fed cow blood (Owasco Meat Co. Inc., Moravia, NY) using membrane covered water-jacketed glass feeders. Adults were maintained on 10% sucrose water in cages approximately 36 x 25 x 25 cm. Larvae were reared in 29.5 x 23 x 8.4 cm plastic containers (LOCK&LOCK Co., Ltd., Seocho-gu, Korea) with ~1.5 L distilled water and Hikari Cichlid Gold fish food pellets (Hikari, Hayward, CA, USA) (ground pellets for 1st instar and whole medium size pellets for 2nd to 4th instars). Food pellets were given daily, as needed depending on larval density and instar. Approximately 800 pupae from the larval containers were placed into cages for each following generation. Additional emerging males and females were stored separately in 2 ml Eppendorf tubes at -80℃ until they were genotyped.

The genotyping of the mosquitoes was done by allele specific polymerase chain reaction (ASPCR) using primers that were allele specific at codon 1016 of the *Vgsc* (one allele has *410L+1016I+1534C* and allele *1534C* has *V410+V1016+1534C*). The genomic DNA from mosquito heads was extracted using an alkali extraction method (Smith et al. 2017). Heads were removed and placed into individual wells of a 96-well PCR plate (Bio-Rad, Hercules CA) with approximately three 2-3-mm diameter Zirconia/Silica beads (BioSpec Products, Bartlesville OK) and 10 µL of 0.2 M NaOH per well. Samples were vortexed for 1 min to pulverize tissue and incubated at 70°C for 10 min. After incubation, 10 µL of neutralization buffer (360 mM Tris-HCl pH 8.0 and 10 mM EDTA) and 80 µL of nuclease-free water (VWR International, Radnor PA) were added to each well. DNA extractions were stored long-term at -70 °C for further analysis if needed. The ASPCR was done using the following thermocycler conditions: For the *1534C* allele, 94˚C for 3 min, 36 x (94˚C for 30 sec, 62˚C for 30 sec, 72˚C for 1 min) and 72˚C (7 min). For the *410L+1016I+1534C* allele, 94˚C for 3 min, 34 x (94˚C for 30 sec, 65˚C for 30 sec, 72˚C for 1 min) and 72˚C (7 min). I used 1µL of extracted DNA as templates for ASPCR. The primers used for each PCR reaction are shown in Table S2. Each PCR reaction was evaluated on a 1% agarose gel and was scored as homozygous V1016 (PCR band only with V1016 primers), homozygous for 1016I (ASPCR band only with 1016I primers) or heterozygous (PCR band with both 1016V and 1016I primers). For each biological replicate, 45 males and 45 females were genotyped. Every PCR plate included control DNA from 2 samples of LKR, 1534C:ROCK and F_1 (control DNA was previously sent for sequencing to validate the expected codon V1016I for each corresponding strain or F_1). In addition to the controls, the codon V1016I was verified for 16 samples from A2F5 and A1F10, eight samples each). The sequencing results for the controls and samples agreed with the results from the gels. Each sample was genotyped using two technical replicates by running PCR reactions and gels twice.

The genotyping results were scored independently by three judges. Each judge assigned a genotype for each mosquito in both technical replicates. If the technical replicates agreed, a final genotype was assigned. A consensus genotype was determined if there was agreement between two out of three judges. If three judges disagreed on the final genotype, then those samples were considered for a third technical replicate. Third replicates were done if there were more than 10 samples per biological replicate for which there was no consensus genotype; otherwise, these samples were dropped from analysis.

Selection of F_9 using deltamethrin

3-7-day old males and females were selected with deltamethrin. The doses used for males and females (0.039 ng/mosquito and 0.078 ng/mosquito, respectively) were chosen to give approximately 80% kill. To conduct the selections, mosquitoes were knocked down with CO_2 and placed in a paper cup on a bucket filled with ice to keep them anesthetized. Deltamethrin in acetone (or acetone only for controls) was applied topically to each mosquito with a PB600-1 repeating dispenser and a 10 μL Hamilton syringe (Hamilton Company, Reno NV). Treated mosquitoes (40) were placed in a paper cup covered with nylon tulle and a cotton ball saturated with distilled water and held at 25˚C for 24 hours. Both male and unmated female survivors were released in disposable cages (dimensions: A-15.7 x 15.7 x 24 inches, Restcloud Chengdu YiShouWeiSheng Technology Co., Ltd, China) and allowed to mate *en masse*. These mosquitoes were reared as described above and their offspring harvested for *Vgsc* genotyping.

Allele competition data analysis

Differences between allele and genotype frequencies across generations were tested using linear mixed models (using the lme4 package (v 1.2–21) in R 3.6.3, based on (Bates et al. 2015) and checked for significance from F-values generated from ANOVA in R (Kuznetsova 2017). Pairwise comparisons between genotype and allele frequencies were done using Tukey's test for post-hoc analysis (using the

"agricolae" package (v 1.3-5)) in R to determine significant differences across generations. The changes in frequencies of the *410L+1016I+1534C* allele between generations F_1 to F_9 in the absence of deltamethrin selection are best represented by a power function model ($F_{1,34} = 276.3$, $r^2 = 0.890$) relative to linear model ($F_{1,34} = 55.76$, $r^2 = 0.621$). To evaluate differences in allele frequencies between cross A and cross B, two models were designed; model 1 accounted for the allele frequencies and generations, whereas the model 2 accounted for the same interaction as model 1, but including the interaction between cross and generation. Similarly, two models were designed to evaluate differences in allele frequencies between males and females; model 3 accounted for the allele frequencies and generations whereas the model 4 accounted for the same interaction as model 3, but including the interaction between sexes and generation.

Deviation from Hardy-Weinberg equilibrium (HWE) within generations was assessed using a chi-square test ($\chi 2$) to compare the observed genotype counts relative to the expected genotype counts calculated using the allele frequencies of the same generation. The level of significance for statistical analyses was $p < 0.05$. Simulations were used to evaluate the likelihood of the observed allele frequency changes due to genetic drift. Simulations were done with R software (R Development Core Team 2020) and scripts applied as in a previous study (Hardstone et al. 2009). The model assumed a diploid and panmictic population with a fixed size of 800 individuals and the initial *410L+1016I+1534C* allele frequency for each generation was defined as the observed frequency in the previous interval. Simulations were repeated 50,000 times per generation and p-values were estimated as the number of simulations in which ending allele frequency was equal or more extreme than the initial value of the interval divided by the total number of simulations. The null hypothesis assumed all fluctuations in allele frequencies could be explained by genetic drift.

A Fisher's combined probability test of either HWE p-values were also used to determine if allele frequency changes across all the generations are in Hardy-Weinberg equilibrium, as a proxy to determine if the changes are due to selection. This method considers multiple independent tests with the same hypothesis and assesses the probability that all hypotheses are true in order to obtain a global p-value (Schaid et al. 2006, Waples 2015).

4.3 Results

The 410L+1016I+1534C allele frequencies decreased drastically over generations in the absence of deltamethrin selection

There were no significant differences in the allele frequencies over generations between crosses A and B for the unselected (ANOVA, p value = 0. 951) or deltamethrin selected generations (ANOVA, p value = 0.174). There were no significant differences in the allele frequencies over generations between males and females in the absence (ANOVA, p value = 0.888) nor presence of deltamethrin selection (ANOVA, p value = 0.774. For this reason, allele frequencies from crosses A and B (and from males and females) were pooled for further analysis.

There was a remarkable fitness disadvantage to the *410L+1016I+1534C* allele, relative to the *1534C* allele, in the absence of insecticide. The frequency of the *410L+1016I+1534C* allele decreased in a trend that is best fitted by a power function model ($F_{1,34} = 276.3$, $r^2 = 0.89$, ANOVA = 2.20×10^{-16}). The fitness cost was most dramatic from the F_1 (0.50) to F_5 (0.12). The frequency of the *410L+1016I+1534C* allele remained relatively unchanged after the F_5 (Fig. 1).

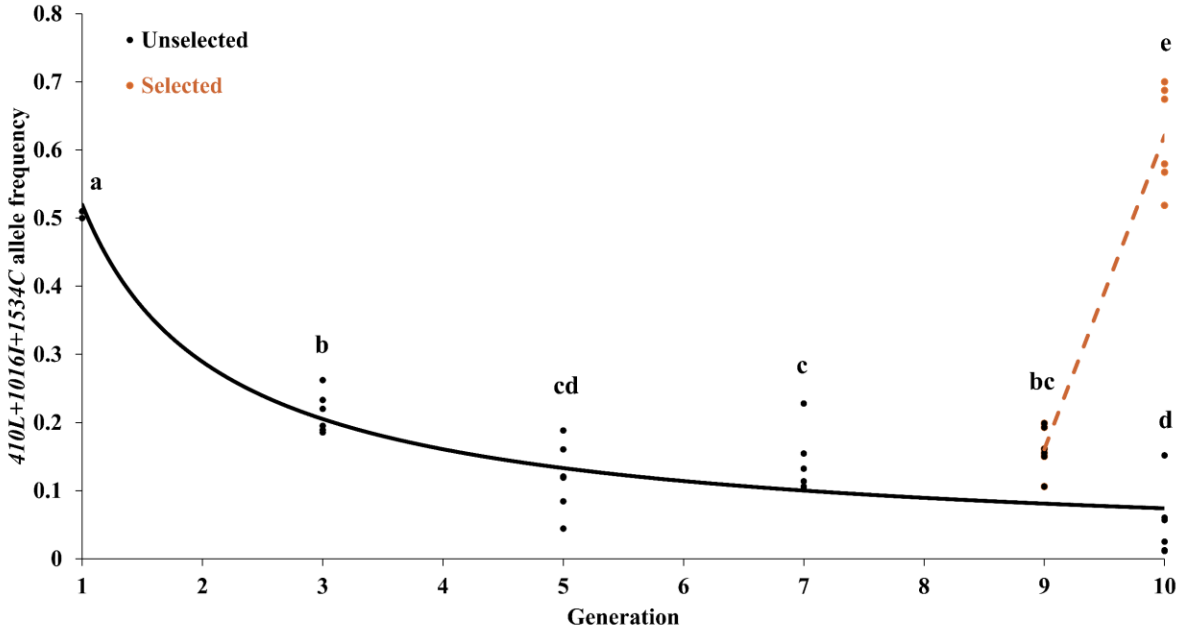

Figure 1. Frequency changes of the *410L+1016I+1534C* alleles over 10 generations in the absence and presence of deltamethrin selection. The solid black line represents the changes in allele frequencies in the absence of deltamethrin exposure are represented by a power function model ($F_{1,34}$ = 276.3, r^2 = 0.89). The dashed orange line represents the changes in allele frequencies from F_9 to F_{10} in the presence of deltamethrin selection (linear model $F_{1,10}$ = 186.1, r^2 = 0.95). Different letters represent significant differences based on Tukey test.

Examination of genotypes at each generation reveals that the reduction in the *410L+1016I+1534C* allele was driven primarily by the fitness costs associated with the *410L+1016I+1534C* homozygote (Fig. 1). For example, the frequency of the *410L+1016I+1534C* homozygote was only 0.026 by the F_3 (Fig. 1) and remained low (below 0.03 from F_3 to F_{10}) in the absence of insecticide. The *1534C/1534C* genotype increased from F_3 (0.59) to F_5 (0.77), and then remained relatively constant through the F_{10}. Similarly, the *1534C/410L+1016I+1534C* genotype decreased from F_3 (0.37) to F_5 (0.21), then remained relatively constant through F_{10}.

The 410L+1016I+1534C allele frequencies increased notably after one cycle of selection with deltamethrin

In sharp contrast to the high fitness cost of the *410L+1016I+1534C* allele in the absence of insecticide, this allele exhibited an extraordinary strong fitness advantage after exposure to deltamethrin. The most dramatic advantage was observed where the frequencies of the homozygotes *410L+1016I+1534C/410L+1016I+1534C* showed a notable increase from F_9 (0.01) to F_{10} (0.48) ($F_{1,10}$ = 60.78, r^2 = 0.86, ANOVA = $1.48x10^{-5}$). On the contrary, the frequencies of the heterozygotes *1534C/410L+1016I+1534C* did not differ significantly after deltamethrin selection from F_9 (0.31) to F_{10} (0.28) ($F_{1,10}$ = 0.154, r^2 = 0.02, ANOVA = 0.702). The frequencies of the homozygotes *1534C/1534C* had a strong reduction from F_9 (0.68) to F_{10} (0.24) ($F_{1,10}$ = 245.5, r^2 = 0.96, ANOVA = $2.29x10^{-8}$). Thus, the changes of the *410L+1016I+1534C/410L+1016I+1534C* homozygotes was carried out at expenses of a decrease in the homozygotes *1534C/1534C*. As expected for a population under selection, the genotype frequencies do not follow the assumptions of HWE (Fisher's combined probability test, df = 72, X^2 = 229.43, p value < 0.0001) (Table 1 and Fig. 2). I was unable to run the Fisher's combined probability test on the simulations from genetic drift because some p values were equal to zero and this violates the assumptions for this test. However, 28 out of 36 simulations were significant and, thus, suggesting a clear trend that changes in alleles frequencies were not due to genetic drift (Table 1).

Table 1. Genotype, allele frequencies for each replicate of the LKR x 1534C:ROCK experiment and their associated Hardy-Weinberg equilibrium (HWE) and genetic drift p-values.

Generation	Sample size	Observed genotype frequency (expected[#])			Allele frequencies		HWE[¥] (p-value)	Genetic drift (p-value)
		1534C/ 1534C	*1534C/ 410L+1016I+1534C*	*410L+1016I+1534C/ 410L+1016I+1534C*	*1534C*	*410L+1016I+1534C*		
AF1-1	83	0.00	1.00	0.00	0.50	0.50	---	---
AF1-2	89	0.00	1.00	0.00	0.50	0.50	---	---
AF1-3	90	0.00	1.00	0.00	0.50	0.50	---	---
BF1-1	86	0.00	0.99	0.01	0.49	0.51	---	---
BF1-2	88	0.00	0.99	0.01	0.49	0.51	---	---
BF1-3	81	0.00	1.00	0.00	0.50	0.50	---	---
AF3-1	88	0.54 (0.59)	0.44 (0.36)	0.01 (0.05)	0.77	0.23	0.079	0.000*
AF3-2	89	0.64 (0.66)	0.35 (0.30)	0.01 (0.03)	0.81	0.19	0.352	0.000*
AF3-3	82	0.52 (0.54)	0.43 (0.39)	0.05 (0.07)	0.74	0.26	0.646	0.000*
BF3-1	81	0.62 (0.61)	0.33 (0.34)	0.05 (0.05)	0.78	0.22	0.989	0.000*
BF3-2	90	0.62 (0.66)	0.38 (0.31)	0.00 (0.04)	0.81	0.19	0.087	0.000*
BF3-3	82	0.65 (0.65)	0.32 (0.31)	0.04 (0.04)	0.81	0.19	0.996	0.000*
AF5-1	81	0.69 (0.70)	0.29 (0.27)	0.01 (0.03)	0.84	0.16	0.669	0.000*
AF5-2	89	0.83 (0.84)	0.17 (0.15)	0.00 (0.01)	0.92	0.08	0.686	0.000*
AF5-3	79	0.91 (0.91)	0.09 (0.08)	0.00 (0.00)	0.96	0.04	0.918	0.000*
BF5-1	87	0.76 (0.77)	0.24 (0.21)	0.00 (0.01)	0.88	0.12	0.441	0.000*
BF5-2	84	0.76 (0.78)	0.24 (0.21)	0.00 (0.01)	0.88	0.12	0.464	0.000*
BF5-3	85	0.71 (0.66)	0.21 (0.31)	0.08 (0.03)	0.81	0.19	0.018*	0.319
AF7-1	68	0.84 (0.71)	0.01 (0.26)	0.15 (0.02)	0.85	0.15	7.08×10^{-14}*	0.346
AF7-2	90	0.54 (0.59)	0.46 (0.35)	0.00 (0.05)	0.77	0.23	0.019*	0.000*
AF7-3	88	0.77 (0.79)	0.23 (0.20)	0.00 (0.01)	0.88	0.11	0.485	0.000*
BF7-1	87	0.74 (0.75)	0.26 (0.23)	0.00 (0.02)	0.87	0.13	0.364	0.159
BF7-2	85	0.79 (0.79)	0.21 (0.19)	0.00 (0.01)	0.89	0.11	0.551	0.128
BF7-3	88	0.79 (0.81)	0.20 (0.18)	0.00 (0.01)	0.90	0.10	0.565	0.000*
AF9-1	89	0.68 (0.72)	0.31 (0.26)	0.00 (0.02)	0.85	0.15	0.219	0.416
AF9-2	83	0.63 (0.65)	0.36 (0.31)	0.01 (0.04)	0.81	0.19	0.339	0.008
AF9-3	88	0.60 (0.64)	0.39 (0.32)	0.00 (0.04)	0.80	0.20	0.066	0.000*
BF9-1	90	0.68 (0.70)	0.32 (0.27)	0.00 (0.02)	0.84	0.16	0.190	0.009*
BF9-2	80	0.71 (0.72)	0.27 (0.26)	0.01 (0.02)	0.85	0.15	0.782	0.000*
BF9-3	85	0.80 (0.79)	0.18 (0.19)	0.01 (0.01)	0.89	0.11	0.998	0.343

Table 1. Continuation.

Generation	Sample size	Observed genotype frequency (expected[#])			Allele frequencies		HWE[¥] (p-value)	Genetic drift (p-value)
		1534C/ 1534C	*1534C/ 410L+1016I+1534C*	*410L+1016I+1534C/ 410L+1016I+1534C*	*1534C*	*410L+1016I+1534C*		
AF10-1	80	0.95 (0.95)	0.05 (0.05)	0.00 (0.00)	0.97	0.03	0.974	0.000*
AF10-2	83	0.88 (0.88)	0.12 (0.11)	0.00 (0.00)	0.94	0.06	0.843	0.427
AF10-3	89	0.97 (0.98)	0.02 (0.02)	0.00 (0.00)	0.99	0.01	0.994	0.000*
BF10-1	88	0.88 (0.89)	0.11 (0.11)	0.00 (0.00)	0.94	0.06	0.852	0.000*
BF10-2	89	0.69 (0.72)	0.30 (0.26)	0.00 (0.02)	0.85	0.15	0.241	0.430
BF10-3	81	0.97 (0.98)	0.02 (0.02)	0.00 (0.00)	0.99	0.01	0.993	0.000*
Selected								
AF10-1	86	0.16 (0.12)	0.32 (0.44)	0.51 (0.45)	0.33	0.67	0.056	0.000*
AF10-2 Sel	88	0.25 (0.18)	0.34 (0.49)	0.41 (0.34)	0.42	0.58	0.019*	0.000*
AF10-3 Sel	80	0.24 (0.09)	0.15 (0.43)	0.61 (0.47)	0.31	0.69	$4.36x10^{-8}$*	0.000*
BF10-1 Sel	20	0.05 (0.09)	0.50 (0.42)	0.45 (0.49)	0.30	0.70	0.696	0.000*
BF10-2 Sel	81	0.39 (0.23)	0.17 (0.49)	0.43 (0.27)	0.48	0.52	$3.02x10^{-8}$*	0.000*
BF10-3 Sel	89	0.33 (0.19)	0.21 (0.49)	0.46 (0.32)	0.43	0.57	$6.73x10^{-7}$*	0.000*
Global X^2 (df = 72) =							229.43	
Global p-value =							0.000*	

[#]Expected genotype frequencies based on the allele frequencies from the same generation.

[¥]The p values of the HWE are based on the observed and expected genotypes within the same generation.

*P-values lower than 0.05 indicate significant differences from the null hypothesis of HWE.

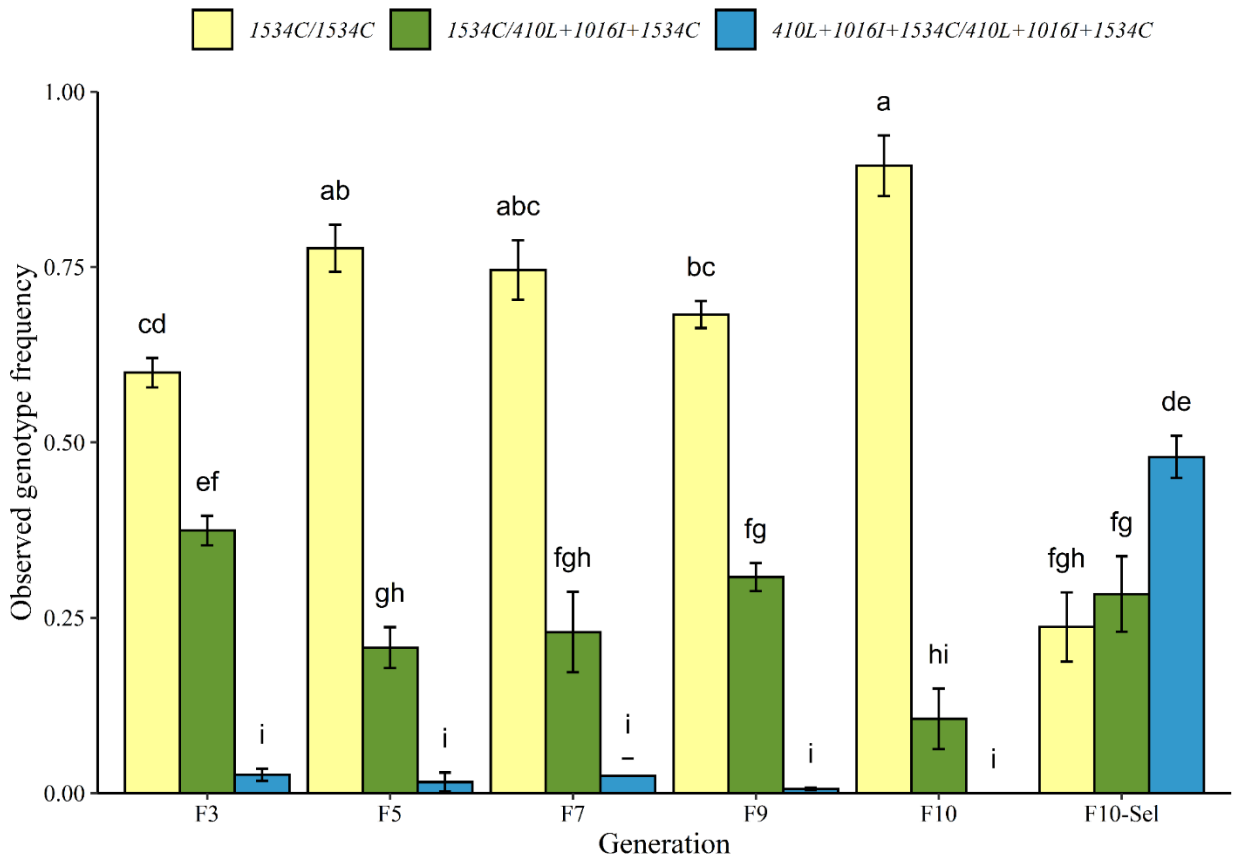

Figure 2. Changes in genotype frequencies over generations in the absence and presence of deltamethrin selection. Different letters represent significant differences based on Tukey test.

4.4 Discussion

My results indicate that the frequencies of the *410L+1016I+1534C* vs. *1534C* alleles are strongly influenced by the fitness disadvantage of the *410L+1016I+1534C* allele in the absence of insecticides, but that in the presence of deltamethrin, this allele has an outstanding fitness advantage. The decrease of the *410L+1016I+1534C* allele across generations in the absence of deltamethrin exposure is driven primarily by the fitness cost of the *410L+1016I+1534C* homozygotes. The fitness cost of the *410L+1016I+1534C* allele was much higher than has been found for other alleles. For example, using a similar population cage experiment, the *989P+1016G* (Smith et al. 2021) and the *F1534C* (Fisher et al. 2022) alleles were shown to have a fitness cost relative to a susceptible allele, but the change in allele and genotype frequencies across generations was lower (frequency of the *kdr* allele decreased in a linear manner and was still greater than 0.3 by the F_7) than those observed in this study. Another previous study used a strain of *A. aegypti* congenic to the pyrethroid-susceptible ROCK strain, but carrying an unknown *kdr* allele (although it was known to carry the V1016I mutation) and measured fitness costs. The frequency of the allele containing the 1016I mutation decreased through 15 generations in the absence of pyrethroid exposure (cross A: $r^2 = 0.527$, $p = 0.0006$ and cross B: $r^2 = 0.569$, $p= 0.0003$, respectively) (Brito et al. 2013) at a rate similar to what was seen for the *1534C* and *989P+1016G* alleles. It would be helpful to know what the allele was in those experiments, as well as what role (if any) the enhanced detoxification enzymes played in the changes in allele frequency.

Given the environmental conditions (larval density, relative humidity and temperature), I predict that a similar fitness cost would occur in field populations of *A. aegypti* where the two *kdr* alleles used in this study are present, but the sources of this cost remain unknown. In other words, I would expect the *1534C* allele to increase in allele frequencies in the absence of deltamethrin exposure. Based on the cross-resistance studies, I predict that applications of different pyrethroids would benefit both resistance alleles considered in population cage experiment because response to pyrethroids did not differ for many pyrethroids between the two strains carrying the alleles conducted in this study (Fan and Scott 2020, Silva

et al. 2021). On the contrary, I would predict that deltamethrin exposure would drastically increase the frequency of the *410L+1016I+1534C* over the *1534C* allele in populations where these alleles coexist. The frequencies of related *kdr* alleles have been measured in field populations in previous studies. Based on data collected from 25 field populations from Brazil, the *1534C* allele was the most common (40.0%) followed by the *410L+1016I+1534C* (38.2%) and *V410+V1016+F1534* (10.4%), the other alleles could not be resolved (remaining 11.4%) (Costa et al. 2020). Another study done in Brazil found that the most common allele was *1016I+1534C* (65.4%), followed by *1534C* (27.5%) and the susceptible *V1016+F1534* (7.2%) (Brito et al. 2018). Unfortunately, this study did not check the presence of the V410L mutation. In Colombia, the most common allele was *1534C* (43.9%), followed by the *V410+V1016+F1534* (25.0%), *410L+1016I+1534C* (22.2%), and other alleles (8.9%) (Granada et al. 2018). In Mexico, the susceptible allele (*V410+V1016+F1534*) was the most common (99.6%) in the year 2000 and there was only one resistance allele (*1534C*) that was extremely rare (0.04%) (Saavedra-Rodriguez et al. 2018). By 2016, the same susceptible allele drastically dropped to (1.6%) and was outcompeted by *416L+1016I+1534C* (68.4%), *1534C* (25.9%) and others (4.01%). In general, the low frequency of the pyrethroid-susceptible allele in these studies suggests that these populations of *A. aegypti* were under pyrethroid exposure and resulted in higher frequencies of the *1016I+1534C* over the *1534C* allele that agrees with my findings. However, since these are field-collected populations it is possible that other mechanisms of resistance are involved and different fitness costs could be present.

My findings show a strong fitness cost associated with the *410L+1016I+1534C* allele in the absence of insecticide exposure, but this allele provides a fitness advantage when exposed to deltamethrin, relative to the *1534C* allele. Changes in genotype frequencies were not in HWE and could not be explained by genetic drift. Given the dramatic fitness cost of the *410L+1016I+1534C* allele relative to the *1534C* allele in the absence of insecticide, it is possible that the functionality of the VGSC is more drastically impaired for the former allele compared to the latter and investigating the physiological reason for the fitness cost would be insightful. For example, experiments looking at the

electrophysical or behavioral differences associated with the *410L+1016I+1534C* allele could be very illuminating.

Acknowledgements

I thank N. Buchon, P. Wang, R. Mertz, R. Norris, and L. Pfannenstiel for their valuable comments.

REFERENCES

Bates, D., M. Mächler, B. Bolker, and S. Walker. 2015. Fitting linear mixed-effects models using lme4. J. Stat. Softw. 67: 1-48.

Bhatt, S., P. W. Gething, O. J. Brady, J. P. Messina, A. W. Farlow, C. L. Moyes, J. M. Drake, J. S. Brownstein, A. G. Hoen, and O. Sankoh. 2013. The global distribution and burden of dengue. Nature 496: 504.

Brito, L. P., L. Carrara, R. M. de Freitas, J. B. P. Lima, and A. J. Martins. 2018. Levels of resistance to pyrethroid among distinct *kdr* alleles in *Aedes aegypti* laboratory lines and frequency of *kdr* alleles in 27 natural populations from Rio de Janeiro, Brazil. Biomed Res Int 2018: 2410819.

Brito, L. P., J. G. Linss, T. N. Lima-Camara, T. A. Belinato, A. A. Peixoto, J. B. Lima, D. Valle, and A. J. Martins. 2013. Assessing the effects of *Aedes aegypti kdr* mutations on pyrethroid resistance and its fitness cost. PLoS One 8: e60878.

CDC. 2016. Zika virus spreads to new areas — Region of the Americas, May 2015–January 2016, pp. 55-58, MMWR Morb Mortal Wkly Rep. Centers for Disease Control and Prevention, Atlanta, Ga.

CDPR. 2018. Total Pounds, Applications, and Acres Treated by County and Chemical. California Department of Pesticide Regulation.

Chang, C., W. K. Shen, T. T. Wang, Y. H. Lin, E. L. Hsu, and S. M. Dai. 2009. A novel amino acid substitution in a voltage-gated sodium channel is associated with knockdown resistance to permethrin in *Aedes aegypti*. Insect Biochem. Mol. Bio. 39: 272-278.

Costa, M. M., K. B. Campos, L. P. Brito, E. Roux, C. M. Rodovalho, D. F. Bellinato, J. B. Pereira Lima, and A. J. Martins. 2020. Kdr genotyping in Aedes aegypti from Brazil on a nation-wide scale from 2017 to 2018. Scientific Reports 10: 13267.

ECDC. 2015. Zika virus epidemic in the Americas: potential association with microcephaly and Guillain-Barré syndrome. European Centre for Disease Prevention and Control, Stockholm, Sweden.

Fan, Y., and J. G. Scott. 2020. The F1534C *voltage sensitive sodium channel* mutation confers 7- to 16-fold resistance to pyrethroid insecticides in *Aedes aegypti*. Pest Man. Sci. 76: 2251-2259.

Fan, Y., P. O'Grady, M. Yoshimizu, A. Ponlawat, P. E. Kaufman, and J. G. Scott. 2020. Evidence for both recombination and mutations in the evolution of *kdr* alleles in *Aedes aegypti*. PLoS Negl Trop Dis 14: e0008154.

Fisher, C. R., A. E. Dressel, J. J. Silva, and J. G. Scott. 2022. A globally distributed insecticide resistance allele confers a fitness cost in the absence of insecticide in *Aedes aegypti*, the yellow fever mosquito. PeerJ Submitted.

Freeman, J. C., L. B. Smith, J. J. Silva, Y. Fan, H. Sun, and J. G. Scott. 2021. Fitness studies of insecticide resistant strains: lessons learned and future directions. Pest Man. Sci. 77: 3847–3856.

Granada, Y., A. Mejía-Jaramillo, C. Strode, and O. Triana-Chavez. 2018. A point mutation V419L in the sodium channel gene from natural populations of *Aedes aegypti* is involved in resistance to λ-cyhalothrin in Colombia. Insects 9: 23.

Haddi, K., H. V. V. Tomé, Y. Du, W. R. Valbon, Y. Nomura, G. F. Martins, K. Dong, and E. E. Oliveira. 2017. Detection of a new pyrethroid resistance mutation (V410L) in the sodium channel of *Aedes aegypti*: a potential challenge for mosquito control. Sci. Rep. 7: 46549.

Hardstone, M. C., B. P. Lazzaro, and J. G. Scott. 2009. The effect of three environmental conditions on the fitness of cytochrome P450 monooxygenase-mediated permethrin resistance in *Culex pipiens quinquefasciatus*. BMC Evol Biol 9: 42.

Harris, A. F., S. Rajatileka, and H. Ranson. 2010. Pyrethroid resistance in *Aedes aegypti* from Grand Cayman. Am. J. Trop. Med. Hyg. 83: 277-284.

INS. 2018. Informe Red de Vigilancia de la Resistencia a Insecticidas (VRI) de uso en salud publica en Colombia. *In* C. Instituto Nacional de Salud (National Institute of Health [ed.].

Kawada, H., S. Z. M. Oo, S. Thaung, K. E., Y. N. M. Maung, H. M. Thu, K. Z. Thant, and N. Minakawa. 2014. Co-occurrence of point mutations in the voltage-gated sodium channel of pyrethroid-resistant *Aedes aegypti* populations in Myanmar. PLoS Negl. Trop. Dis. 8: e3032.

Kushwah, R. B. S., C. L. Dykes, N. Kapoor, T. Adak, and O. P. Singh. 2015. Pyrethroid-resistance and presence of two knockdown resistance (*kdr*) mutations, F1534C and a novel mutation T1520I, in Indian *Aedes aegypti*. PLoS Negl. Trop. Dis. 9: e3332.

Kuznetsova, A. B., P. B.; Christensen, R. H. B. . 2017. lmerTest Package: Tests in Linear Mixed Effects Models. J Stat Softw 82: 1-26.

Moyes, C. L., J. Vontas, A. J. Martins, L. C. Ng, S. Y. Koou, I. Dusfour, K. Raghavendra, J. Pinto, V. Corbel, J.-P. David, and D. Weetman. 2017. Contemporary status of insecticide resistance in the major *Aedes vectors* of arboviruses infecting humans. PLoS Neglect. Trop. D. 11: e0005625.

Murcia, O., B. Henríquez, A. Castro, S. Koo, J. Young, R. Márquez, D. Pérez, L. Cáceres, and A. Valderrama. 2019. Presence of the point mutations Val1016Gly in the voltage-gated sodium channel detected in a single mosquito from Panama. Parasite Vector 12: 62.

R Development Core Team 2020. R: A language and environment for statistical computing computer program, version By R Development Core Team, Vienna, Austria.

Rinkevich, F. D., C. A. Leichter, T. A. Lazo, M. C. Hardstone, and J. G. Scott. 2013. Variable fitness costs for pyrethroid resistance alleles in the house fly, *Musca domestica*, in the absence of insecticide pressure. Pestic. Biochem. Physiol. 105: 161-168.

Saavedra-Rodriguez, K., F. V. Maloof, C. L. Campbell, J. Garcia-Rejon, A. Lenhart, P. Penilla, A. Rodriguez, A. A. Sandoval, A. E. Flores, G. Ponce, S. Saul Lozano, and W. C. Black. 2018. Parallel evolution of *vgsc* mutations at domains IS6, IIS6 and IIIS6 in pyrethroid resistant *Aedes aegypti* from Mexico. Sci. Rep. 8: 6747.

Schaid, D. J., A. J. Batzler, G. D. Jenkins, and M. A. Hildebrandt. 2006. Exact tests of Hardy-Weinberg equilibrium and homogeneity of disequilibrium across strata. Amer. J. Human Genet. 79: 1071–1080.

Silva, J. J., C. N. Couam, and J. G. Scott. 2021. Levels of cross-resistance to pyrethroids conferred by the *Vssc* knockdown resistance allele 410L+1016I+1534C in *Aedes aegypti*. PLoS Negl Trop Dis 15: e0009549.

Smith, L. B. 2019. Fitness advantages and disadvantages of pyrethroid resistance mechanisms in the yellow fever mosquito, *Aedes aegypti*. PhD, Cornell Ithaca, NY.

Smith, L. B., S. Kasai, and J. G. Scott. 2017. Voltage-sensitive sodium channel mutations S989P+V1016G in *Aedes aegypti* confer variable resistance to pyrethroids, DDT and oxadiazines. Pest Manag. Sci. 74: 737-745.

Smith, L. B., J. J. Silva, C. Chen, L. Harrington, and J. G. Scott. 2021. Fitness costs of individual and combined pyrethroid resistance mechanisms, *kdr* and CYP-mediated detoxification, in *Aedes aegypti*. PLoS Negl Trop Dis. 15: e009271.

Srisawat, R., N. Komalamisra, C. Apiwathnasorn, P. Paeporn, R. Sittiruk, Y. Rongsriyam, and Y. Eshita. 2012. Field-collected permethrin-resistant *Aedes aegypti* from central Thailand contain point mutations in the domain IIS6 of the sodium channel gene (*kdr*). SE Asian J. Trop. Med. 43: 1380-1386.

Waples, R. S. 2015. Testing for Hardy–Weinberg proportions: have we lost the plot? J. Hered. 106: 1-19.

WHO. 2013. Dengue and severe dengue. World Health Organization, Geneva.

Yactayo, S., J. E. Staples, V. Millot, L. Cibrelus, and P. Ramon-Pardo. 2016. Epidemiology of chikungunya in the Americas. J Infect Dis 214: S441-S445.

4.5 Supplementary materials

Table S1. List of *kdr* alleles found in *A. aegypti.* Amino acid numbering based on *Musca domestica* VGSC, GenBank: CAA65448.1.

Allele	Reference
410L	(Granada et al. 2018)
410L+1534C	(Haddi et al. 2017, Saavedra-Rodriguez et al. 2018)
410L+1016I+1534C	(Saavedra-Rodriguez et al. 2018)
989P+1016G	(Srisawat et al. 2010)
989P+1016G+1534C	(Kawada et al. 2014)
1011M+1016G	(Murcia et al. 2019)
1016I+1534C	(Harris et al. 2010)
1016G+1763Y	(Chang et al. 2009)
1520I+1534C	(Kushwah et al. 2015)
1534C	(Fan et al. 2020)

Table S2. List of primers used for genotyping the V1016I mutation from LMRKDR:RK and 1534C:ROCK.

Allele	Primer name	Sequence (5' to 3')
1016V	E20-Sus1	CATGATCGTGTTCCGGGTATTG
	V1R ARMS	CAAAAGCAAGGCTAAGAAAAGGTTAAGTGC
1016I	E20-Res2	GCACTCATTCATGATCGTGTTCCGGGTATTA
	I1R ARMS-2	CAAAAGCAAGGCTAAGAAAAGGTTAAGTATT

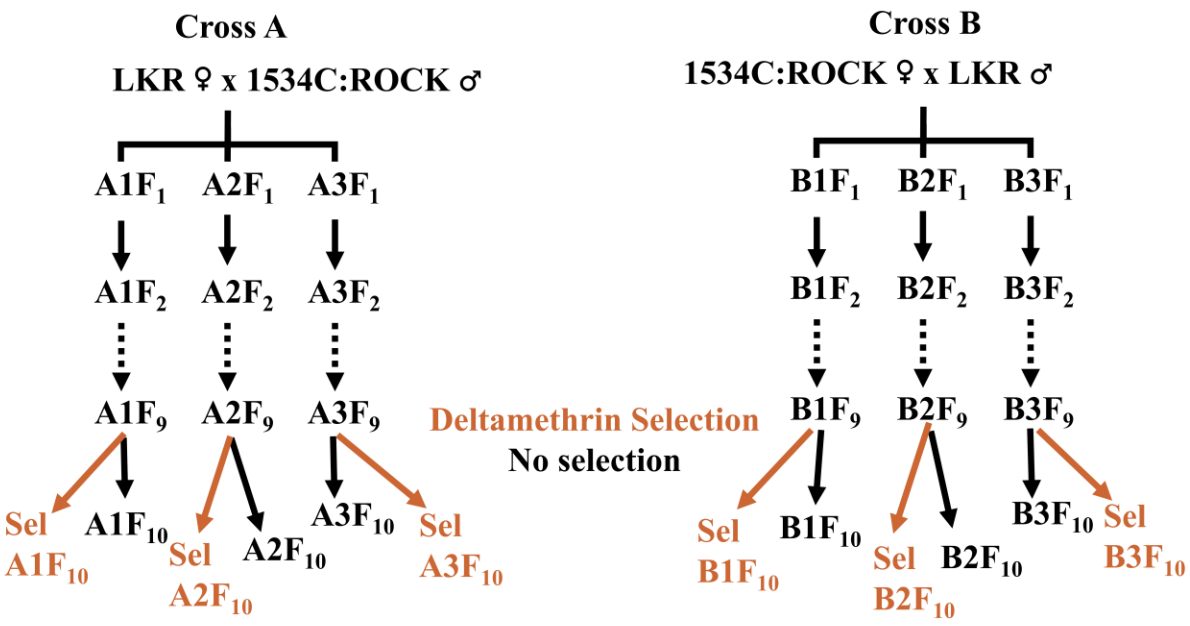

Figure S1. Diagram of the allele competition experiment. Each strain had a different *kdr* allele (LKR and 1534C:ROCK strains had the *410L+1016I+1534C* and *1534C* alleles, respectively). For each reciprocal cross (400 females and 200 males) the offspring were separated into three biological replicates. A subset of mosquitoes from F_9 were selected with deltamethrin and survivors were allowed to mate. The F_{10} from unselected and selected mosquitoes are colored in black and brown, respectively.

CHAPTER 5

FUTURE DIRECTIONS

The main thrust of my thesis research was to understand role of the *voltage-gated sodium channel* (*Vgsc*) gene in pyrethroid resistance and its fitness costs in the yellow fever mosquito, *Aedes aegypti.* This thesis contributed the fields of entomology, insect physiology and toxicology by studying the exon conservation of the VGSC across insect orders and within species, evaluating the levels of cross-resistance to pyrethroids, DDT and oxadiazines conferred by the *kdr* allele *410L+1016I+1534C*, and the fitness costs associated to this allele in the absence of deltamethrin exposure. To continue expanding knowledge in the fields of science mentioned above, the future directions of my thesis dissertation are explained in this chapter.

When I studied the exon conservation of the VGSC between insect orders (Chapter 2), there was high amino acid identity but also evidenced the increase in the number of alternative, mutually exclusive and 5' or 3' alternative splice site exons from Diplura to Diptera. From a biological perspective, this finding indicates that multiple isoforms of the VGSC leads to several functional proteins, and it would be very interesting to study how these isoforms affect the properties of the sodium channel. The best approach for this would be to examine the different isoforms by heterologous expression of in *Xenopus* oocytes.

My results (Chapter 3) showed differences in the levels of resistance to 1*R-cis αS* cypermethrin and deltamethrin conferred between the *410L+1016I+1534C* and *1534C* alleles. Although the structure-activity relationship of pyrethroids has been explored since the 1970s, my results are the first to show how specific *kdr* alleles provide different levels of pyrethroid resistance depending on the diastereoisomer configuration. However, most insecticides bioassays done to date use a mix of isomers. Hence, future studies conducting bioassays with individual isomer configurations would reveal possible structure-activity relationships that remained overlooked for decades. In addition to studying isomer configurations

of pyrethroids, it would be highly valuable to better understand which mutations or combination of mutations from the *410L+1016I+1534C* allele are responsible for the increased levels of resistance to 1*R-cis αS* cypermethrin, deltamethrin and flumethrin compared to the *1534C*. In fact, being able to compare the levels of resistance to 1*R-cis αS* cypermethrin and deltamethrin between strains of the same genetic background but carrying multiple *kdr* alleles derived from the *410L+1016I+1534C* (e.g. *410L+1016I+1534C*, *410L+1534C*, *1016I+1534C*, and *1534C*) would elucidate the interaction between the aforementioned pyrethroids and the VGSC. Such elucidation could by conducted by using CRISPR-Cas9 system to introduce the 410L and, independently, introduce the 1016I mutations into the background of the congenic strain carrying the *1534C* allele to obtain two new strains with different *kdr* alleles (*410L + 1534C* and *1016I + 1534C*).

In chapter 4, fitness costs were found for the *410L+1016I+1534C* allele after 10 generations in the absence of insecticide exposure relative to the *1534C* allele. However, there was a strong increase after deltamethrin exposure relative to the *1534C* allele. The decrease of the *410L+1016I+1534C* allele across generations was reflected in a constantly lower number of homozygote resistant mosquitoes relative to the heterozygotes. The outstanding decrease in the frequencies of the *410L+1016I+1534C* allele relative to *1534C* raises the motivation to evaluate if the stark decrease in the frequency of the *410L+1016I+1534C* allele would be similar when in competition with a different *kdr* allele (e.g. *989P+1016G*)? To answer this question, I would propose to conduct another population cage experiment under the same environmental conditions where two congenic populations (each carrying either the *410L+1016I+1534C* or *989P+1016G* alleles) are allowed to mate *en masse*. Testing the fitness cost of the *989P+1016G* allele in the presence of *410L+1016I+1534C* allele would be relevant because, as observed in chapter 3, the *989P+1016G* allele conferred higher levels of resistance to multiple pyrethroids relative to the *410L+1016I+1534C* and *1534C* alleles. Thus, there is a clear advantage when mosquito populations carry the *989P+1016G* allele in the presence of pyrethroid exposure, but it would be interesting to see what happens to the frequencies of these alleles in the eventual case when

populations carrying these alleles coexist in the absence of pyrethroid selection. Another alternative for future directions would be to identify the factors that explain the fitness costs associated with the *410L+1016I+1534C* allele. Two previous studies found a decrease of resistance alleles (*989P+1016G* and *1016I*) by conducting similar population cage experiments as done in my project but did not find effects when looking at life history traits. However, it is possible that fitness costs could be observed for different resistance alleles such as those tested in my project. I would suggest measuring the net reproductive rate (R_0), mating competition, sex ratio and body size under the same environmental parameters as done in this study. Since these alleles are located in the *Vgsc* gene, it is likely that fitness costs could be detected in experiments that address the nervous system (courtship behavior, locomotion, and/or predator avoidance).